Copyright Warning & Restrictions

The copyright law of the United States (Title 17, United States Code) governs the making of photocopies or other reproductions of copyrighted material.

Under certain conditions specified in the law, libraries and archives are authorized to furnish a photocopy or other reproduction. One of these specified conditions is that the photocopy or reproduction is not to be "used for any purpose other than private study, scholarship, or research." If a, user makes a request for, or later uses, a photocopy or reproduction for purposes in excess of "fair use" that user may be liable for copyright infringement,

This institution reserves the right to refuse to accept a copying order if, in its judgment, fulfillment of the order would involve violation of copyright law.

Please Note: The author retains the copyright while the New Jersey Institute of Technology reserves the right to distribute this thesis or dissertation

Printing note: If you do not wish to print this page, then select "Pages from: first page # to: last page #" on the print dialog screen

Order Number 9426996

Estimation and cancellation of friction in control systems

Mentzelopoulou, Sofia, Ph.D.

New Jersey Institute of Technology, 1994

U·M·I
300 N. Zeeb Rd.
Ann Arbor, MI 48106

ABSTRACT

ESTIMATION AND CANCELLATION OF FRICTION IN CONTROL SYSTEMS

by
Sofia Mentzelopoulou

The research reported in this dissertation concerns the estimation and cancellation of friction in control systems. For purposes of analysis, the Coulomb friction model, the "extended" Coulomb friction model as well as dynamic friction models are used. In addition, for systems with multiple degrees-of-freedom, a general matrix representation of friction is presented.

For the design of the friction estimators, the theory of nonlinear observers is applied. In particular, for a system with multiple degrees-of-freedom, holonomic constraints, and multiple friction sources, three different observers are presented to estimate the friction force or torque. The first (Generalized Coulomb Friction Observer) is designed by assuming that friction is described by the classical Coulomb model; the second (Generalized Tracking Observer) considers friction as a system unknown constant input; and the third (Generalized Dynamic Friction Observer) is designed by assuming that friction is described by a dynamic model.

For the analysis of the performance of the proposed estimators, two cases are considered. First considered is the case where both the system "positions" and "velocities" are available for measurements. Second considered is the case where only the system "positions" can be measured. In the first case, the observers use the measurements of the states to estimate the friction forces. In the second case, an additional reduced-order velocity observer is used to estimate the unmeasured "velocities".

The problem of friction cancellation in a system with multiple degrees-of-freedom, external inputs and friction sources is also addressed. Necessary and

sufficient conditions are derived for cancellation of the friction. The conditions are based on the relative distribution of the system inputs and friction sources at the different system degrees–of–freedom. When cancellation is possible, a control law for accomplishing it is presented.

The effectiveness of the proposed algorithms for friction estimation and cancellation is demonstrated by simulations. The observers are applied and compared in systems with linear as well as nonlinear dynamics.

Finally, experimental data for the different friction compensators are taken and compared, using an experimental apparatus built for this purpose. The results of the experiments confirm the theory and demonstrate that friction can be estimated and cancelled by the algorithms developed in this research.

ESTIMATION AND CANCELLATION OF FRICTION IN CONTROL SYSTEMS

by
Sofia Mentzelopoulou

A Dissertation
Submitted to the Faculty of
New Jersey Institute of Technology
in Partial Fulfillment of the Requirements for the Degree of
Doctor of Philosophy

Department of Electrical and Computer Engineering

May 1994

APPROVAL PAGE

ESTIMATION AND CANCELLATION OF FRICTION IN CONTROL SYSTEMS

Sofia Mentzelopoulou

Dr. Bernard Friedland, Dissertation Advisor — Date
Distinguished Professor of Electrical Engineering, NJIT

Dr. Timothy Chang, Committee Member — Date
Assistant Professor of Electrical and Computer Engineering, NJIT

Dr. Denis Blackmore, Committee Member — Date
Professor of Mathematics, NJIT

Dr. Avraham Harnoy, Committee Member — Date
Associate Professor of Mechanical Engineering, NJIT

Dr. Farshad Khorrami, Committee Member — Date
Assistant Professor of Electrical Engineering, Polytechnic University

Dr. Brian Stewart Randal Armstrong-Hélouvry, — Date
Committee Member
Assistant Professor of Electrical Engineering and Computer Science,
University of Wisconsin - Milwaukee

BIOGRAPHICAL SKETCH

Author: Sofia Mentzelopoulou

Degree: Doctor of Philosophy

Date: May 1994

Undergraduate and Graduate Education:

- Doctor of Philosophy in Electrical Engineering
  New Jersey Institute of Technology, Newark, NJ, USA, 1994
- Master of Science in Electrical Engineering,
  Rochester Institute of Technology, Rochester, NY, USA, 1990
- Diploma in Electrical Engineering,
  National Technical University of Athens, Athens, Greece, 1989.
- *Certificat Pratique de Langue Française (premier degré)*,
  Université de Paris Sorbonne, Paris IV, France, 1983

Major: Electrical Engineering

Presentations and Publications:

Journal Publications

Friedland, B., S.E. Mentzelopoulou, and G.E. Antoniou. 1993. "On a Property of Compensators Designed by the Separation Principle." *IEEE Transactions on Automatic Control*, AC-38(2): 370- 372.

Mentzelopoulou, S.E., G.E. Antoniou, and N.J. Theodorou. 1993. "Design of a Periodic Feedback Control Law for Systems With Higher Dimension." *IEE Proceedings Part-D*, 140(4): 225-230.

Glentis, G.O., S.E. Mentzelopoulou, and G.E. Antoniou. 1993. "Transfer Function Determination of Multidimensional Singular Systems Using the FFT." *International Journal of Systems Science*, 24(1): 211-218.

Mentzelopoulou, S.E., R. Hormis, G.E. Antoniou, and C.N. Manikopoulos. 1993. "On the Factorization of 2-D Polynomials via Neural Networks." *Neural, Parallel and Scientific Computations*, 1: 271-286.

Mentzelopoulou, S.E., G.E. Antoniou, and C.N. Manikopoulos. 1992. "Realization of Separable Nth- Order 2-D All- Pass Digital Filters." *International Journal of Electronics,* 73(6): 1143-1147.

Antoniou, G.E., S.E. Mentzelopoulou, and C.N. Manikopoulos. 1992. "Computation of the Transfer Function of the Fornasini-Marchesini Two Dimensional State Space Models." *Control Theory and Advanced Technology*, 8(1): 153-166.

Mentzelopoulou, S.E., and N.J. Theodorou. 1991. "Nth Dimensional Minimal State Space Realization." *IEEE Transactions on Circuits and Systems*, 38(3): 340-343.

Antoniou, G.E., S.E. Mentzelopoulou, and C.N. Manikopoulos. 1991. "Two Dimensional Systems: A Simple Proof of the Cayley Hamilton Theorem." *International Journal of Systems Science*, 22(1): 225-228.

Antoniou, G.E., S.E. Mentzelopoulou, and G.O. Glentis. 1991. "Transfer Function Determination of two Dimensional Generalized Systems via the DFT." *IEE Proceedings Part D*, 138(4): 327-330.

Manikopoulos, C.N., S.E. Mentzelopoulou, and G.E. Antoniou. 1991. "Minimal Circuit and State Space Realization of Three Terms Separable Denominator 2-D Filters." *International Journal of Electronics*, 71(5): 723-731.

Mentzelopoulou, S.E., and G.E. Antoniou. 1990. "Generalized Two Dimensional Systems: Leverrier Faddeeva Algorithm." *Control Theory and Advanced Technology*, 6(3): 441-449.

Antoniou, G.E., C.N. Manikopoulos, and S.E. Mentzelopoulou. 1990. "Two-Dimensional Modified Cauer Form: Circuit and State Space Realization." *IEE Electronic Letters*, 26(4): 258-259.

Antoniou, G.E., and S.E. Mentzelopoulou. 1990. "An Algorithm for the Transfer Function Determination of General Singular Doubly Indexed Dynamical Systems." *Control Theory and Advanced Technology*, 6(4): 697-703.

Conference Publications

Mentzelopoulou, S.E., and B. Friedland. 1994. "Experimental Evaluation of Friction Estimation and Compensation Techniques." to be presented at the *1994 American Control Conference*, Baltimore, MD.

Mentzelopoulou, S.E., and B. Friedland. 1994. "On Adaptive Estimation of Dynamic Friction in a Multiple Degree-of-Freedom System," submitted to the *33rd IEEE Conference on Decision and Control*, Orlando, FL.

Friedland, B., and S.E. Mentzelopoulou. 1993. "On Estimation of Dynamic Friction." *32nd IEEE Conference on Decision and Control,* San Antonio, TX, 2: 1919-1924.

Friedland, B., S.E. Mentzelopoulou, and Y.J. Park. 1993. "Friction Estimation in Multimass Systems." *1993 American Control Conference,* San Francisco, CA, 2: 1927-1931.

Mentzelopoulou, S.E. 1993. "Friction Estimation in a Two-Link Robot Arm Manipulator." *2nd IEEE Regional Conference on Control Systems*, Newark, NJ, 54-57.

Mentzelopoulou, S.E., B. Friedland, D. Hur, and O. Manzhura. 1993. "Experimental Measurements and Compensation of Friction." *2nd IEEE Regional Conference on Control Systems*, Newark, NJ, 162-165.

Antoniou, G.E., B. Friedland, and S.E. Mentzelopoulou. 1993. "Parameter Estimation in Normal and Diabetic Individuals via Nonlinear Observers." *2nd IEEE Regional Conference on Control Systems*, Newark, NJ, 145-158, 1993.

Mentzelopoulou, S.E., G.E. Antoniou, and B. Friedland. 1993. "Nonlinear Observers: An Application to the Spread of an Epidemic." *19th IEEE Annual Northeast Bioengineering Conference*, Newark, NJ, 78-79.

Friedland, B., and S.E. Mentzelopoulou. 1992. "On Adaptive Friction Compensation Without Velocity Measurement." *1st IEEE Conf. on Control and Applications*, Dayton, OH, 2: 1076-1081.

This dissertation is dedicated to
my grandmother, Olga,
who I loved so much and lost so suddenly on May 12th, 1994

ACKNOWLEDGMENT

I would like to express my appreciation and sincere gratitude to my research advisor Dr. Bernard Friedland for his patient guidance, counsel and support during the course of this research.

I also gratefully acknowledge the encouragement afforded by the Department of Electrical and Computer Engineering, New Jersey Institute of Technology. Thanks are also due to other members of my thesis committee, Drs. Timothy Chang, Denis Blackmore, Avraham Harnoy, Farshad Khorrami and Brian Armstrong-Hélouvry for taking time to review this work and for their valuable comments and suggestions.

Also my gratitude is extended to the members of the Control System Laboratory at New Jersey Institute of Technology. I am particularly grateful to Mr. David Hur and Ms. Oksana Manzhura for their help in setting up the experimental apparatus. I also wish to express my gratitude to my friends and members of the Hellenic Student Association who have given me encouragement during this doctoral program.

Thanks are also due to the National Science Foundation who supported this research, under Grant MSS9215636.

Most of all thanks are extended to my family for their love, support, patience and inspiration provided me at moments of frustration and despair. Particularly, I thank my husband for his help, encouragement, support and patience all those years. I gratefully thank also my grandma for the beautiful drawings and for the love and inspiration. My thanks are also extended to my mother for her love, encouragement and support. Finally, I ask the forgiveness of them who passed away, for not being with them their last moments.

TABLE OF CONTENTS

LIST OF FIGURES

NOMENCLATURE

a	friction coefficient (scalar or vector)
$a(v)$	"extended" Coulomb friction coefficient
$a_1,\ a_2\ a_3,\ a_4$	parameters of $a(v)$
$\hat{a}$	the estimate of a
$\mathcal{A}$	diagonal matrix which contains the friction coefficients
B	the control matrix
e_v	error between the actual and estimated velocity
e_a	error between the actual and estimated friction coefficient
e_F	error between the actual and estimated friction
e_f	error between the actual and estimated normalized friction f
E	the kinetic energy
f	the normalized friction force
$\hat{f}$	the estimate of f
F	friction force
$\hat{F}$	the estimate of F
$g_1,\ g_2$	feedback gains
$g(x, v, w)$	the total nonfrictional system forces
k_v, K_v	gain of the velocity observer
k_ω	gain of the angular velocity observer
k_F, K_F	gain of the CFO and GCFO observers, respectively
$k_1,\ k_2$	gains of TO observer
$K_1,\ K_2$	gains of GTO observer
$k_a,\ k_{f1},\ k_{f2}$	gains of DFO observer
$k_d,\ k_{d1},\ k_{d2}$	gains of DFOb observer
$K_a,\ K_{f1},\ K_{f2}$	gains of GDFO observer
m	mass
$M(x)$	mass matrix
t	time
T, T_q	transformation matrices
u	the non-frictional input (acceleration) to the ideal system
$\bar{u}$	input to compensate for friction
U	the friction distribution matrix
v	velocity of the mass
$\hat{v}$	the estimate of v
w	the total non-frictional input to the actual system
$\mathtt{w}$	non-frictional feedback to the motor
x	position of the mass
z	state of TO and GTO observer
z_F	state of CFO and GCFO observer
$z_a,\ z_f$	states of DFO and GDFO observers

θ	angular position
θ_r	reference angular position
$\phi(\cdot)$	even function
$\mathbf{\Psi}$	Jacobian matrix
$\|\|\mathbf{\Psi}\|\|$	the norm of the Jacobian matrix
ω	angular velocity
$\hat{\omega}$	the estimated angular velocity

PREFACE

Friction is a paradox. Most mechanical systems need friction to operate. It is undesirable, however, in control systems since its presence limits the system static accuracy and causes limit cycles (the "slip–stick" phenomenon) at low velocities. It still remains as a phenomenon not very well defined and explained.

To reduce friction in a control system, passive techniques (such as improved lubrication, air bearings, magnetic bearings) are commonplace. These techniques, however, are not always adequate, and sometimes active friction cancellation techniques are used. The simplest of these is dither: noise inserted at the point of control. This technique is very simple, but it cannot always be used in high precision operation since it may result in unacceptable vibrations. More recently control engineers have sought to ameliorate the effects of friction by using more sophisticated measures to counteract its effects such as high gain PD control, model based feedback, joint torque control, model reference adaptive control or adaptive pulse width control.

In this dissertation, three methods for estimating and compensating friction are presented. Two of them are model–based while the third considers friction as an unknown bias system parameter. A comparative study of the methods is conducted by simulations and experimentally.

The thesis is organized as follows: Chapter 1 contains a brief historic and scientific introduction concerning research in the area of friction. Chapters 2, 3 and 4 deal with the estimation of Coulomb and "extended" Coulomb friction for the cases of one degree–of–freedom systems with measurable "position" and "velocity", one degree–of–freedom systems with unmeasurable "velocity" and multiple degree–of–freedom systems, respectively. In Chapter 5 the problem of friction cancellation is addressed in a multiple degree–of–freedom system with multiple friction forces and controls. Chapters 6 and 7 deal with the estimation of "dynamic" friction in a single

and multiple degree-of-freedom system, respectively. Chapter 8, presents experimental results. The algorithms proposed in the previous chapters are implemented on an experimental apparatus and experimental data are collected, analyzed and interpreted. Finally, in Chapter 9, the work presented in this thesis is summarized and suggestions for future research are presented.

CHAPTER 1

FRICTION: AN EVERYDAY PHYSICAL PHENOMENON

Friction is an important phenomenon that appears in most everyday operations in many of which it is necessary. In control applications, however, friction is often undesirable because it effects precision and accuracy in system performance as well as system stability.

Owing to its importance, many researchers have been involved with friction, trying to explain and describe the friction phenomenon and to give some solutions to the problem of friction compensation. According to Armstrong–Hélouvry (1991), who published a monograph with an extensive friction historical background, the first researcher, who studied the friction phenomenon was Leonardo Da Vinci in 1452. Leonardo described friction as a force independent of the contact area, opposite to the motion and proportional to the perpendicular to the surface force. His work, after being hidden for years, was rediscovered by Amontons in 1699 and later developed by Coulomb (1785) (Figure 1.1a). They all described the friction in a system with nonzero velocity. This friction was called kinetic friction. In 1833 Morin introduced static friction which corresponds to velocities very close to zero or zero. A few years later, in 1866, Reynolds described viscous friction which appears in contact with liquids. The combination of those three different friction forces, static, kinetic and viscous, constitutes the basic zero–memory friction model which is extensively used by researchers until the present (Figure 1.1b). Finally, in 1902, a better explanation for the transition period between static and kinetic friction at low velocities was given by Stribeck. (Figure 1.1c)

The systematic study of friction became the science of tribology during the first half of the 20th century. One goal of the new science was to explain the friction phenomenon by better understanding the surface topography. Another goal was the

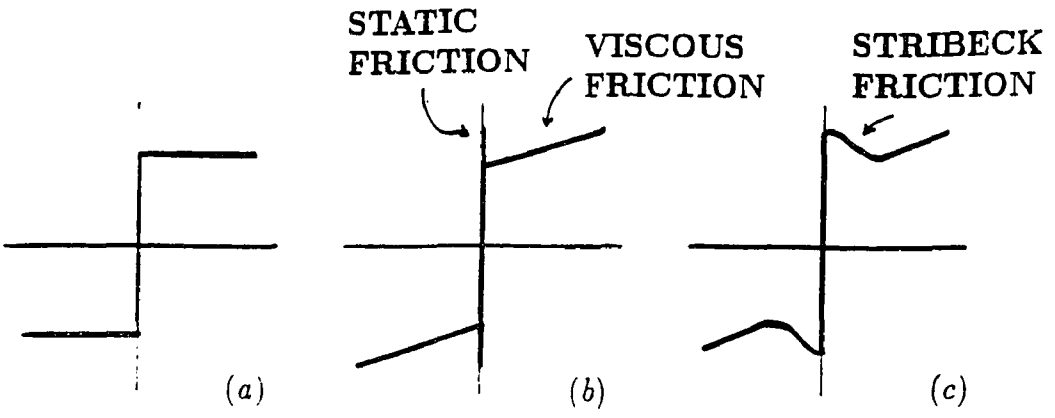

Figure 1.1 Classical friction models (friction versus velocity) (a) Coulomb kinetic friction model, (b) Static plus viscous friction model and (c) Static plus viscous plus Stribeck friction model.

development of better lubricants which can be very effective in the reduction of the friction between two surfaces.

After the World War II, a more theoretical approach to the phenomenon of friction in control systems started to appear. For the analysis, theoretical tools like describing function theory, mathematical modeling and state space techniques have been developed and used. In addition, numerous experiments have been conducted in order to observe and describe the friction phenomenon.

1.1 Mathematical Models of Friction

Several mathematical models have been proposed to describe the effects of friction in different applications. These models can be classified into two different categories:

- "zero memory" models
- "dynamic" models

1.1.1 Zero Memory Friction Models

The first proposed zero memory friction model is the Coulomb model described as

$$F = a\text{sgn}(v)$$

where F is the friction, a is the friction magnitude, and v is the velocity. The friction magnitude a is generally proportional to the normal force F_n:

$$a = cF_n$$

where c is the "coefficient of friction", a dimensionless parameter. The normal force F_n may be time varying, depending upon what is happening elsewhere in the system. This investigation regards the product $a = cF_n$ as an undetermined parameter to be estimated.

Tustin (1947) proposed a model that considers friction to be a decaying exponential function of the relative velocity,

$$F = [F_k + (F_s - F_k)e^{-v/v_c}]\text{sgn}(v)$$

where F_s, F_k and F is static, kinetic and total friction, respectively, while v and v_c is the velocity and the characteristic velocity at which starts the kinetic friction, respectively. This model helps to describe the macroscopic limit cycle behavior that takes place in servo-mechanisms with a negative viscous friction force.

Bo and Pavulescu (1982) presented an exponential model of the form:

$$F = [F_k + (F_s - F_k)e^{-(\frac{v}{\alpha})^n}]\text{sgn}(v)$$

In the above equation α and n are adjustable empirical parameters. More precisely, n has been found to range from 0.5 to 1.0. Fuller (1984) suggested n to be very large if there is effective lubrication.

Armstrong-Hélouvry (1991) explored the friction behavior of a brush type d-c servo motor driven mechanism with gearing. For his analysis he employed Tustin's

model and specified the parameters of the model to fit the experimental data. Specifically, he found $F_s = 9.56$, $F_s - F_k = 1.13$ and $v_c = 0.019$. Furthermore, he examined different empirical models in order to describe Stribeck friction. More precisely, he used Tustin's model $(F_s - F_k)e^{-v/v_s}$, a Gaussian model $(F_s - F_k)e^{-(v/v_s)^2}$, a Gaussian model with offset $(F_s - F_k)e^{-((v-v_0)/v_s)^2}$, a Lorentzian model, proposed by Hess and Soom, $(F_s - F_k)\frac{1}{1+(\frac{v}{v_s})^2}$ and a polynomial model. He concluded that the models to consider are the "two-break" Gaussian model, the Lorentzian model and the Gaussian with offset. In addition, for compliant motion, he applied the Bo and Pavulescu model with $n = 2$ and α to be 0.0053 or 0.035.

Canudas de Wit et al. (1991) addressed the problem of modeling and compensation of friction at velocities close to zero. A new model, linear in parameters, with zero memory, which captures the downward bends at low velocity was used to adaptively compensate for friction. This model, in combination with an adaptive computed torque method, was tested experimentally in a robot manipulator.

Gogoussis and Donath (1987, 1990, 1993), proposed a model which describes Coulomb friction in the bearings and transmissions of robot manipulators. In addition, they studied friction and its effects for the forward dynamics problem for robots.

1.1.2 Dynamic Friction Models

Dynamic friction includes hysteresis effect at zero velocity (Figure 1.2). The dynamic friction models can be divided to those having a state space form and to those without a state space description.

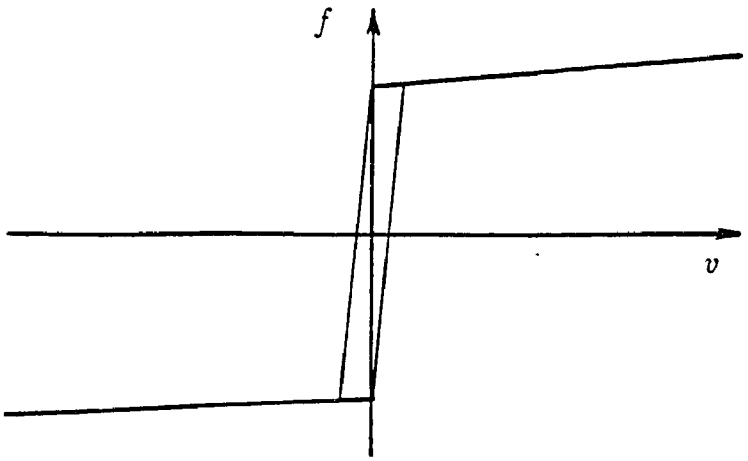

Figure 1.2 Dynamic friction model has hysteresis effect at zero velocity.

1.1.2.1 Dynamic Friction Models Not in State Space Form

Derjaguin et al. (Armstrong–Hélouvry, 1991) studied the transient behavior of the static friction, and proposed the following model

$$F_s(t) = F_k + (F_{s\infty} - F_k)\frac{t}{t+\gamma}$$

where $F_{s\infty}$ is the steady state static friction, F_k is the kinetic friction and γ is the characteristic rise time of static friction.

Kato et al. (1972, 1974) proposed a different model to describe the transient behavior of static friction

$$F_s(t) = F_k + (F_{s\infty} - F_k)(1 - e^{-\gamma t^n})$$

The parameters γ and n depend on the application, the nature of the materials in contact, and the existence of a lubricant. For conformable contacts, Kato found γ to range from 0.04 to 0.64 and n from 0.36 to 0.67.

Karnopp (1985) provided a method for modeling dynamic systems that contain slip–stick friction, which results in a set of differential equations.

Hess and Soom (1990) employed a model of the form

$$F = [F_k + F_v|v| + (F_s - F_k)\frac{1}{1 + (\frac{v(t-\tau_L)}{v_s})^2}]\text{sgn}(v)$$

where the last term of the above equation corresponds to the Stribeck friction. Furthermore they described the frictional lag with respect to velocity that occurs when velocity changes sign, with a pure time delay τ_L which is increasing as the lubricant viscosity and the perpendicular to the surfaces force increase. Evidence of the existence of that lag had been reported earlier by Sampson et al. (1943), Rabinowicz (1958), Bell and Burdekin (1966, 1969), Rice and Ruina (1983) and Walrath (1984) through experimental data.

Haessig and Friedland (1991) presented a model called the "bristle model" which is an approximation designed to capture the true nature of sticking.

Armstrong–Hélouvry (1993) applied dimensional and perturbation analysis to the problem of slip stick encountered during the motion of machines. The friction model studied ("seven–parameter" model) is the one of Hess and Soom, motivated by current tribological results and incorporates Coulomb, viscous and Stribeck friction with frictional lag and rising static friction. In addition, he examined Kato's model for a nonconformable contact and found $\gamma = 1.66$ and $n = 0.65$ (Armstrong–Hélouvry, 1991).

Polycarpou and Soom (1992) reported experimental data which verifies the seven–parameter model of Armstrong–Hélouvry.

1.1.2.2 Dynamic Friction Models in State Space Form

The dynamic friction models proposed in the literature have the following generic form

$$\begin{aligned} F &= \gamma(f, v) \\ \dot{f} &= \xi(f, v) \end{aligned}$$

where f is the normalized friction force, and $\gamma(f, v)$ and $\xi(f, v)$ are functions that characterize the specific friction model.

Dahl (1976) studied the friction in small rotations of ball bearings with a spring force and proposed the following friction model

$$\dot{f} = cv|1 - f\,\mathrm{sgn}(v)|^i \mathrm{sgn}[1 - f\,\mathrm{sgn}(v)] \tag{1.1}$$

$$F = af \tag{1.2}$$

where i determines the slop of the friction curve, c is a constant that determines the width of the hysteresis and a is a constant that specifies the magnitude of the force.

Ruina (1980) presented a dynamic model to describe the friction present at the relative motion of the earth's crystal plates. His model has the form:

$$\dot{f} = -\frac{v}{L}[f + b\ln\frac{v}{v_o}]$$

$$F = F_o + a\ln\frac{v}{v_o} + f$$

where L is the characteristic length controlling the evolution of f.

Walrath (1984) presented an experimental friction model to describe the bearing friction behavior,

$$\tau\dot{F} = -F + T\,\mathrm{sgn}(v)$$

where T is the constant rolling friction torque, v is the relative gimball velocity and τ is an adjustable model parameter. Furthermore, based on this model, he designed a digital adaptive controller for an airborne optical pointing and tracking telescope.

Haessig and Friedland (1991) proposed the "reset integrator model," which is numerically more efficient than their bristle model and exhibits behavior similar to the model proposed by Karnopp (1985). Specifically, the "reset integrator" friction model is described as follows

$$\dot{f} = c[v - \phi^{-1}(v)]$$

$$F = af$$

where c is a constant that determines the width of the hysteresis and $\phi^{-1}(f)$ is the inverse function of $\phi(\cdot)$. Function $\phi(\cdot)$ is an odd function that varies between ± 1.

Linker and Dieterich (1992) performed tests involving step changes and pulses in normal load, during constant velocity sliding, and they proposed a model similar to the one that was proposed by Ruina.

Canudas de Wit et al. (1993) proposed a new dynamic model for friction that captures most of the friction behavior:

$$\begin{aligned} \dot{f} &= v - \frac{|v|}{g(v)} f \\ F &= \sigma_0 f + \sigma_1 \dot{f} + \sigma_2 v \end{aligned}$$

where $g(\cdot)$ is a function that depends on many factors such as material properties, lubrication, temperature, and σ_0, σ_1 and σ_2 are the stiffness, damping and viscous friction parameters, respectively.

Harnoy and Friedland (1993) developed a model to describe dynamic friction on lubricated surfaces. The model is developed for a short journal bearing, but can be extended to other geometries of sliding surfaces. Furthermore, in Harnoy et al. (1994), an improved dynamic model is proposed for the resistance forces to the rotation of a journal, in a lubricated sleeve bearing at low speed.

1.2 Friction Compensation

Many researchers have been involved, through the years, with the problem of friction compensation in specific applications, using several empirical methods as well as classical control feedback design techniques. One of the earliest techniques to eliminate the effects of friction is dither (injection of noise at the control input) which is simple and effective. It may, however, cause random oscillations in the system due to the effects of the noise. Hence it cannot be used in high precision operations. Other methods proposed in the literature can be classified into two different categories as follows:

- Friction compensation without explicitly estimating the magnitude of the friction
- Friction cancellation by estimating the friction

1.2.1 Friction Compensation Without Estimating Friction

Tou and Schulthesis (1953) extend the describing function analysis technique to cover problems of static and sliding friction in feedback systems. In particular it has been shown that the use of integral equalization in series with the loop may easily lead to instability. Essentially equivalent minor loop equalizers, however, may yield an entirely satisfactory system.

Shen et al. (1962, 1964) found that a system which is subjected to dry friction can be stabilized by using nonlinear passive compensation. Specifically, for small ramp inputs it is necessary to increase the damping by a derivative control which becomes saturated for high ramp rates. To decrease the steady–state error at high ramp rates and achieve stability a dead zone before the integrator is used. Additionally they proposed an input adaptive system to adjust the magnitude of the saturation and of the dead zone.

Friedland et al. (1976) designed a servo for a gyro test table. In the design, friction was represented as an independent random walk and the feedback law was calculated based on the theory of linear optimal control.

Kubo et al. (1986) proposed a controller with a fixed kinetic friction feedback, to avoid over–compensation of friction in empirically tuned controllers, since he observed that friction does not always destabilize the system.

Townsend and Salisbury (1987) used describing function analysis to study the friction in a control system and proposed integral control to compensate it. In addition they study the stability of the system response to various inputs.

Southward et al. (1991) proposed a nonlinear compensation force, for slip–stick friction, to supplement a PD control law applied to one degree–of–freedom mechanical systems.

Armstrong–Hélouvry (1991) used a dither signal that is slightly greater in magnitude than the magnitude of static friction and a reduction of number in the rms contact force error was observed. Also he demonstrated a technique involving closed loop constant velocity glides and measuring average torque.

Wu and Paul (1980), Luh et al. (1983), Mukerjee and Ballard (1985), Pfeffer et al. (1989) proposed a technique, called "joint torque control," which is based on the output torque sensing and control, to compensate kinetic friction.

Dupont (1993, 1993a, 1994) used a PD controller for friction compensation and proposed stability conditions to avoid the "stick–slip" phenomenon.

1.2.2 Friction Cancellation by Estimation

Gilbart and Winston (1974) presented a model reference adaptive control system built of analog components, used to control the pointing of a tracking telescope.

Craig (1987) identified adaptively kinetic and viscous friction parameters. Cheok et al. (Armstrong–Hélouvry, 1991) used an optimization procedure to identify the slip–stick friction parameters.

Canudas de Wit et al. (1987, 1991) proposed an adaptive algorithm to compensate the effects of friction on line. Canudas de Wit, and Seront (1990) designed a feedback law to robustify the closed loop system properties, under a possible inexact friction compensation, which may provoke limit–cycles.

Yang and Tomizuka (1988) presented an adaptive pulse width control scheme to provide precise positioning of a control object under the influence of static, Coulomb friction and backlash. In addition Tung et al. (1991, 1993) proposed and used repetitive control for improving low velocity tracking performance.

Brandenburg et al. (1988, 1991) and Schäfer et al. (1991, 1993) studied the stability of an elastic two–mass system with Coulomb friction and backlash, and proposed the conditions to ensure optimal operation down to the lowest speeds and standstill. They also, applied a model reference adaptive control structure to adapt the parameters of Coulomb friction.

Friedland and Park (1991) presented an adaptive algorithm to compensate Coulomb friction, which entails the use of an observer designed based on the Coulomb friction model.

Maqueira et al. (1993) presented a practical adaptive friction compensation technique for line–of–sight pointing and stabilization. The Coulomb friction level and a spatial time constant are estimated and used to update a simple friction reference model which generates commands to cancel friction disturbances using relative rate feedforward.

Baril (1993) proposed a robust nonlinear friction compensator to complement a linear controller that considers friction as an uncertain disturbance.

1.3 Contribution of the Research Presented in This Thesis

New results in the area of friction estimation and cancellation are presented in this research. Specifically

- The Coulomb friction observer, introduced by Friedland and Park (1991), is extended to the case of unmeasurable velocity by introducing a velocity observer coupled to the friction observer. The development of the theory includes a methodology for determining the observer parameters to ensure convergence (where possible) or boundedness of the estimation error when Coulomb friction as well "extended" Coulomb friction (static plus viscous plus Stribeck friction) is estimated.

- The Coulomb friction observer with and without the additional velocity observer is extended to systems with multiple degrees-of-freedom and friction sources. To this end, a general model for the friction vector force is introduced. In addition, for the multiple mass system case a feedback control law is designed to cancel the friction totally or partially, depending on the system topology.

- For estimating dynamic friction, a "Dynamic Friction Observer" is introduced which is designed based on a dynamic friction model.

- Based on the theory of observers the "Tracking Observer" is proposed which assumes friction an unknown system input.

To demonstrate the effectiveness of the methods developed in this thesis various applications including linear and nonlinear dynamics are illustrated. A comparative study of the proposed algorithms is conducted through simulations as well as experimentally. In the simulations, the algorithms are tested in systems with linear and nonlinear dynamics. In the experiments a particular experimental apparatus, built for this purpose, was used to demonstrate the ability of the proposed methods to estimate and cancel the friction in a real hardware application.

CHAPTER 2

ADAPTIVE COMPENSATION OF "EXTENDED" COULOMB FRICTION IN A SINGLE DEGREE–OF–FREEDOM SYSTEM

2.1 Introduction

The problem considered in this chapter is the estimation and cancellation of Coulomb plus viscous plus Stribeck friction —which we call "extended" Coulomb friction— that may be present in a control system with one degree–of–freedom, using the theory of reduced order observers.

Two different observers are proposed and compared in estimating the friction force. The first observer (CFO), proposed by Friedland et al. (1991), is designed based on the Coulomb friction model; the second (TO) is a "tracking" observer which considers friction as an unknown constant system input, the estimation of which generally leads to integral control action (Friedland, 1986).

Global stability is shown when the acceleration of the system is finite. The observers estimates converge to the true value of friction for a particular range of the observer gains.

Finally, favorable simulation results verify the good performance of the designed friction compensators.

2.2 Statement of the Problem

An "ideal" (i.e., frictionless) mechanical system with a single degree–of–freedom, has the following dynamic description

$$\begin{aligned} \dot{x} &= v \\ \dot{v} &= u \end{aligned} \tag{2.1}$$

where x, v and u are the position, the velocity and the input (acceleration) due to all forces to the system, respectively.

Furthermore, for the above system (2.1) the input u is assumed to be of the form:

$$u = -g_1(x - x_r) - g_2 v \tag{2.2}$$

where x_r is a reference position and the coefficients g_1 and g_2 may be selected to satisfy desired performance specifications (Friedland, 1986).

Next, let us consider the same system as (2.1) with the addition of the friction phenomenon effects. This new system can be called "actual" and is described as follows:

$$\begin{aligned} \dot{x} &= v \\ \dot{v} &= w - F(a, v) \end{aligned} \tag{2.3}$$

where $F(a, v)$ is the friction force and w is the system non-frictional input. The friction force includes static plus viscous plus Stribeck friction and is described by the "extended" Coulomb model

$$F(a, v) = a(v)\ \mathrm{sgn}(v) \tag{2.4}$$

where $a(v)$ is the friction parameter and is an even function of velocity. Specifically, according to Armstrong-Hélouvry, (1991) and Canudas de Wit, (1990, 1991), the friction coefficient $a(v)$ can be represented in general by the following form

$$a(v) = a_1 + a_2 e^{-a_3|v|} + a_4|v| \tag{2.5}$$

where a_1 is the coefficient corresponding to the static friction, a_4 corresponds to the viscous friction and a_2 and a_3 to the Stribeck friction. All the coefficients are considered for the analysis positive and constant.

The problem considered in this chapter is the estimation and cancellation of the friction in system (2.3) such that the latter becomes equivalent to the ideal system (2.1).

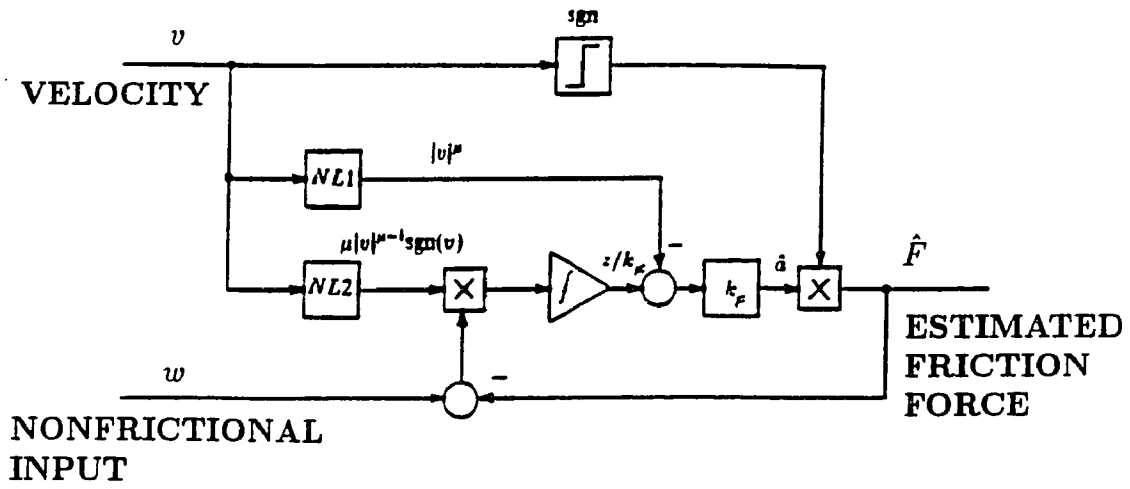

Figure 2.1 Block diagram of the Coulomb friction observer (CFO)

2.3 Estimation and Cancellation of Friction

Defining $\hat{a}$ and $\hat{F}$ to represent the estimates of a and F respectively, the following observers are proposed to estimate the friction force in the system.

2.3.1 Coulomb Friction Observer (CFO)

The observer has the following structure:

$$\hat{a} = z_F - k_F|v|^{\mu} \tag{2.6}$$

$$\hat{F} = \hat{a}\ \mathrm{sgn}\ (v) \tag{2.7}$$

where the variable z_F is given as

$$\dot{z}_F = k_F\ \mu|v|^{\mu-1}(w - \hat{F})\ \mathrm{sgn}(v) \tag{2.8}$$

and k_F and μ are parameters to be chosen by the designer to ensure convergence of the error to zero. (The conditions under which these parameters can be so chosen are discussed in the next section.)

A block diagram representation of this observer is shown in Figure 2.1

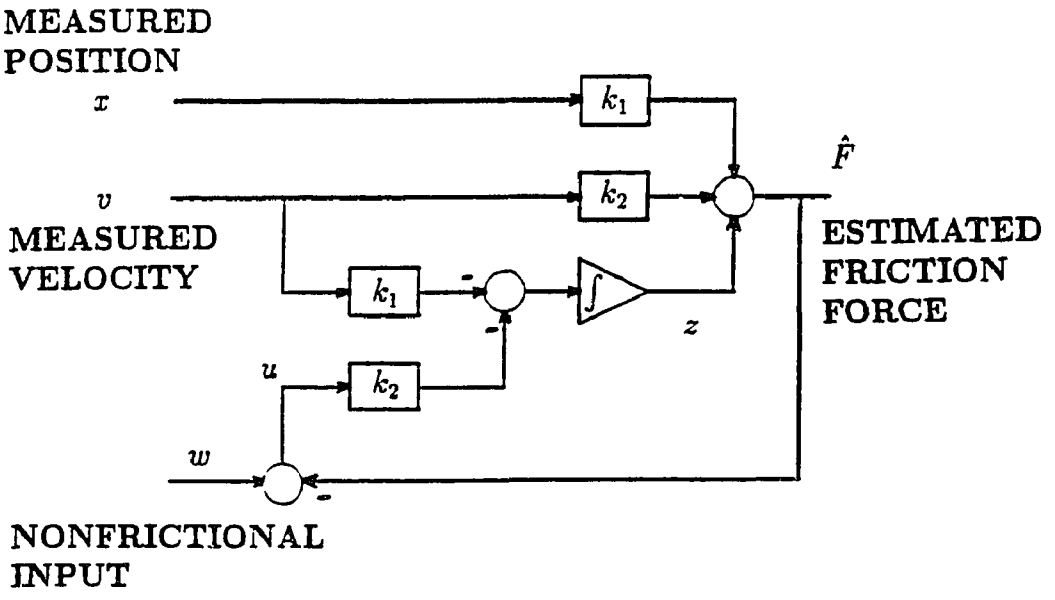

Figure 2.2 Block diagram of the tracking observer (TO)

2.3.2 Tracking Observer (TO)

This observer is based on the tracking of the total friction force $F(a, v)$. Its dynamics are given by

$$\hat{F} = z + k_1 x + k_2 v \tag{2.9}$$

$$\dot{z} = -k_1 v - k_2(w - \hat{F}) \tag{2.10}$$

where z is the observer state and k_1, k_2 are the observer gains to be chosen by the designer to ensure convergence of the error to zero.

A block diagram representation of this observer is shown in Figure 2.2

2.3.3 Cancellation of Friction

To cancel the friction in system (2.3), the input w has to be in the form

$$w = u + \hat{F} \tag{2.11}$$

where u is the control that would be used in the absence of friction. It can be easily shown that friction cancellation becomes more effective as $\hat{F}$ approaches $F(a, v)$.

2.4 Error Analysis and Selection of Observer Gains

To evaluate the performance of the observers and to establish conditions for the gains k_F, k_1 and k_2, the error under the real and the estimated parameters has to be considered.

2.4.1 Coulomb Friction Observer (CFO)

Define the error e_a between the actual a and the estimated friction parameter $\hat{a}$ to be

$$e_a = a - \hat{a} \tag{2.12}$$

Differentiating both sides of the above equation (2.12) and using (2.3), (2.4), (2.6), (2.8), (2.7) and (2.11), yields

$$\begin{aligned}
\dot{e}_a &= \dot{a} - \dot{\hat{a}} \\
&= \frac{\partial a}{\partial v}\dot{v} - \dot{z}_F + k_F\,\mu \mid v \mid^{\mu-1}\ \dot{v}\,\mathrm{sgn}(v) \\
&= \frac{\partial a}{\partial v}\dot{v} - k_F\,\mu \mid v \mid^{\mu-1}\ [w - \hat{F} - \dot{v}]\,\mathrm{sgn}(v) \\
&= \frac{\partial a}{\partial v}\dot{v} - k_F\,\mu \mid v \mid^{\mu-1}\ [w - \hat{F} - w + F(a,v)]\,\mathrm{sgn}(v) \\
&= -k_F\,\mu \mid v \mid^{\mu-1}\ e_a + \frac{\partial a}{\partial v}\dot{v}
\end{aligned} \tag{2.13}$$

The above differential equation describes the rate of change of the error e_a. The following conditions are sufficient for exponential stability of the estimation error:

1. $k_F > 0$
2. $\mu > 0$
3. $\frac{\partial a}{\partial v}\dot{v}$ is bounded.

assuming that v is bounded away from zero.

Notice that for a constant friction coefficient, the third condition does not apply, and the results are the same as presented in Friedland et al. (1991).

Next it will be shown that Condition 3 is always valid if the acceleration of the system is bounded. To this end, the following lemma will be used.

Lemma 2.1 *If a is described by (2.5), then the partial derivative of a with respect to v is bounded.*

Proof

Differentiating equation (2.5), yields

$$\frac{\partial a}{\partial v} = (-a_2 a_3 e^{-a_3|v|} + a_4)\mathrm{sgn}(v) \tag{2.14}$$

By careful examination of the right hand side of equation (2.14), it can be concluded that

$$-a_2 a_3 \leq -a_2 a_3 e^{-a_3|v|} < 0$$

and

$$a_4 - a_2 a_3 \leq (-a_2 a_3 e^{-a_3|v|} + a_4) < a_4 \tag{2.15}$$

Next, comparing equations (2.14) and (2.15) yields

$$|\frac{\partial a}{\partial v}| \leq \max(|a_4 - a_2 a_3|, |a_4|) \tag{2.16}$$

The proof is complete. △

Using the Lemma 2.1, Condition 3 is satisfied if the acceleration $\dot{v}$ of the system is bounded. The boundedness condition is not a serious restriction since in general it is valid. As an example consider the sinusoidal motion of a mass. In this case the velocity is sinusoidal as well as the acceleration, thus the acceleration is bounded and Condition 3 is valid. For the case however of a square wave reference position, the velocity contains delta functions at the changes of the direction of the displacement. In those instants the acceleration becomes infinite and the proposed observer loses track. Nevertheless, the duration of an infinite acceleration is very small comparing to the overall motion of the system which gives the opportunity to the observer to recover.

2.4.2 Tracking Observer (TO)

Define the error e_F as

$$e_F = F(a,v) - \hat{F} \tag{2.17}$$

Differentiating both sides of the above equation (2.17) and using (2.3), (2.4), (2.9), (2.10), and (2.11), yields

$$\begin{aligned} \dot{e}_F &= \dot{F}(a,v) - \dot{\hat{F}} \\ &= -\dot{z} - k_1 v - k_2 \dot{v} + \dot{F}(a,v) \\ &= k_2 e_F + \dot{F}(a,v) \end{aligned} \tag{2.18}$$

In order for the solution of this differential equation to remain in a neighborhood of the origin (the size of which depends on $\dot{F}$), the following conditions must be valid:

1. $k_2 < 0$
2. $\dot{F}(a,v)$ bounded.

Notice that there is no restriction for k_1.

The second condition can be simplified as follows, assuming that $v \neq 0$:
$\frac{\partial a}{\partial v}\dot{v}$ bounded.
This condition is always valid, according to Lemma 2.1, if the acceleration of the system is bounded.

2.5 Simulation Results: One Mass System

For the simulations, we consider the ideal system (2.1), with input u given by (2.2) where the gains g_1 and g_2 are chosen to be $g_1 = 200$ and $g_2 = 20$. The closed loop ideal system, with this input u, has a natural frequency of $10\sqrt{2}$ and a damping factor 0.707. In addition, the actual system, given by (2.3), has the same input u as the ideal system, while the friction is given by

$$F(a,v) = (40 + 20e^{-|v|} + 2|v|)\,\mathrm{sgn}(v)$$

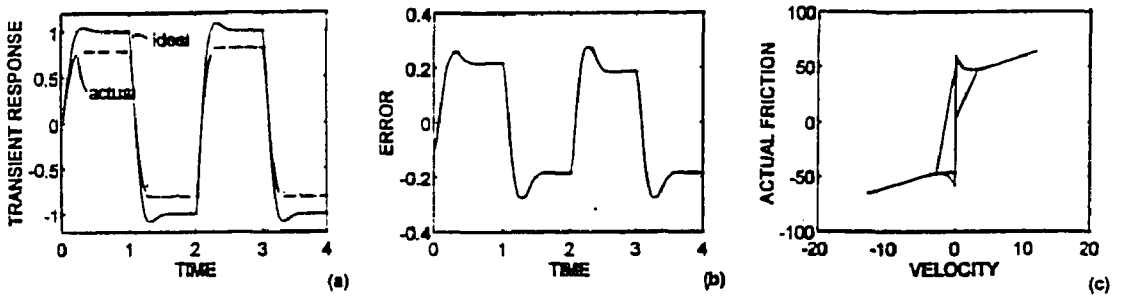

Figure 2.3 (a) Transient response of ideal system and actual without friction cancellation (b) Error between the transient responses of the ideal system and the actual without friction cancellation (c) Actual friction.

The reference position is a square wave with amplitude 1 and frequency of 0.5 Hz. Moreover, white noise with a rms value of 0.1 is assumed present in all measurements. Notice that the chosen level of noise is comparable to the noise of a typical sensor and the quantization noise present in the experiments described in Chapter 8.

Figures 2.3a,b show a comparison of the behavior of the transient response of the ideal system (where friction is not present) and the actual (where friction is present) without including friction cancellation in the feedback. Additionally, Figure 2.3c shows the friction considered present in the actual system.

Figure 2.4 show the transient response of the ideal and the actual system versus time, the error between the ideal system and the actual (with friction compensation) versus time, and the estimated friction versus velocity, respectively, when the CFO observer is used and for different values of the observer gains. As it can be seen from the graphs, the performance of the overall system improves as the gain k_F increases. An increase, however, of the observer gain μ results in a better friction estimate.

The performance of the tracking observer, (TO), is shown in Figure 2.5 As it can be seen from the graphs, the performance of the overall system improves as the gain k_2 increases.

From these results it would appear that observer performance can be improved indefinitely by increasing the gains. But when estimation noise is considered, it is found, as expected, that increasing the gains improves the transient response at the expense of increased steady state rms error.

Comparing the performances of the two observers it can be seen that both are satisfactory. The CFO, however, seems to be able to track more the detailed characteristics of friction than the TO.

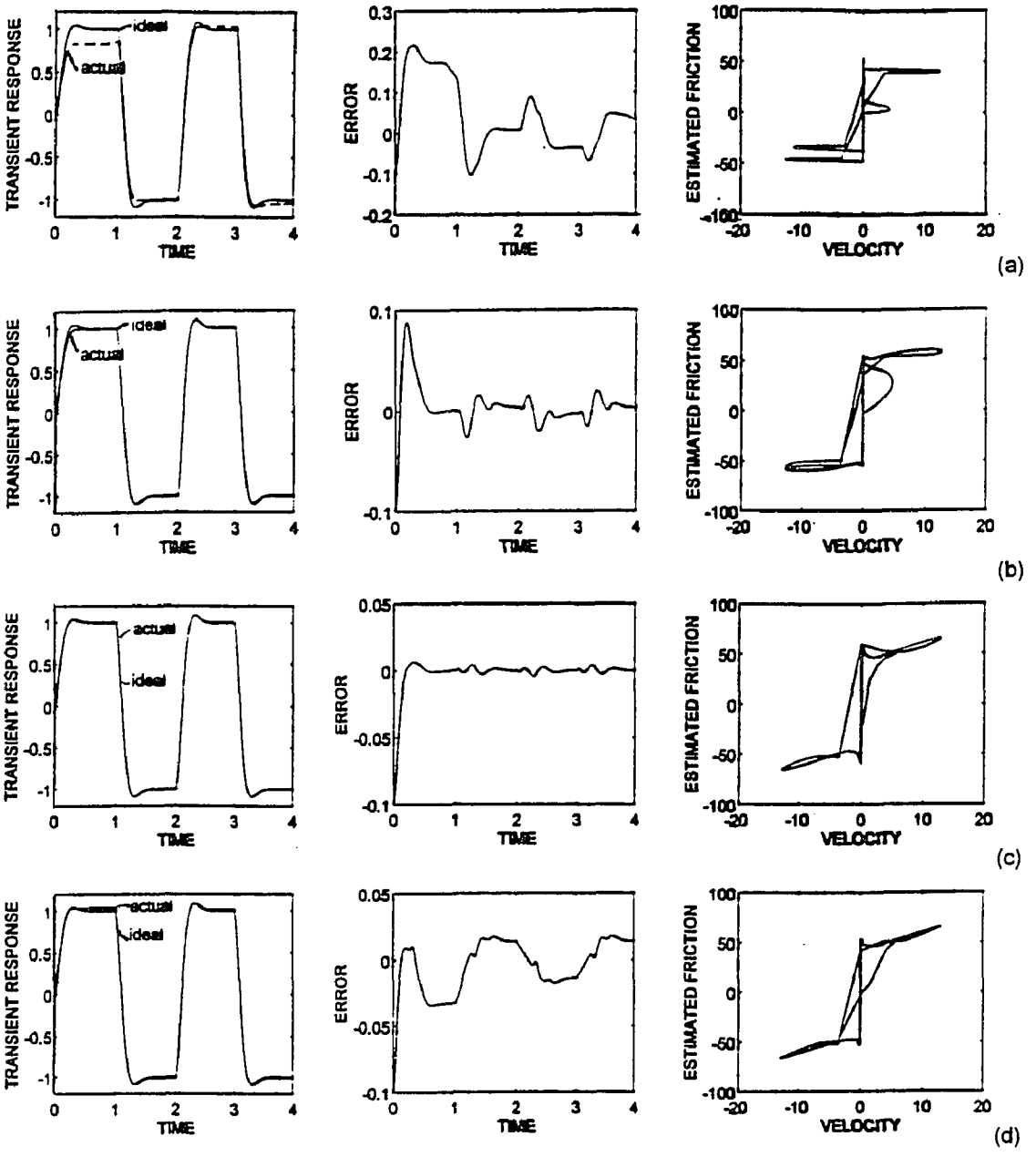

Figure 2.4 Performance of the CFO compensator for (a) $k_F = 1$, $\mu = 1$ (b) $k_F = 10$, $\mu = 1$ (c) $k_F = 100, \mu = 1$ (d) $k_F = 10$, $\mu = 2$

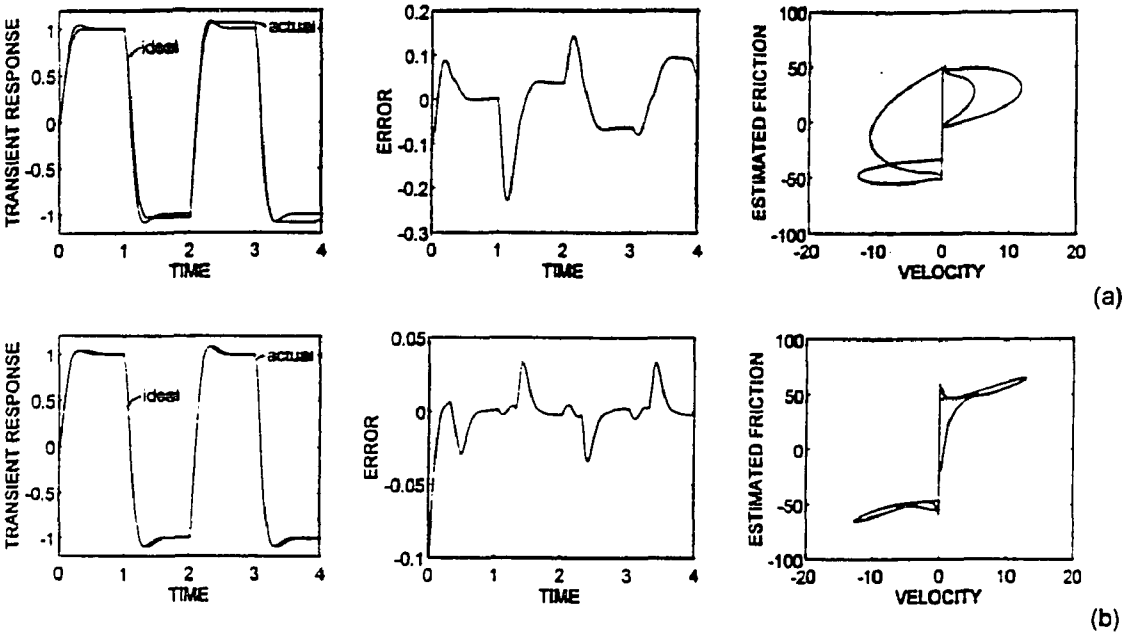

Figure 2.5 Performance of the TO compensator for (a) $k_1 = 0$, $k_2 = -10$ (b) $k_1 = 0$, $k_2 = -100$

CHAPTER 3

ADAPTIVE COMPENSATION OF "EXTENDED" COULOMB FRICTION IN A SINGLE DEGREE–OF–FREEDOM SYSTEM WITHOUT VELOCITY MEASUREMENTS

3.1 Introduction

In numerous applications the velocity measurements required in the friction observers, described in Chapter 2, are not available. Considered in this chapter is the estimation and cancellation of "extended" Coulomb friction (Coulomb plus viscous plus Stribeck friction) that may be present in a single degree–of–freedom system, using the theory of reduced order observers, when velocity cannot be measured. A two stage nonlinear observer is introduced which simultaneously estimates the velocity and the friction force. The observer consists of one of the friction observers proposed in the previous chapter combined in cascade with a velocity observer.

The conditions for asymptotic stability of the overall observer are derived for the case of estimating Coulomb as well as "extended" Coulomb friction. The observer converges to the true value of friction for a particular range of observer gains.

Finally, favorable simulation results verify the good performance of the friction compensator.

3.2 Statement of the Problem

Consider the ideal system

$$\begin{aligned} \dot{x} &= v \\ \dot{v} &= u \end{aligned} \tag{3.1}$$

and

$$u = -g_1(x - x_r) - g_2 v \tag{3.2}$$

where x, v and u are the position, the velocity and the input (acceleration) due to all non–frictional forces to the system. x_r is a reference position and the coefficients g_1 and g_2 may be selected to satisfy desired performance specifications (Friedland, 1986).

Next, let us consider the actual system

$$\begin{aligned} \dot{x} &= v \\ \dot{v} &= w - F(a, v) \end{aligned} \tag{3.3}$$

where $F(a,v)$ is the friction force and w is the system non–frictional input. The friction force is represented by the "extended" Coulomb model

$$F(a,v) = a(v)\ \mathrm{sgn}(v) \tag{3.4}$$

and the friction coefficient $a(v)$ is described as follows:

$$a(v) = a_1 + a_2 e^{-a_3|v|} + a_4|v| \tag{3.5}$$

where a_1 is the coefficient corresponding to the Coulomb friction, a_4 corresponds to the viscous friction and a_2 and a_3 to the Stribeck friction.

To achieve friction cancellation, the input w must be of the form

$$w = u - \hat{F}$$

where $\hat{F}$ is the estimate of the friction.

The problem considered in this chapter is the estimation and cancellation of friction in system (3.3) such that the latter becomes equivalent to the ideal system (3.1), assuming that only the position x is measurable.

3.3 Friction Estimation Without Velocity Measurements

To estimate the friction force (3.4), it is necessary to estimate the velocity. To this end, a velocity observer is added in cascade to the friction observers, presented in

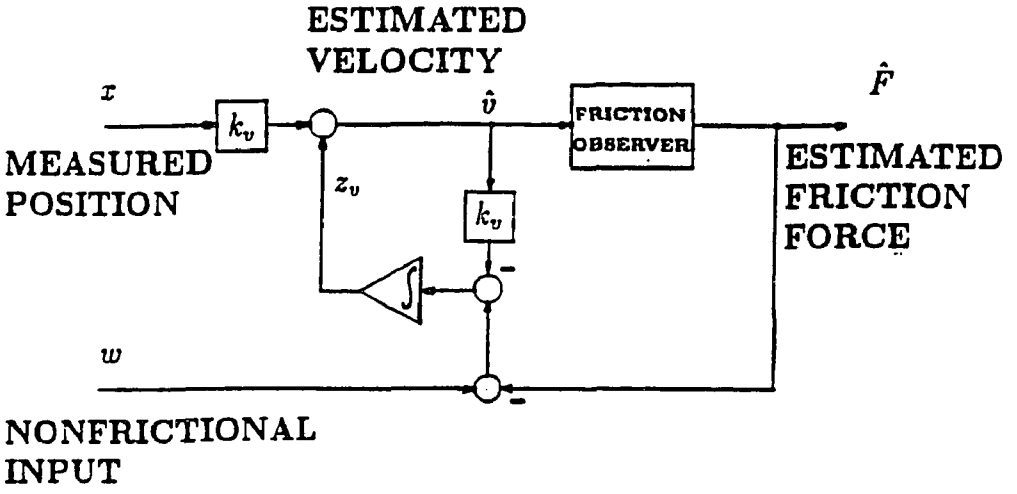

Figure 3.1 Two stage observer for estimating the friction force in the absence of velocity measurements.

the previous chapter. The structure of the resulting nonlinear observer is shown in Figure 3.1. The velocity observer uses the measured position and the estimate of the friction to provide an estimate of the velocity, and the friction observers use the estimate of the velocity to estimate the friction.

3.3.1 Velocity Observer

The dynamics of the velocity observer are defined by:

$$\hat{v} = z_v + k_v x \tag{3.6}$$

where $\hat{v}$ is the estimate of the velocity v, k_v is the corresponding observer gain, and the variable z_v is given as

$$\dot{z}_v = -k_v \hat{v} + u \tag{3.7}$$

When the velocity observer is used, the estimate $\hat{v}$ replaces the true velocity v in the friction observers, as will become apparent next.

3.3.2 Coulomb Friction Observer (CFO)

When the velocity observer is used, the CFO observer takes the form

$$\hat{a} = z_F - k_F|\hat{v}| \tag{3.8}$$

$$\hat{F} = \hat{a}\,\mathrm{sgn}(\hat{v}) \tag{3.9}$$

where the variable z_F is given as

$$\dot{z}_F = k_F\,(w - \hat{F})\,\mathrm{sgn}(\hat{v}) \tag{3.10}$$

and k_F is a parameter to be chosen by the designer to ensure convergence of the error to zero. (The conditions under which k_F can be so chosen are discussed in the next section). Notice that the observer (3.8)–(3.10) is the same as (2.6)–(2.8) when $\mu = 1$.

3.3.3 Tracking Observer (TO)

When the velocity observer is used, the tracking observer takes the form

$$\hat{F} = z + k_1 x + k_2 \hat{v} \tag{3.11}$$

$$\dot{z} = -k_1 \hat{v} - k_2(w - \hat{F}) \tag{3.12}$$

where z is the observer state and k_1, k_2 are the observer gains to be chosen by the designer to ensure convergence of the error to zero.

3.4 Error Analysis and Selection of Observer Gains

To evaluate the performance of the observers and to establish conditions for the gains k_v, k_F, k_1 and k_2, the error under the real and the estimated parameters has to be considered. Define

$$e_v = v - \hat{v} \tag{3.13}$$

$$e_F = F(a,v) - \hat{F} \tag{3.14}$$

Next, the error analysis will be studied for each of the two friction observers.

3.4.1 Coulomb Friction Observer (CFO)

To simplify the analysis, the special case of a constant friction coefficient a (Coulomb friction) will first be considered followed by the more general case where a is a function of the velocity ("extended" Coulomb friction).

3.4.1.1 Coulomb Friction

Differentiating both sides of the equations (3.13) and (3.14) and using (3.3), (3.4), (3.6), (3.7), (3.8), (3.10) and (3.9), yields

$$\begin{aligned} \dot{e}_v &= \dot{v} - \dot{\hat{v}} \\ &= -F(a,v) + w - \dot{z}_v - k_v\dot{x} \\ &= -F(a,v) + \hat{F} + u - u + k_v\hat{v} - k_v v \\ &= -k_v e_v - e_F \end{aligned} \tag{3.15}$$

and

$$\begin{aligned} \dot{e}_F &= \dot{F}(a,v) - \dot{\hat{F}} \\ &= [-\dot{z}_F + k_F\ \dot{\hat{v}}\ \mathrm{sgn}(\hat{v})]\mathrm{sgn}(\hat{v}) \\ &= -k_F\ [w - \hat{F} - \dot{\hat{v}}] \\ &= -k_F\ [u - \dot{z}_v - k_v\dot{x}] \\ &= k_F\ k_v e_v \end{aligned} \tag{3.16}$$

Summarizing, we have

$$\dot{e}_v = q_1(e_v, e_F) = -k_v e_v - e_F \tag{3.17}$$

$$\dot{e}_F = q_2(e_v, e_F) = k_F k_v\ e_v \tag{3.18}$$

It is easily seen that the equilibrium point of the above linear differential equations (3.17) and (3.18), is the origin i.e., $e_{v_0} = e_{F_0} = 0$. The global asymptotic stability for this system of equations is determined by the nature of the Jacobian matrix

$$\Psi = \left[\begin{array}{cc} \frac{\partial q_1}{\partial e_v} & \frac{\partial q_1}{\partial e_F} \\ \frac{\partial q_2}{\partial e_v} & \frac{\partial q_2}{\partial e_F} \end{array} \right]_{e=0} = \left[\begin{array}{cc} -k_v & -1 \\ k_F k_v & 0 \end{array} \right] \tag{3.19}$$

Calculating the characteristic polynomial of Ψ we get

$$| s\mathbf{I} - \Psi | = s^2 + k_v s + k_F k_v$$

If $k_v > 0$, and $k_F > 0$, the eigenvalues of Ψ lie in the open left half plane. and the equilibrium point $e = 0$ is globally asymptotically stable.

3.4.1.2 "Extended" Coulomb Friction

Following the same procedure as for the previous case, yields

$$\dot{e}_v = q_1(e_v, e_F) \tag{3.20}$$

$$\dot{e}_F = q_2(e_v, e_F) + \frac{\partial a}{\partial v}\dot{v} \tag{3.21}$$

where $q_1(e_v, e_F)$ and $q_2(e_v, e_F)$ are given by (3.17) and (3.18) respectively. The above linear differential equations are not homogeneous. The following conditions are sufficient to ensure stability in a neighborhood of the point $e_{v_0} = e_{F_0} = 0$,

1. Real$[eig(\Psi)] < 0.0$
2. $\frac{\partial a}{\partial v}\dot{v}$ is bounded.

where matrix Ψ is given by (3.19).

According to the results of the previous subsection, sufficient conditions for 1 to hold, are:

1a. $k_F > 0$

1b. $k_v > 0$

Finally, using Lemma 2.1, Condition 2 is always valid if the acceleration of the system is finite.

Notice that for a constant friction coefficient, Condition 2 does not apply, yielding to the results presented for the previous case.

3.4.2 Tracking Observer (TO)

As in the previous section, the special case of a constant friction coefficient a will first be considered, followed by the more complicated case where a is a function of the velocity.

3.4.2.1 Coulomb Friction

Differentiating both sides of equations (3.13) and (3.14) and using (3.3), (3.4), (3.6), (3.7), (3.11) and (3.12), yields

$$\begin{aligned} \dot{e}_v &= \dot{v} - \dot{\hat{v}} \\ &= -F(a,v) + w - \dot{z}_v - k_v\dot{x} \\ &= -F(a,v) + \hat{F} + u - u + k_v\hat{v} - k_v v \\ &= -k_v e_v - e_F \end{aligned} \tag{3.22}$$

and

$$\begin{aligned} \dot{e}_F &= \dot{F}(a,v) - \dot{\hat{F}} \\ &= -\dot{z} - k_1 v - k_2\dot{\hat{v}} \\ &= k_1\hat{v} + k_2 u - k_1 v - k_2(\dot{z}_v + k - v\dot{x}) \\ &= -(k_1 + k_2 k_v)e_v \end{aligned} \tag{3.23}$$

The equilibrium point for the above differential equations (3.22) and (3.23), is the origin, as it can easily be shown, i.e., $e_{v_0} = e_{F_0} = 0$. Since the differential equations are linear, the conditions for global asymptotic stability are determined by the nature of the Jacobian matrix Ψ,

$$\Psi = \begin{bmatrix} -k_v & -1 \\ -k_1 - k_2 k_v & 0 \end{bmatrix} \tag{3.24}$$

If $k_v > 0$ and $(k_1 + k_2 k_v) < 0$, the eigenvalues of Ψ lie in the open left half plane and the errors, e_v and e_F, converge globally to zero.

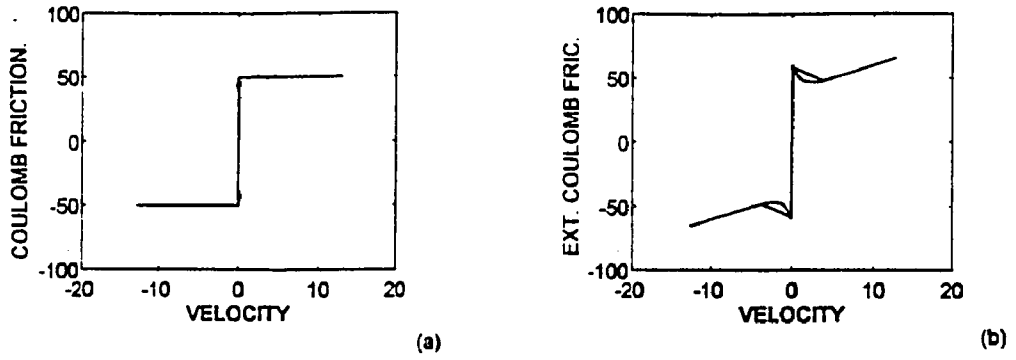

Figure 3.2 (a) Actual Coulomb friction (b) Actual "extended" Coulomb friction.

3.4.2.2 "Extended" Coulomb Friction

Following the same procedure as for the previous subsection, yields

$$\dot{e}_v = -k_v e_v - e_F \tag{3.25}$$

$$\dot{e}_F = -(k_1 + k_2 k_v) e_v + \dot{F} \tag{3.26}$$

The above linear differential equations are not homogeneous. The following conditions are sufficient to ensure stability in a neighborhood of the point $e_{v_0} = e_{F_0} = 0$,

1. Real$[eig(\Psi)] < 0.0$
2. $\dot{F}$ bounded.

where matrix Ψ is given by (3.24).

According to the results of the previous subsection, sufficient conditions for 1 to hold, are:

1a. $k_v > 0$

1b. $k_1 + k_2 k_v < 0$

Finally, using Lemma 2.1, Condition 2 is always valid if the acceleration of the system is finite.

Notice that for a constant friction coefficient, Condition 2 does not apply and the results are the same as presented for the previous case.

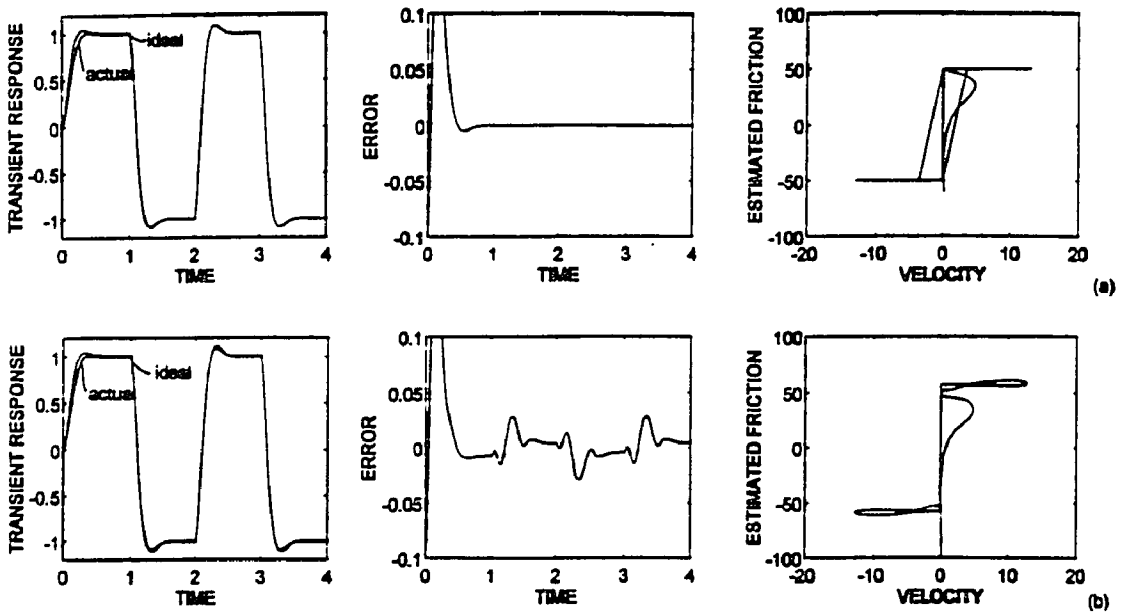

Figure 3.3 Performance of the CFO compensator, with $k_F = 10$, $k_v = 100$, in estimating (a) Coulomb friction (b) "extended" Coulomb friction

3.5 Simulation Results: One Mass System (continued)

For the simulations, we consider the ideal system (3.1), where the input u is given by (3.2) and the gains g_1 and g_2 are chosen to be $g_1 = 200$ and $g_2 = 20$. The closed loop ideal system, with this input u, has a natural frequency of $10\sqrt{2}$ and a damping factor 0.707. In addition, the actual system, given by (3.3), has the same input u as the ideal. At the simulations Coulomb friction is considered as follows

$$F(a, v) = 50 \text{ sgn}(v)$$

while the "extended" Coulomb friction is given by

$$F(a, v) = (40 + 20e^{-|v|} + 2|v|) \text{ sgn}(v)$$

(Figures 3.2a,b). The reference position is a square wave with amplitude 1 and frequency of 0.5 Hz. Moreover, white noise with a rms value of 0.1 is assumed to be present in all measurements.

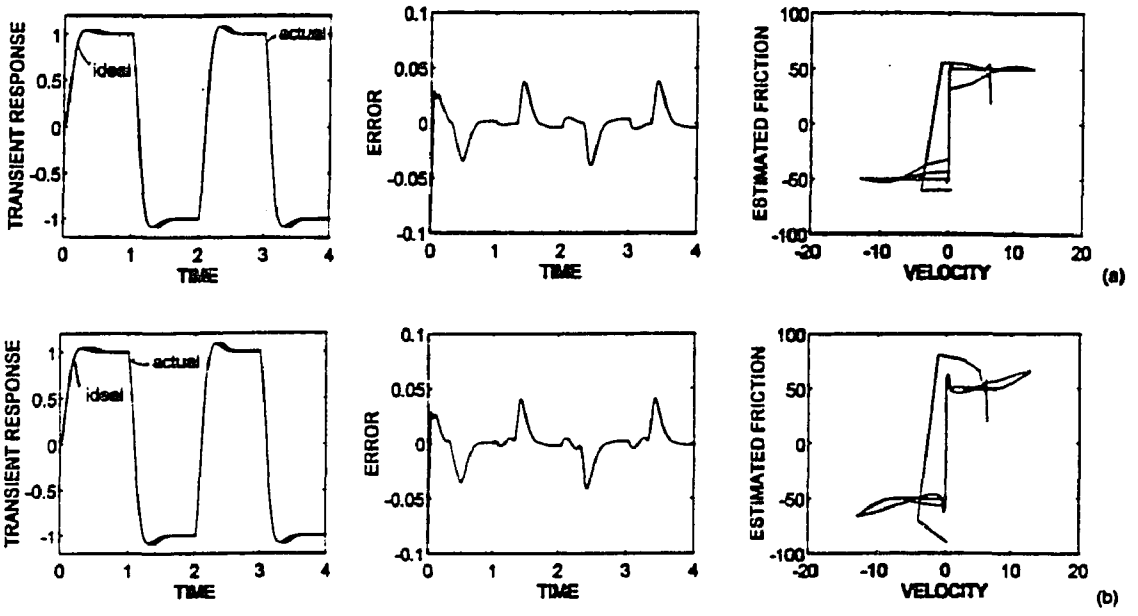

Figure 3.4 Performance of the TO compensator, with $k_1 = 0$, $k_2 = -100$ $k_v = 100$, in estimating (a) Coulomb friction (b) "extended" Coulomb friction

Figure 3.3 show the error between the transient responses of the ideal system and the actual (with friction compensation) versus time, and the estimated friction versus velocity when both the CFO and velocity observers are used to estimate and cancel Coulomb or "extended" Coulomb friction. Similarly, the performance of the tracking observer, (TO), with the additional velocity observer is shown in Figure 3.4 As can be seen from the graphs, the ill-effects of velocity observer are negligible and the friction can be estimated and cancelled successfully.

CHAPTER 4

ADAPTIVE ESTIMATION OF "EXTENDED" COULOMB FRICTION IN A MULTIPLE DEGREE–OF–FREEDOM SYSTEM

4.1 Introduction

In this chapter, the problem of friction estimation in a multiple degree–of–freedom system, is considered, under the assumption that friction is described by the "extended" Coulomb model. The results of this chapter are an extension of those presented in Chapters 2 and 3, for systems with multiple friction sources and multiple degrees–of–freedom.

Two different observers, generalizations of those presented before, are considered. The first is the generalized Coulomb friction observer designed based on a static friction model (GCFO); the second is the generalized tracking observer (GTO). For the analysis two cases are considered:

1. All the states are available for measurement.
2. Only position can be measured.

In the first case, the nonlinear observers use the measurements of the states to estimate the friction forces. In the second case, when only the positions and not the velocities are measurable, an additional observer is used to provide estimates of the velocities which are inputs to the friction observers.

Finally, favorable simulation results verify the theoretical analysis. Excellent performance of the proposed system in the presence of white noise is demonstrated by simulations.

4.2 Statement of the Problem

A system with multiple degrees–of–freedom consists of one or more masses characterized by translational motion in one or more directions and/or rotational motion.

In the following analysis the case of rotational motion perpendicular to planar translational will be considered as well as translational motion in three dimensions.

The dynamic model that describes such a system is the following:

$$\dot{x} = v \tag{4.1}$$

$$M(x)\dot{v} = g(x, v, w) - F(a, v) \tag{4.2}$$

where

$$x = [x_1\ x_2\ \cdots\ x_n]' \tag{4.3}$$

$$v = [v_1\ v_2\ \cdots\ v_n]' \tag{4.4}$$

and x_i and v_i are the ith "position" and "velocity". The mass matrix $M(x)$ is symmetric and positive definite. The vector $g(x, v, w)$ is a function of position and velocity as well as of the external input w to the system and represents the total non–frictional system force vector; $F(a, v)$ is the friction vector.

Assuming that the friction between two surfaces is described by the Coulomb model, it can be shown (see Appendix A), that the friction force vector can be written in the following form:

$$F(a, v) = U\ \mathcal{A}\ \mathrm{sgn}(U'v) \tag{4.5}$$

where

$$\mathcal{A} = \mathrm{diag}\{a\} = \begin{bmatrix} a_1 & \cdots & 0 \\ \vdots & \ddots & \vdots \\ 0 & \cdots & a_\nu \end{bmatrix} \tag{4.6}$$

The vector a contains the unknown friction coefficients and U is a known, $n \times \nu$, matrix (where ν is the number of different friction forces).

Now, if friction is described by the "extended" Coulomb model, the friction coefficients a_i are written as

$$a_i = a_{i1} + a_{i2}e^{-a_{i3}|\bar{v}_i|} + a_{i4}|\bar{v}_i| \tag{4.7}$$

where a_{i1}, a_{i2}, a_{i3} and a_{i4} are parameters which are assumed constants in this investigation, and $\bar{v}_i$ is the ith element of the vector $U'v$. In this case, the matrix friction coefficient $\mathcal{A}$ takes the form

$$\mathcal{A} = \mathcal{A}_1 + \mathcal{A}_2 e^{-\mathcal{A}_3 \text{diag}\{|U'v|\}} + \mathcal{A}_4 \text{diag}\{|U'v|\} \tag{4.8}$$

where

$$\mathcal{A}_i = \text{diag}\{a_{1i} \cdots a_{\nu i}\} \tag{4.9}$$

for $i = 1, 2, 3, 4$.

The problem considered in this chapter is the estimation of the friction force vector $F(a, v)$ in the system (4.1)–(4.2).

4.3 Observers Dynamics

For the estimation of the friction vector $F(a, v)$, assuming availability of the measurements of the positions and velocities, two nonlinear observers are studied.

4.3.1 Generalized Coulomb Friction Observer (GCFO)

Let $[U'v]_i$ represent the ith element of the vector $U'v$. Then, if $\hat{a}$ and $\hat{F}$ are the estimate vectors of a and $F(a, v)$ respectively, the following observer to estimate the friction vector $F(a, v)$ is proposed.

$$\hat{F} = US(v)\hat{a} \tag{4.10}$$

$$\hat{a} = z_F - K_F\, h(|U'v|) \tag{4.11}$$

with

$$\dot{z}_F = K_F\, D(v)\, S(v)\, U'\, M^{-1}(x)\, [g(x, v, w) - US(v)\, \hat{a}] \tag{4.12}$$

where

$$S(v) = \text{diag}\{\text{sgn}([U'v]_1),\ \cdots\ , \text{sgn}([U'v]_\nu)\} \tag{4.13}$$

$$h(|U'v|) = \begin{bmatrix} h_1(|U'v|) \\ \vdots \\ h_\nu(|U'v|) \end{bmatrix} \tag{4.14}$$

$$D(v) = \text{diag}\{\frac{\partial h_i(|U'v|)}{\partial(|U'v|)}\} \tag{4.15}$$

and K_F is a matrix to be chosen by the designer to ensure convergence of the error to zero. (The conditions under which K_F can be so chosen, are discussed in the next section.)

It is seen from (4.14)–(4.15) that $h(|U'v|)$ is a vector with elements that are functions which are analytic and monotonic in their arguments. Moreover, the matrix $D(v)$ is diagonal, the elements of which are the partial derivatives of the functions $h_i(\cdot)$ with respect to their arguments.

4.3.2 Generalized Tracking Observer (GTO)

Assuming again that $\hat{F}$ is the estimate vector of $F(a, v)$, the following alternate observer for friction estimation is proposed:

$$\hat{F} = z + K_1 x + K_2 v \tag{4.16}$$

with

$$\dot{z} = -K_1 v - K_2 M^{-1}(x)\,[g(x, v, w) - \hat{F}] \tag{4.17}$$

where K_1 and K_2 are matrices to be chosen by the designer to ensure boundedness of the error.

4.4 Selection of Gains and Error Analysis

To determine the gains K_F, K_1 and K_2, the error between the true and the estimated friction parameters is considered.

4.4.1 Generalized Coulomb Friction Observer (GCFO)

The error between the true vector a and its estimate $\hat{a}$ is calculated for the purpose of determining K_F and assessing performance. Let

$$e_a = a - \hat{a} \tag{4.18}$$

Differentiating both sides of the above equation (4.18), and using (4.11), (4.12) and (4.2), yields

$$\begin{aligned}\dot{e}_a &= \dot{a} - \dot{\hat{a}} \\ &= \dot{a} - \dot{z} + K_F \frac{\partial h(|U'v|)}{\partial(|U'v|)} \frac{\partial(|U'v|)}{\partial(U'v)} \frac{\partial(U'v)}{\partial v} \dot{v} \\ &= -K_F\, D(v)\, S(v)\, U'\, M^{-1}\, U\, S(v)\, e + \dot{a} \end{aligned} \tag{4.19}$$

The above differential equation is not homogeneous if vector a is not a constant. If the gain K_F is picked to ensure exponential stability and $\dot{a}$ is bounded, the error will be bounded in a neighborhood of the origin (Brockett, 1970).

Next, it is shown that $\dot{a}$ is bounded when the friction coefficient matrix is given by (4.8).

In order for the rate of change of a to be bounded, each coefficient $\dot{a}_i$ should be bounded, for every $i = 1, \cdots, \nu$. Now, using equation (4.7) yields

$$\dot{a}_i = \frac{\partial a_i}{\partial \bar{v}_i} \frac{\mathrm{d}\bar{v}_i}{\mathrm{d}t} \tag{4.20}$$

According to Lemma 2.1, $\dfrac{\partial a_i}{\partial \bar{v}_i}$ is bounded. Furthermore, $\dfrac{\mathrm{d}\bar{v}_i}{\mathrm{d}t}$ represents the system relative accelerations which can be assumed to be bounded.

4.4.2 Generalized Tracking Observer (GTO)

In order to evaluate the performance of the observer, the error between the true and the estimated friction forces is considered.

$$e_F = F - \dot{F} \tag{4.21}$$

Differentiating both sides of (4.21), and using (4.16), (4.17) and (4.2), yields

$$\begin{aligned}\dot{e}_F &= \dot{F} - \dot{\hat{F}} \\ &= \dot{F} - \dot{z} - K_1 v - K_2 \dot{v} \\ &= K_2\, M^{-1}(x)\, e_F + \dot{F} \end{aligned} \tag{4.22}$$

The above differential equation is not homogeneous if vector F is not a constant. If the gain K_2 is picked to ensure exponential stability and $\dot{F}$ is bounded, the error will be bounded in a neighborhood of the origin (Brockett, 1970).

Next, it is shown that $\dot{F}$ is bounded when the friction coefficients a_i are described by (4.7).

The friction force vector is written in the form:

$$F = U\ S(v)\ a \tag{4.23}$$

and

$$\dot{F} = \dot{U}\ S(v)a + U\dot{S}(v)a + US(v)\dot{a} \tag{4.24}$$

If the friction coefficient vector a is constant the last term is zero; otherwise it is bounded as shown in Section 4.4.1. U is in general a function of the positions x. It is reasonable to assume that the states x as well as the velocities are bounded and so are the matrices U and $\dot{U}$. In addition, matrix $S(v)$ contains the sign of the relative system velocities. Assuming that $[U'v]_i \neq 0$, $S(v)$ is real, bounded, and $\dot{S}(v) = 0$. Finally, since all the terms of equation (4.24) are bounded, $\dot{F}$ is bounded.

4.5 Friction Estimation Without Velocity Measurements

In the foregoing analysis, assuming that the entire state vector of the system was available for measurement, two nonlinear observers were proposed to estimate the friction force vector. In this section, however, only the position x is assumed measurable. Therefore, in order to estimate the unmeasurable velocities, an additional nonlinear reduced order state observer is used. This observer is combined in cascade with the observers of the previous sections to estimate the friction vector. A block diagram representation of the cascade structure of the velocity and friction observers is shown in Figure 4.1.

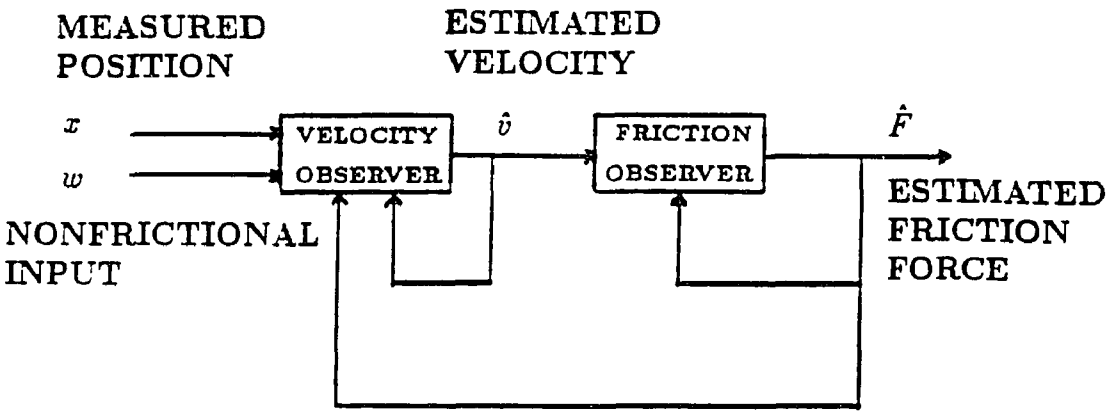

Figure 4.1 Cascade structure of velocity and friction observers.

4.5.1 Velocity Observer "Architecture"

Assuming $\hat{v}$ represents the estimate of the velocity v, the following nonlinear, reduced-order state observer is proposed:

$$\hat{v} = z_v + K_v x \tag{4.25}$$

with

$$\dot{z}_v = -K_v \hat{v} + M^{-1}(x)\,[g(x, \hat{v}, w) - \hat{F}] \tag{4.26}$$

where K_v is the design parameters matrix.

The latter observer uses as inputs the measurements of the positions x as well as the estimates of the previously proposed observers (4.10)–(4.12) or (4.16)–(4.17), to estimate the velocities.

4.6 Combining Velocity and Friction Observers

When the velocity observer is used, the estimate $\hat{v}$ replaces in the friction observers the true velocity v.

4.6.1 Generalized Coulomb Friction Observer (GCFO)

When the velocity observer is used, the GCFO observer (4.11)-(4.12) takes the form:

$$\begin{aligned} \dot{z}_F &= K_F D(\hat{v}) S(\hat{v}) U' M^{-1}(x) \left[g(x, \hat{v}, w) - U S(\hat{v}) \hat{a} \right] \\ \hat{a} &= z_F - K_F h(|U'\hat{v}|) \qquad (4.27) \\ \hat{F} &= U S(\hat{v}) \hat{a} \qquad (4.28) \end{aligned}$$

To determine the gains K_F and K_v, the error under the real and the estimated parameters has to be considered. To this end define

$$\begin{aligned} e_v &= v - \hat{v} \qquad (4.29) \\ e_a &= a - \hat{a} \qquad (4.30) \end{aligned}$$

Differentiating both sides of (4.29) and (4.30), and using (4.2), (4.27) and (4.25), yields

$$\begin{aligned} \dot{e}_v &= q_v(e_v, e_a, v, a) \qquad (4.31) \\ \dot{e}_a &= q_a(e_v, e_a, v, a) + \dot{a} \qquad (4.32) \end{aligned}$$

where

$$\begin{aligned} q_v(e_v, e_a, v, a) &= M^{-1}(x) \left[g(x, v, w) - g(x, \hat{v}, w) \right] - M^{-1}(x) \left\{ S(v) a - S(v - e_v)[a - e_a] \right\} \\ &\quad - K_v e_v \\ q_a(e_v, e_a, v, a) &= K_F D(v - e_v) S(v - e_v) U' K_v e_v \end{aligned}$$

The above differential equations are not homogeneous if vector a is not a constant. If the gains K_v and K_F are picked to ensure exponential stability and $\dot{a}$ is bounded, the error will be bounded in a neighborhood of the origin (Brockett, 1970).

The Jacobian matrix $\mathbf{\Psi}$ of equations (4.31) and (4.32), calculated at $e_v = e_a = 0$, is

$$\mathbf{\Psi} = \begin{bmatrix} -K_v + M^{-1}(x) g_v(x, v, w) & -M^{-1}(x)\, U S(v) \\ K_F D(v) S(v) U' K_v & 0 \end{bmatrix}$$

where $g_v(x,v,w) = \frac{\partial g(x,v,w)}{\partial v}$. For the above calculations of partial derivatives it is assumed, that $v \neq e_v$, and $a \neq e_a$. If the gain matrices can be picked such that Ψ has eigenvalues in the left half plane, $||\Psi||$ bounded and $||\dot{\Psi}||$ is sufficiently small, the estimation error is exponentially stable.

4.6.2 Generalized Tracking Observer (GTO)

When the reduced order velocity observer is used, the GTO observer, for the friction forces (4.16), (4.17) takes the form

$$\begin{aligned} \dot{z} &= -K_1\hat{v} - K_2 M^{-1}(x)\,[g(x,\hat{v},w) - \hat{F}] \\ \hat{F} &= z + K_1 x + K_2 \hat{v} \end{aligned} \tag{4.33}$$

To determine the gains K_1, K_2 and K_v, the error under the real and the estimated parameters has to be considered. The components of the vector error are:

$$e_v = v - \hat{v} \tag{4.34}$$

$$e_F = F(a,v) - \hat{F} \tag{4.35}$$

The analysis is similar to the one presented for the GCFO observer in the previous section.

The differential equations describing the rate of change of the estimation errors are the following

$$\begin{aligned} \dot{e}_v &= M^{-1}(x)[g(x,v,w) - g(x,\hat{v},w)] - M^{-1}(x)e_F - K_v e_v \\ \dot{e}_F &= -(K_1 + K_2 K_v)e_v + \dot{F}(a,v) \end{aligned} \tag{4.36}$$

The above differential equations are not homogeneous. If the gains K_v, K_1 and K_2 are picked to ensure exponential stability and $\dot{F}(a,v)$ is bounded, the error will be bounded within the origin (Brockett, 1970).

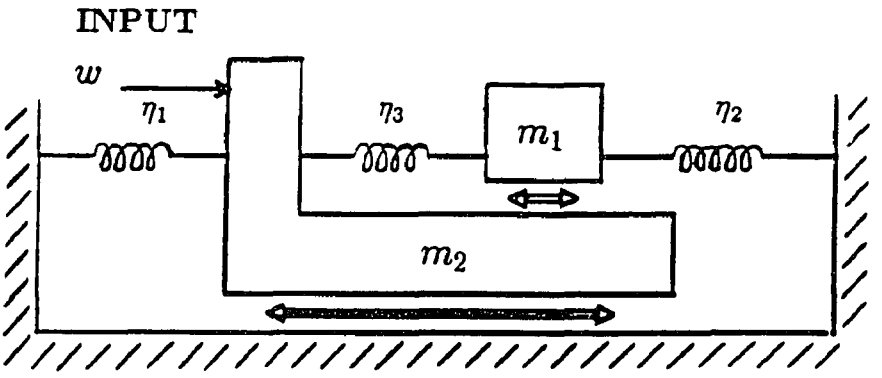

Figure 4.2 The two-mass system.

The Jacobian matrix Ψ of equations (4.36) and (4.36), calculated at $e_v = e_F = 0$, is

$$\Psi = \begin{bmatrix} -K_v + M^{-1}(x)g_v(x,v,w) & -M^{-1}(x) \\ -(K_1 + K_2K_v) & 0 \end{bmatrix}$$

where $g_v(x,v,w) = \frac{\partial g(x,v,w)}{\partial v}$. If the gain matrices can be picked such that Ψ has eigenvalues in the left half plane, $||\Psi||$ bounded and $||\dot{\Psi}||$ is sufficiently small, the estimation error is exponentially stable.

4.7 Example 1: Two-Mass System

Let us consider the system, shown in Figure 4.2, which consists of two masses m_1 and m_2, one on top of the other. In this system friction appears between the two masses as well as between the second mass and the ground.

The system differential equations are

$$\begin{aligned} m_1\dot{v}_1 &= -(\eta_2 + \eta_3)x_1 + \eta_3 x_2 - F_1 \\ m_2\dot{v}_2 &= \eta_3 x_1 - (\eta_1 + \eta_3)x_2 - F_2 + w \end{aligned} \tag{4.37}$$

where η_1, η_2, η_3 are the spring constants, m_1, m_2 are the masses, while x_1, v_1, x_2, v_2 are the displacement and the velocity of the masses m_1 and m_2 respectively, and w is the input. F_1, F_2 are the total friction forces of the first and the second mass,

respectively, and are described as follows

$$F_1 = a_1 \text{sgn}(v_1 - v_2) \tag{4.38}$$

$$F_2 = a_2 \text{sgn}(v_2) - a_1 \text{sgn}(v_1 - v_2) \tag{4.39}$$

The problem considered in this example is the estimation of the friction forces that appear in the two-mass system.

First let us rewrite the system differential equations in the standard form (4.1), (4.2):

$$\begin{aligned} \dot{x} &= v \\ M\dot{v} &= g(x, v, w) - F(a, v) \end{aligned}$$

where

$$F(a, v) = [F_1 \;\; F_2]' = U\mathcal{A}\,\text{sgn}(U'v)$$

and

$$x = [x_1 \quad x_2]', \quad v = [v_1 \quad v_2]'$$

$$g(x, v, w) = \begin{bmatrix} -(\eta_2 + \eta_3)x_1 + \eta_3 x_2 \\ \eta_3 x_1 - (\eta_1 + \eta_3)x_2 + w \end{bmatrix} \tag{4.40}$$

$$M = \begin{bmatrix} m_1 & 0 \\ 0 & m_2 \end{bmatrix}, \; U = \begin{bmatrix} 1 & 0 \\ -1 & 1 \end{bmatrix}, \; \mathcal{A} = \begin{bmatrix} a_1 & 0 \\ 0 & a_2 \end{bmatrix} \tag{4.41}$$

Next the two observers proposed in the chapter will be designed and simulated.

4.7.1 Observers Dynamics

Generalized Coulomb Friction Observer (GCFO)

Choose $h(|U'v|)$ to be

$$h(|U'v|) = |U'v| = \begin{bmatrix} |v_1 - v_2| \\ |v_2| \end{bmatrix} \tag{4.42}$$

Then, according to (4.15), the matrix D becomes

$$D = \text{diag}\{d_1, d_2\} = \text{diag}\{1, 1\} \tag{4.43}$$

Moreover, using (4.13), $S(v)$ is

$$S(v) = \text{diag}\{\text{sgn}(v_1 - v_2), \text{sgn}(v_2)\} \tag{4.44}$$

Finally, substituting (4.42)–(4.44) into (4.11) and (4.12), the GCFO observer takes the form

$$\hat{F}_1 = (z_{F1} - k_{F1}|\hat{v}_1 - \hat{v}_2|)\text{sgn}(\hat{v}_1 - \hat{v}_2) \tag{4.45}$$

$$\hat{F}_2 = (z_{F2} - k_{F2}|\hat{v}_2|)\text{sgn}(\hat{v}_2) - \hat{F}_1 \tag{4.46}$$

and

$$\begin{aligned}
\dot{z}_{F1} &= k_{F1}\text{sgn}(\hat{v}_1 - \hat{v}_2)\{(m_1)^{-1}[-(\eta_2 + \eta_3)x_1 + \eta_3 x_2 - \hat{F}_1] \\
&\quad -(m_2)^{-1}[\eta_3 x_1 - (\eta_1 + \eta_3)x_2 - \hat{F}_2]\} \\
\dot{z}_{F2} &= k_{F2}\text{sgn}(\hat{v}_2)(m_2)^{-1}[\eta_3 x_1 - (\eta_1 + \eta_3)x_2 - \hat{F}_2]
\end{aligned}$$

where the gain $K_F = \text{diag}\{k_{F1}, k_{F2}\}$.

Generalized Tracking Observer (GTO)

According to (4.16) and (4.17), the GTO observer for the friction forces has the following form

$$\hat{F}_1 = z_1 + k_{11}x_1 + k_{21}\hat{v}_1 \tag{4.47}$$

$$\hat{F}_2 = z_2 + k_{12}x_2 + k_{22}\hat{v}_2 \tag{4.48}$$

and

$$\begin{aligned}
\dot{z}_1 &= -k_{11}\hat{v}_1 - k_{21}(m_1)^{-1}[-(\eta_2 + \eta_3)x_1 + \eta_3 x_2 - \hat{F}_1] \\
\dot{z}_2 &= -k_{12}\hat{v}_2 - k_{22}(m_2)^{-1}[\eta_3 x_1 - (\eta_1 + \eta_3)x_2 + w - \hat{F}_2]
\end{aligned}$$

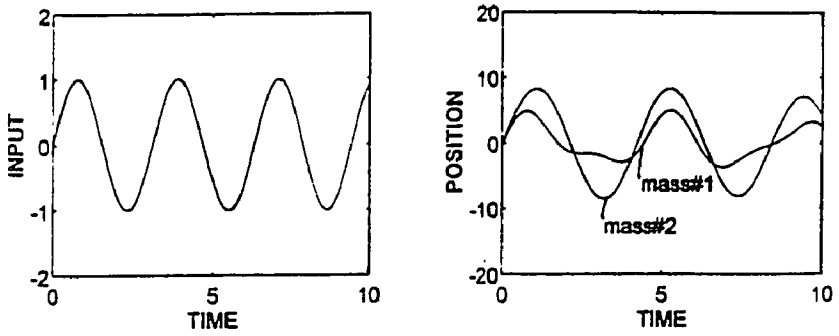

Figure 4.3 System input and transient responses.

where the observer gain matrices were picked to be diagonal, i.e

$$K_1 = \text{diag}\{k_{11}, k_{21}\}$$

$$K_2 = \text{diag}\{k_{21}, k_{22}\}$$

Velocity Observer "Architecture".

Assuming that only the position is available for measurements, the observer to estimate the velocity is the following

$$\hat{v}_1 = z_{v_1} + k_{v_1} x_1 \tag{4.49}$$

$$\hat{v}_2 = z_{v_2} + k_{v_2} x_2 \tag{4.50}$$

and

$$\dot{z}_{v_1} = -k_{v_1}\hat{v}_1 + (m_1)^{-1}[-(\eta_2+\eta_3)x_1 + \eta_3 x_2 - \hat{F}_1]$$

$$\dot{z}_{v_2} = -k_{v_2}\hat{v}_2 + (m_2)^{-1}[\eta_3 x_1 - (\eta_1+\eta_3)x_2 + w - \hat{F}_2]$$

where, $K_v = \text{diag}\{k_{v_1}, k_{v_2}\}$.

4.7.2 Simulation Results

For the simulations, the values of the system parameters are assumed to be $m_1 = 10$, $m_2 = 50$, $\eta_1 = 100$, $\eta_2 = 50$, $\eta_3 = 20$, $a_1 = 10$ and $a_2 = 20$. The measurements of the positions are considered to be contaminated with white noise with a rms value

of 0.1. The input is sinusoidal with frequency π Hz. The system input and transient response are shown in Figure 4.3.

The results for the GCFO observer are shown in Figures 4.4a and 4.5a. The observer gain matrices used in the simulations are

$$\begin{aligned} K_F &= \text{diag}\{500, 700\} \\ K_v &= \text{diag}\{10, 10\} \end{aligned}$$

Figures 4.4b and 4.5b show the results for the GTO observer. The observer gain matrices used in the simulations are

$$\begin{aligned} K_1 &= \text{diag}\{0, 0\} \\ K_2 &= \text{diag}\{-1000, -5000\} \\ K_v &= \text{diag}\{10, 10\} \end{aligned}$$

The estimation of "extended" Coulomb friction is shown in Figures 4.5a,b. In the simulations the gains for the observers remain unchanged, while the friction coefficients are described as follows

$$\begin{aligned} a_1 &= 20 + 10e^{-|v_1 - v_2|} + |v_1 - v_2| \\ a_2 &= 40 + 20e^{-|v_2|} + 2|v_2| \end{aligned}$$

As it can be seen from the simulations, the GCFO observer that is designed based on a Coulomb friction model, performs better: The GTO observer needs a relatively high gain to track the details of the friction force, which results in a high overshoot in the observer transient response.

4.8 Example 2: Two Link Robot Arm

The dynamic equation describing the motion of a two robot arm manipulator is (Grossman, 1991) (Figure 4.6)

$$M(\theta)\dot{\omega} + F_c(\theta, \omega) + F_g(\theta) = w - F(a, \omega) \tag{4.51}$$

where

$$\theta = \begin{bmatrix} \theta_1 & \theta_2 \end{bmatrix}' \tag{4.52}$$

$$\omega = \begin{bmatrix} \omega_1 & \omega_2 \end{bmatrix}' \tag{4.53}$$

are vectors containing the angular positions and velocities of the two links respectively.

Matrix $M(\theta)$ is the inertia matrix and can be written analytically as follows:

$$M(\theta) = \begin{bmatrix} M_{11} & M_{12} \\ M_{21} & M_{22} \end{bmatrix} \tag{4.54}$$

with

$$\begin{aligned} M_{11} &= I_1 + I_2 + m_1 b_1^2 + m_2(l_1^2 + b_2^2) + 2m_2 l_1 b_2 \cos\theta_2 \\ M_{12} &= I_2 + m_2 b_2^2 + m_2 l_1 b_2 \cos\theta_2 \\ M_{21} &= M_{12} \\ M_{22} &= I_2 + m_2 b_2^2 \end{aligned}$$

where m_i, l_i are the mass and the length of the ith link, b_i is the distance from the ith joint to the center of gravity of the ith link, and I_i is the moment of inertia of the ith link about the center of gravity.

The vector $F_c(\theta, \omega)$ represents the coriolis and centrifugal forces of the system while $F_g(\theta)$ is the gravitational force vector. The analytic expressions of the vectors $F_c(\theta, \omega)$ and $F_g(\theta)$ are

$$F_c(\theta, \omega) = \begin{bmatrix} -m_2 l_1 b_2 (2\omega_1 + \omega_2)\omega_2 \sin(\theta_2) \\ m_2 l_1 b_2 \omega_1^2 \sin(\theta_2) \end{bmatrix} \tag{4.55}$$

and

$$F_g(\theta) = \begin{bmatrix} (m_1 b_1 + m_2 l_1)\cos(\theta_1) + m_2 b_2 \cos(\theta_1 + \theta_2) \\ m_2 b_2 \cos(\theta_1 + \theta_2) \end{bmatrix} g \tag{4.56}$$

where g is the gravitational acceleration.

The input vector w is the sum of all the external input forces applied to the system.

Friction is assumed present at the two joints and is described in (4.51) by the vector $F(a,\omega)$, where

$$\begin{aligned} F(a,\omega) &= \begin{bmatrix} F_1 \\ F_2 \end{bmatrix} = \begin{bmatrix} a_1 \mathrm{sgn}(\omega_1) \\ a_2 \mathrm{sgn}(\omega_2) \end{bmatrix} \\ &= \underbrace{\mathrm{diag}\{\mathrm{sgn}(\omega_1), \mathrm{sgn}(\omega_2)\}}_{S(\omega)} \underbrace{\begin{bmatrix} a_1 \\ a_2 \end{bmatrix}}_{a} \end{aligned}$$

The vector a contains the unknown constant Coulomb friction coefficients a_1, and a_2.

The problem considered in this example, is the estimation of the friction vector $F(a,\omega)$.

4.8.1 Friction Observer "Architecture"

Generalized Coulomb Friction Observer (GCFO)

Assume $\hat{a}$ and $\hat{F}$ to be the estimate of a and $F(a,\omega)$ respectively. Then, the GCFO observer takes the form:

$$\hat{a} = z_F - K_F |\hat{\omega}| \tag{4.57}$$

$$\hat{F} = S(\hat{\omega})\hat{a} \tag{4.58}$$

with

$$\dot{z}_F = K_F S(\hat{\omega}) M^{-1}(\theta)[w - F_c(\theta,\hat{\omega}) - F_g(\theta) - \hat{F}] \tag{4.59}$$

where $M^{-1}(\theta)$ is the inverse of the inertia matrix $M(\theta)$ and K_F is a matrix to be chosen by the designer to ensure convergence of the error to zero. Notice that the inertia matrix is positive definite, and can always be inverted.

Velocity Observer "Architecture"

Assuming $\hat{\omega}$ represents the estimate of the velocity ω, the velocity observer takes the form:

$$\hat{\omega} = z_\omega + K_\omega \theta \tag{4.60}$$

with

$$\dot{z}_\omega = M^{-1}(\theta)[u - F_c(\theta, \hat{\omega}) - F_g(\theta) - \hat{F}] - K_\omega \hat{\omega} \tag{4.61}$$

where K_ω is the designed parameters matrix.

The latter observer uses as inputs the measurements of the angular position θ as well as the estimates of the previously proposed observer (4.57) to estimate the velocities of the links.

4.8.2 Simulation Results

To verify the performance of the observers described above, a simulation study was performed. The values of the system parameters were assumed to be $m_1 = 0.7718$ kg, $m_2 = 0.2713$ kg, $l_1 = 0.205$ m, $l_2 = 0.224$ m, $I_1 = 0.00863$ kg-m^2, $I_2 = 0.00132$ kg-m^2, $k_1 = 0.04$ m, $k_2 = 0.065$ m and $g = 9.8$ m/s^2. The measurements of angular positions were considered to be contaminated with white noise with an rms value of 0.5. The applied inputs were $u_1 = \sin(2t)$ and $u_2 = 0$. The values of the friction coefficients were assumed to be $a_1 = 0.001$ and $a_2 = 0.005$. The gain matrices K_F and K_ω were selected as

$$K_F = \begin{bmatrix} .01 & 0 \\ .01 & 0.005 \end{bmatrix}, \quad K_\omega = \begin{bmatrix} 1 & 0.5 \\ 1 & 10 \end{bmatrix}$$

The results are shown in Figure 4.7. As can be seen from the figure, friction can be estimated successfully in a system with nonlinear dynamics.

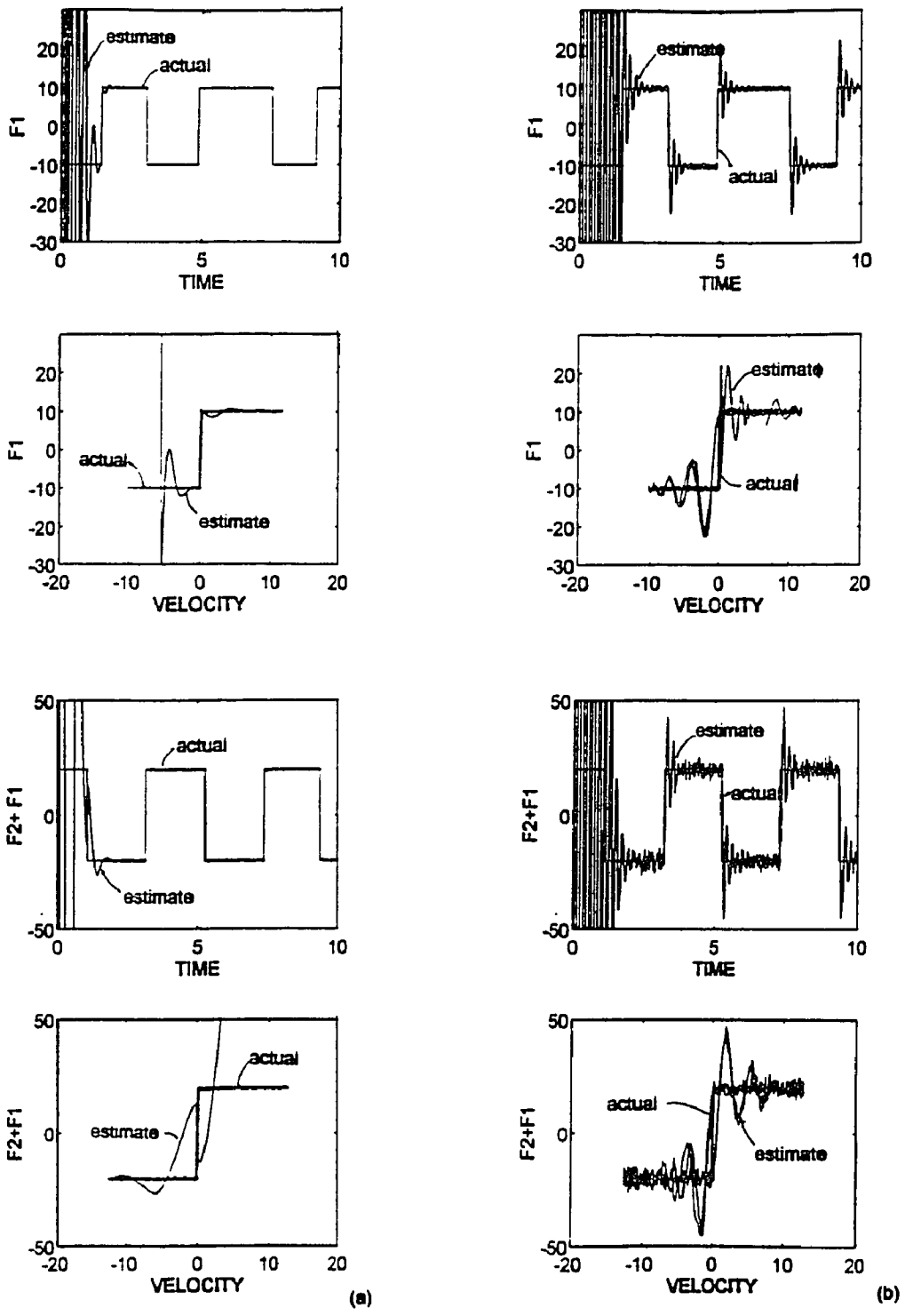

Figure 4.4 (a) Performance of the GCFO observer in estimating Coulomb friction F_1 between the two masses and $(F_1 + F_2)$ between the second mass and the ground (b) Performance of the GTO observer in estimating the system friction forces.

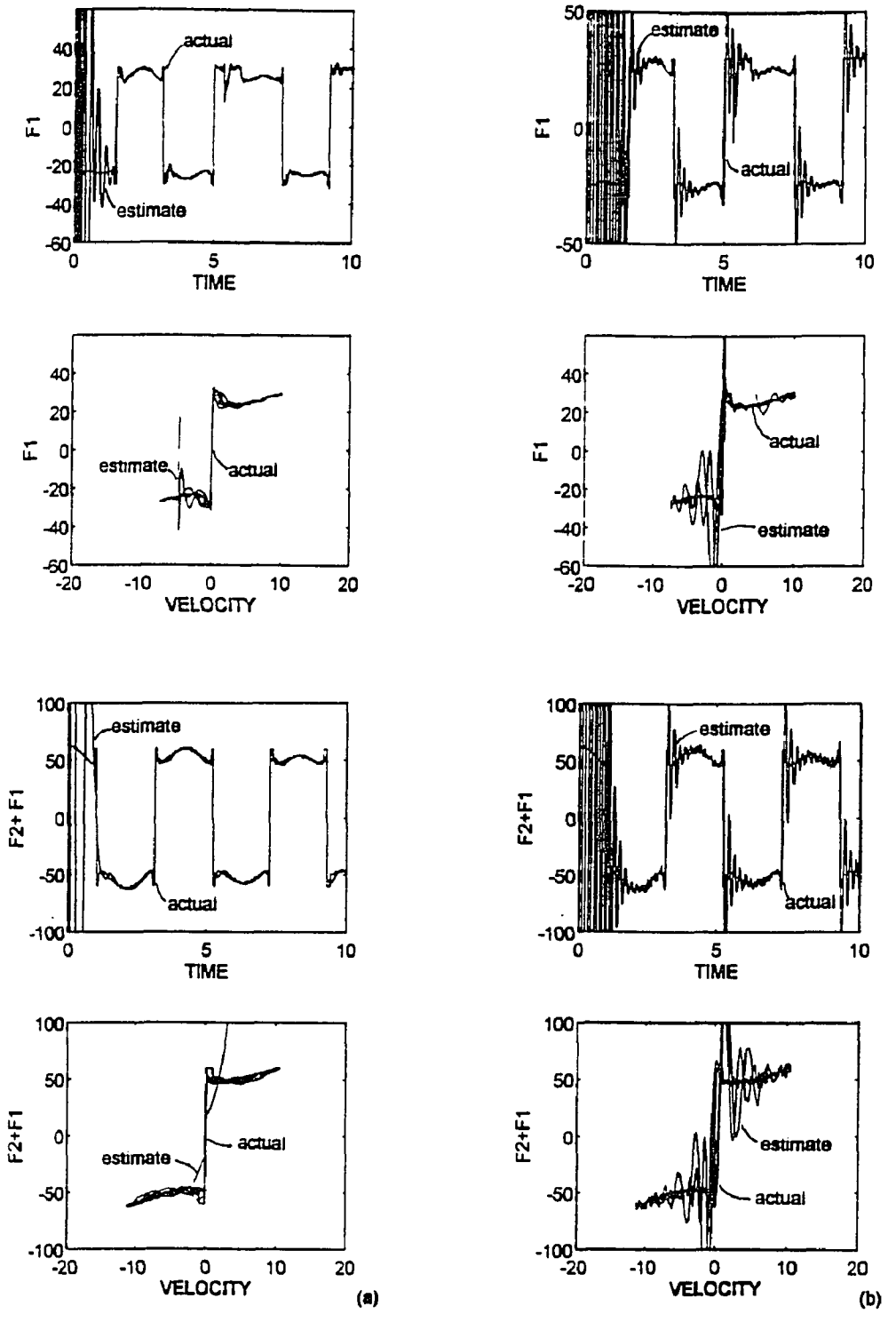

Figure 4.5 (a) Performance of the GCFO observer in estimating "extended" Coulomb friction F_1 between the two masses and $(F_1 + F_2)$ between the second mass and the ground (b) Performance of the GTO observer in estimating the system friction forces.

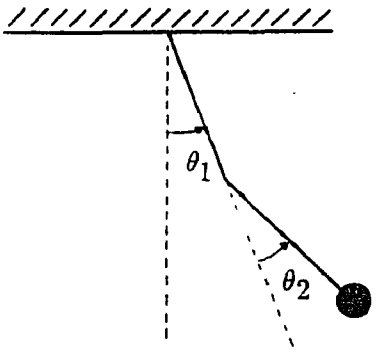

Figure 4.6 The two link robot arm.

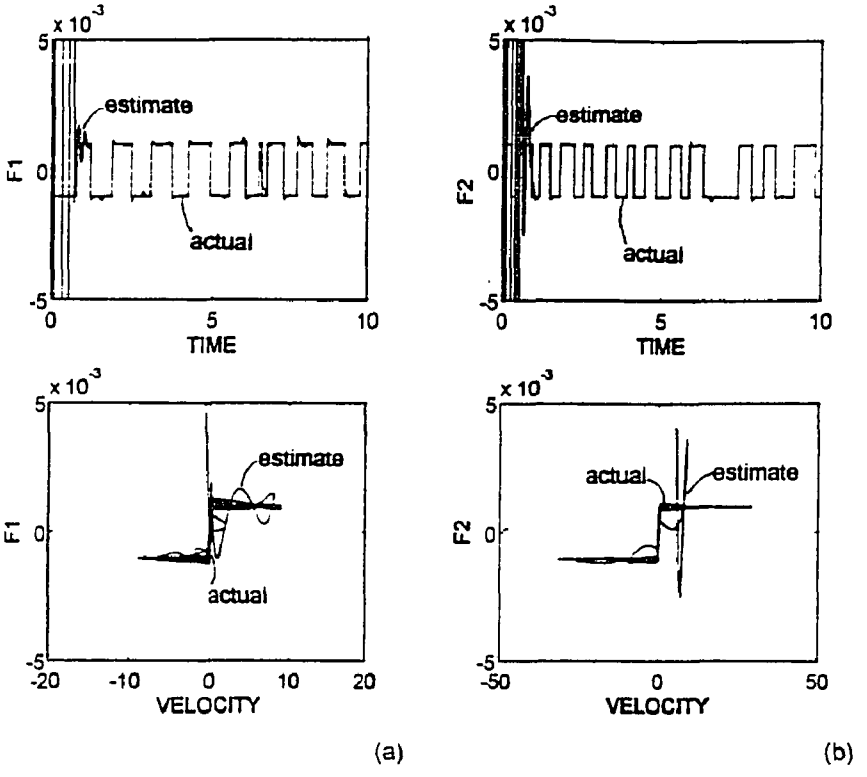

Figure 4.7 Performance of the GCFO observer in estimating Coulomb friction (a) Actual and estimated friction F_1 (b) Actual and estimated friction F_2.

CHAPTER 5

FRICTION CANCELLATION IN A SYSTEM WITH MULTIPLE INPUTS AND FRICTION SOURCES

5.1 Introduction

The problem considered in this chapter is the cancellation of friction in systems with multiple inputs and friction sources. This problem has been considered in the past by many researchers. Techniques such as high gain PD control, model–based feedback, dither, joint torque control, model reference adaptive control, adaptive pulse width control were proposed.

In this chapter an investigation is conducted concerning the relation between the system topology and friction cancellation in a system linear with respect to the inputs. In particular, topological conditions are derived, based on the distribution of the inputs and the friction forces in the system, which determine whether total or partial friction cancellation is possible. When cancellation is possible, an appropriate feedback control law is designed to cancel the friction. The method leads to total or partial friction cancellation, depending on the topology of the system.

The proposed feedback design can be combined with the algorithms for friction estimation proposed in the previous chapters (or, for that matter, another friction estimation method) to cancel the friction forces.

Simulation results demonstrate the effectiveness of the method.

5.2 Statement of the Problem

The general dynamic model that describes a system which is linear with respect to the inputs, is

$$\dot{x} = v \tag{5.1}$$

$$M(x)\dot{v} = g(x,v) + Bw - F \tag{5.2}$$

where

$$x = [x_1\ x_2\ \cdots\ x_n]' \tag{5.3}$$

$$v = [v_1\ v_2\ \cdots\ v_n]' \tag{5.4}$$

and x_i and v_i are the ith "position" and "velocity," respectively. The matrix $M(x)$ is the known mass matrix which is symmetric and positive definite. The vector $g(x, v)$ and the matrix B are also assumed to be known and w is a $r \times 1$ vector of the external system inputs; F is the friction vector which can be written as follows

$$F = U\bar{F} \tag{5.5}$$

where the vector $\bar{F}$ contains the different friction forces, i.e.

$$\bar{F} = [\ \bar{F}_1\ \ \cdots \bar{F}_\nu\ ]' \tag{5.6}$$

and U is the friction "distribution" matrix (Appendix A).

The problem considered in this chapter is the determination of an appropriate feedback control law to cancel the friction vector $\bar{F}$. This problem, however, doesn't have always a solution, as it will become apparent by the analysis that follows. In the next section, necessary and sufficient conditions will be derived to determine which of the friction forces can be cancelled.

5.3 Design of Feedback Control Law

The input w of the system can be written as

$$w = u + \bar{u} \tag{5.7}$$

where u is the input designed for the system with no friction to satisfy some performance criteria, and $\bar{u}$ is the input that will be designed to eliminate or cancel (when possible) the effects of friction.

The problem of friction cancellation can be reformulated as follows: Find an appropriate input $\bar{u}$ such that

$$B\bar{u} = U\bar{F} \tag{5.8}$$

assuming that B is a $n \times r$ matrix, where n is the number of the system states and r the number of the system inputs. The conditions under which equation (5.8) has a solution are examined below and a feedback control law is designed when possible to do so.

5.3.1 Perfect Friction Cancellation

Perfect friction cancellation is possible under certain topological conditions between the distribution of the inputs and the distribution of the friction forces in the system.

- $n = r$ and $\text{rank}B = r$

  In this case the input $\bar{u}$ takes the form

$$\bar{u} = B^{-1}U\bar{F} \tag{5.9}$$

- $n > r$ and $\text{rank}B = r$ and $U_2\bar{F} = 0$

  where the matrix U_2 is defined as

$$KU = \begin{bmatrix} U_1 \\ U_2 \end{bmatrix} \tag{5.10}$$

  and the matrix K is determined such that

$$KB = \begin{bmatrix} B_1 \\ 0 \end{bmatrix}$$

  If the above conditions are satisfied, friction can be cancelled perfectly by the following input

$$\bar{u} = B_1^{-1}U_1\bar{F} \tag{5.11}$$

- $n \geq r$ and rank$B < r$ and $U_2\bar{F} = 0$

  where U_2 is defined by (5.10). If the above conditions are satisfied, then more than one solution may be found for (5.8). To determine a solution, the algorithm, proposed in Appendix B, may be used.

5.3.2 Partial Friction Cancellation

- $n > r$ and rank$B = r$ and $U_2\bar{F} \neq 0$

  where U_2 is defined by (5.10).

  In this case friction can be cancelled partially by the following input

$$\bar{u} = B_1^{-1}U_1\bar{F} \tag{5.12}$$

- $n \geq r$ and rank$B < r$ and $U_2\bar{F} \neq 0$

  where U_2 is defined by (5.10). To determine a solution, the algorithm proposed in Appendix B may be used.

- $n < r$ and rank$B \leq n$,

  then a solution that minimizes the least mean square error is proposed. Specifically,

$$\bar{u} = (B'B)^{-1}B'U\bar{F} \tag{5.13}$$

  In the special case where rank$B = n$, the algorithm given in Appendix B may be used in order to determine an appropriate input $\bar{u}$.

Note 1

The theory presented in this section is based on the knowledge of the friction distribution matrix U, the control matrix B, the mass matrix M, and the vector friction force $\bar{F}$. In the case where $\bar{F}$ is not known, the GCFO and GDFO observers, proposed

in Chapter 4 and 7, respectively, can be used to estimate the unknown forces. The GTO observer, however, as is proposed in Chapters 4 and 8, assumes that U is unknown, and estimates F instead of $\bar{F}$, which may be very important for some applications. The modified GTO observer, (MGTO), able to estimate $\bar{F}$, has the following form

$$\hat{F} = z + K_{m1}x + K_{m2}v \tag{5.14}$$

with

$$\dot{z} = -K_{m1}v - K_{m2}M^{-1}[g(x,v,w) - U\hat{F}] \tag{5.15}$$

where $\hat{F}$ is the estimate vector of $\bar{F}$, and K_{m1} and K_{m2} are matrices to be chosen by the designer to ensure convergence of the estimation error to zero. To determine the matrices K_{m1} and K_{m2}, the same procedure as that followed in Chapter 4 can be applied. The MGTO observer is similar to the GTO, and can be used to estimate Coulomb as well as dynamic friction satisfactorily. When the observers are used, the input w uses the estimates of the friction instead of the actual friction force.

Note 2

If the matrix $\bar{B}$ contains some zero rows, then friction forces that cannot be cancelled may exist in the system. In this case, for simplicity, we can eliminate these forces from the equation (5.8) before we proceed to apply the conditions for partial or perfect friction cancellation. To this end, the following procedure should be followed:

Step 1: Assume that the zero rows in B are the i_1st, $\cdots$, i_lth. Then, eliminate those rows, and create a submatrix $\bar{B}$ of B, which contain no zero rows.

Step 2: Check if there are any non zero elements in the i_1st, $\cdots$, i_lth rows of the matrix U. If there are, it is assumed that they belong to the j_1st, $\cdots$, j_sth columns. This means that there exist friction forces that cannot be cancelled. The friction forces $\bar{F}_i$ that are the j_1st, $\cdots$, j_sth elements of the vector $\bar{F}$ cannot be cancelled due

to the relative distribution of the system inputs with the one of the frictions on the different system degrees-of-freedom.

Step 3: Eliminate the rows i_1st, $\cdots$, i_lth as well as the columns j_1st, $\cdots$, j_sth from the matrix U and create a new submatrix $\bar{U}$. Finally create a submatrix $\bar{F}_n$ which results from $\bar{F}$ after eliminating the j_1st, $\cdots$, j_sth elements.

Considering the matrix simplifications proposed above, equation (5.8) can be rewritten as follows

$$\bar{B}\bar{u} = \bar{U}\bar{F}_n \tag{5.16}$$

5.4 Example: Two–Mass System (Continued)

Let us consider again the two-mass system (Figure 4.2). The system differential equations are

$$m_1\dot{v}_1 = -(\eta_2 + \eta_3)x_1 + \eta_3 x_2 - F_1 \tag{5.17}$$

$$m_2\dot{v}_2 = \eta_3 x_1 - (\eta_1 + \eta_3)x_2 + w - F_2 \tag{5.18}$$

where F_1 and F_2 are the total friction forces applied to the top and bottom mass respectively. For the above system,

$$F_1 = \bar{F}_1$$

$$F_2 = \bar{F}_2 - \bar{F}_1$$

where $\bar{F}_1$ is the friction that exists between the two masses, and $\bar{F}_2$ is the friction between the second mass and the ground.

It can be easily seen that when the input is applied on the bottom mass, only $\bar{F}_2$ can be totally cancelled. This can also be shown by following the analysis developed in the present chapter.

Step 1: Form matrices M, B, U and $\bar{F}$ using equations (5.17)-(5.18), as

$$M = \begin{bmatrix} m_1 & 0 \\ 0 & m_2 \end{bmatrix}, \quad B = \begin{bmatrix} 0 \\ 1 \end{bmatrix} \quad U = \begin{bmatrix} 1 & 0 \\ -1 & 1 \end{bmatrix} \quad \bar{F} = \begin{bmatrix} \bar{F}_1 \\ \bar{F}_2 \end{bmatrix}$$

Step 2: The first row of matrix B is zero. Thus, we have to check if there exist any nonzero elements in the first row of the matrix U. As it can be seen, the element which belongs to the first row and first column of U is nonzero. Therefore, eliminate the first row of B, the first row and column of U and the first element F_1 of the friction vector, and create the submatrices $\bar{B}$, $\bar{U}$ and $\bar{F}_n$, as

$$\bar{B} = 1, \quad \bar{U} = 1, \quad \bar{F}_n = \bar{F}_2$$

Step 3: Solve the equation (5.16). By doing so, we get

$$\bar{u} = \bar{F}_2$$

as expected.

Notice that in the case where the friction observers proposed previously were used, the input $\bar{u}$ would be equal to the estimate of the second friction $\bar{F}_2$ and not the actual $\bar{F}_2$.

For the simulations the actual system has an input w of the form

$$w = \bar{F}_2 + \sin(2t)$$

The ideal system, however, does not contain the force $\bar{F}_2$ and has an input equal to $\sin(2t)$. In addition, the actual friction is assumed to be described by the "Coulomb" model, while the GCFO observer is used to estimate the friction.

The results of the simulations are shown in Figure 5.1. As it can be seen from the graphs, the response of the actual system is very much closer to the response of the ideal when friction cancellation is applied.

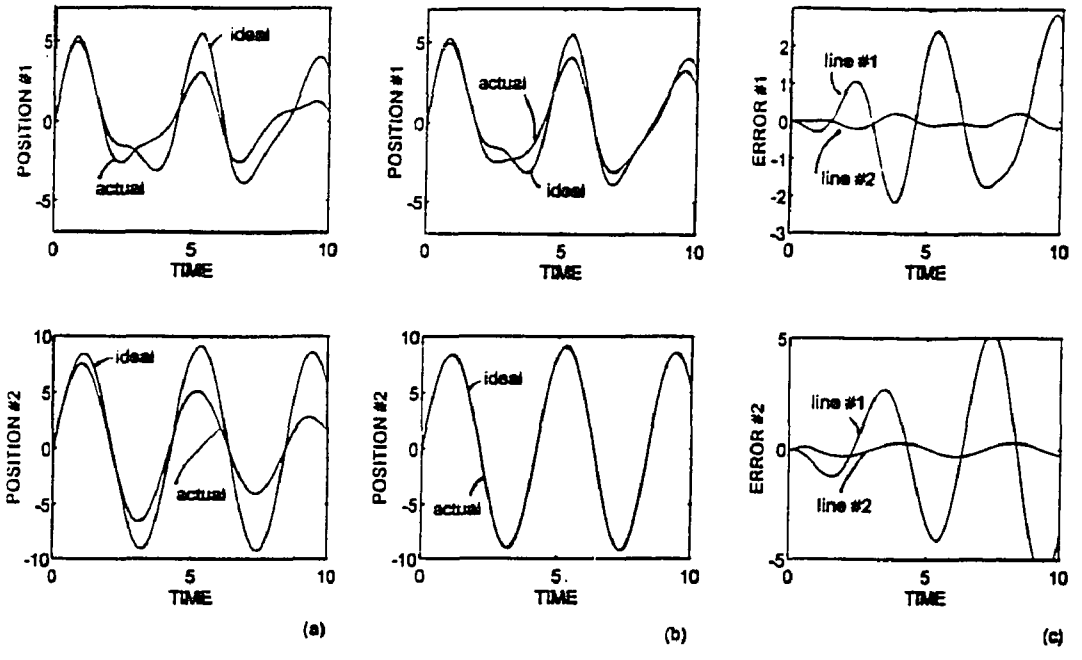

Figure 5.1 (a) Transient responses of the masses of the actual system (with friction and without friction cancellation) and the ideal system (b) Transient responses of the masses of the actual system (with friction and friction cancellation) and the ideal system (c) Lines #1 and #2 show the error between the transient responses of Figures (a) and (b) respectively.

CHAPTER 6

ADAPTIVE COMPENSATION OF DYNAMIC FRICTION IN A SINGLE DEGREE–OF–FREEDOM SYSTEM

6.1 Introduction

The problem considered in this chapter is the estimation and cancellation of friction in a single degree–of–freedom system assuming that friction is described by a dynamic model, (Dahl, 1976, Haessig et al., 1991) rather than a memoryless model that has been considered in the previous chapters.

Evidence is mounting that friction is a dynamic phenomenon, i.e., that a zero–memory nonlinearity does not adequately capture the true nature of friction (Dahl, 1976, Haessig et al., 1991, Armstrong–Hélouvry, 1991, Hess et al., 1991, Canudas et al., 1993) The dynamic effects of friction, however, are often small and difficult to measure. Therefore it would be natural to ask whether it is permissible to ignore them in designing a compensation technique that relies upon a model of the friction.

In the present chapter the performance of three friction estimators are compared. The first (CFO) is the one proposed by Friedland et al. (1991), and is designed based on the Coulomb friction model. The second proposed observer (TO) is based on the tracking of the total friction force F as an unknown bias (also presented in the previous chapters). The third observer (DFO), proposed in this chapter, incorporates an assumed dynamic friction model (i.e., Dahl or the reset–integrator).

If the velocity is not directly measured, another reduced–order observer is used to estimate it. Conditions for stability of the estimators are derived in the absence of a velocity observer and in the presence thereof.

To compare the performance of the proposed observers in estimating dynamic friction, simulations were conducted.

6.2 Statement of the Problem

The dynamic process studied is assumed to be a single mass acted upon by a friction force F and a control force w. Accordingly, the overall dynamics of the process are represented by

$$\dot{x} = v \tag{6.1}$$

$$\dot{v} = w - F \tag{6.2}$$

where x and v are the position and velocity of the mass, respectively. The friction force F is given by

$$F = af \tag{6.3}$$

$$\dot{f} = \xi(v, f) \tag{6.4}$$

where the parameter a is the coefficient of friction that multiplies the normalized friction f, and $\xi(v, f)$ is assumed to be a bounded function as long as v and f are bounded.

The function $\xi(v, f)$ varies between the different friction models. Specifically, for the "reset integrator" friction model

$$\xi(v, f) = c[v - \phi^{-1}(f)] \tag{6.5}$$

where c is a constant that determines the width of the hysteresis and $\phi^{-1}(f)$ is the inverse function of $\phi(\cdot)$. $\phi(v) = -\phi(-v)$ is a function of the velocity which can be assumed to vary between ± 1. For implementation purposes suitable analytical approximations for $\phi(\cdot)$ and its inverse should be used.

Another model, considered in this thesis is the Dahl model. For this model the function $\xi(v, f)$ has the following form:

$$\xi(v, f) = cv|1 - f\phi(v)|^i \text{sgn}[1 - f\phi(v)] \tag{6.6}$$

where i determines the slope of the friction curve.

Now, as has already been mentioned in the Chapters 2 and 3, for friction cancellation, the input w should be of the form

$$w = u + \hat{F} \tag{6.7}$$

where $\hat{F}$ is the estimate of friction and u is given as

$$u = -g_1(x - x_r) - g_2 v \tag{6.8}$$

with x_r to be a reference position and the coefficients g_1 and g_2 to be selected to satisfy desired performance specifications.

The problem considered in this chapter is the estimation and cancellation of dynamic friction F in the system (6.1)-(6.2).

6.3 Observer Dynamics

Defining $\hat{a}$, $\hat{f}$ and $\hat{F}$ to represent the estimates of a, f and F, respectively, the dynamics of the three friction observers studied below are:

6.3.1 Coulomb Friction Observer (CFO)

This observer is designed based upon a Coulomb friction model and is described as follows

$$\hat{F} = (z_F - k_F \mid v \mid^{\mu})\text{sgn}(v) \tag{6.9}$$

$$\dot{z}_F = k_F \, \mu |v|^{\mu-1}(w - \hat{F}) \, \text{sgn}(v) \tag{6.10}$$

where z_F is the observer state and k_F is the observer gain to be chosen by the designer to ensure convergence of the error to zero.

6.3.2 Tracking Observer (TO)

This observer is based upon the tracking of the total friction force F. Its dynamics are given by:

$$\hat{F} = z + k_1 x + k_2 v \tag{6.11}$$

$$\dot{z} = -k_1 v - k_2(w - \hat{F}) \tag{6.12}$$

where z is the observer state and k_1, k_2 are the observer gains to be chosen by the designer to ensure convergence of the error to zero.

6.3.3 Dynamic Friction Observer (DFO)

This observer is designed based upon a dynamic model for f, and estimates of the friction coefficient a and the normalized friction force f. Specifically

$$\hat{a} = z_a + k_a \hat{f} v \tag{6.13}$$

$$\hat{f} = z_f + k_{f1} x + k_{f2} v \tag{6.14}$$

with

$$\begin{aligned} \dot{z}_a &= -k_a v \xi_1(v, \hat{f}) - k_a \hat{f}(w - \hat{F}) \\ \dot{z}_f &= -k_{f1} v - k_{f2}(w - \hat{F}) + \xi_1(v, \hat{f}) \end{aligned}$$

and

$$\hat{F} = \hat{a}\hat{f} \tag{6.15}$$

where z_a, z_f are the observer states and k_a, k_{f1} and k_{f2} are the observer gains to be chosen by the designer to ensure convergence of the error to zero. The function $\xi_1(\cdot,\cdot)$ corresponds to the dynamic friction model based on which the observer is designed, and may not be the same as the function $\xi(\cdot,\cdot)$ used to describe the actual friction model.

6.4 Selection of Gains and Error Analysis

To establish conditions for the gains k_F, k_1, k_2, k_a, k_{f1} and k_{f2}, we consider the error between the true friction force F and its estimate $\hat{F}$:

$$e_F = F - \hat{F} \tag{6.16}$$

Differentiating both sides of the above equation and using (6.4) through (6.15), an analytic expression for each observer is derived that describes the rate of change of the estimation error e_F.

6.4.1 Coulomb Friction Observer (CFO)

The differential equation of the error e_F is

$$\begin{aligned} \dot{e}_F &= \dot{F} - \dot{\hat{F}} \\ &= \dot{F} - \dot{z}_F \operatorname{sgn}(v) - k_F \mu |v|^{\mu-1} \dot{v} \\ &= \dot{F} - k_F \mu |v|^{\mu-1} e_F \end{aligned} \tag{6.17}$$

The following conditions are sufficient for exponential stability of the estimation error in a neighborhood of zero:

1. $\mu > 0$
2. $k_F > 0$
3. dF/dt bounded

assuming that v is bounded away from the origin. Notice that Condition 2 is assumed to be valid by the statement of the problem as long as the system velocity and friction force remain bounded.

6.4.2 Tracking observer (TO)

The differential equation of the error e_F is

$$\begin{aligned} \dot{e}_F &= \dot{F} - \dot{\hat{F}} \\ &= \dot{F} - \dot{z} - k_1 v - k_2 \dot{v} \\ &= k_2 e_F + \dot{F} \end{aligned} \tag{6.18}$$

In order for the solution of this differential equation to remain in a neighborhood of the origin, the following conditions must be valid:

1. $k_2 < 0$

2. dF/dt bounded

Notice that there is no restriction on k_1.

6.4.3 Dynamic Friction Observer (DFO)

This observer is second order, therefore two differential equations are needed to describe the propagation of the error. Define

$$e_a = a - \hat{a} \tag{6.19}$$

$$e_f = f - \hat{f} \tag{6.20}$$

Then, differentiating equations (6.19) and (6.20) and using (6.13) and (6.14) yields

$$\begin{aligned} \dot{e}_f &= \dot{f} - \dot{\hat{f}} \\ &= k_{f2} a e_f + k_{f2} f e_a - k_{f2} e_a e_f + \xi(v, f) - \xi_1(v, \hat{f}) \end{aligned} \tag{6.21}$$

and

$$\begin{aligned} \dot{e}_a &= \dot{a} - \dot{\hat{a}} \\ &= -k_a(f + k_{f2} v - e_f)(a e_f + f e_a - e_a e_f) \end{aligned} \tag{6.22}$$

The above differential equations are not homogeneous if the model for which the observer is designed does not match the actual friction model.

The Jacobian matrix $\mathbf{\Psi}$ of equations (6.21), calculated at $e_f = e_a = 0$, is

$$\mathbf{\Psi} = \begin{bmatrix} k_{f2} a + \xi_{1f}(v, f) & k_{f2} f \\ -k_a a(f + k_{f2} v) & -k_a f(f + k_{f2} v) \end{bmatrix} \tag{6.23}$$

where $\xi_1 f(v, f) = \frac{\partial \xi_1(v, f)}{\partial f}$. If the gains can be picked such that $\mathbf{\Psi}$ has eigenvalues in the left half plane, $||\mathbf{\Psi}||$ bounded and $||\dot{\mathbf{\Psi}}||$ is sufficiently small, the estimation error is exponentially stable and will converge in a neighborhood of the origin (the size of which depends on $|\xi(v, f) - \xi_1(v, f)|$).

To find the conditions under which matrix Ψ has eigenvalues in the left half plane the Routh-Hurwitz criterion can be applied. Using this criterion it is found that it is sufficient to pick the gains as follows:

1. $k_a f(f + v k_{f2}) > 0$
2. $0 < k_{f2} < \dfrac{k_a f(f + v k_{f2}) + \xi_{1f}(v, f)}{a}$
3. $\dfrac{\partial \xi_1(v, f)}{\partial f} < 0$

The requirement that the rate of change of $\xi(v, f)$ with respect to f is less than zero is satisfied if $\xi(v, f)$ describes the Dahl model, (6.6), or the "reset-integrator" model (6.5):

If the DFO observer is designed based on Dahl friction model, then $\xi_1(v, f)$ is given by (6.6) and Condition 3 is always satisfied since

$$\frac{\partial \xi_1(v, f)}{\partial f} = -c\, v\, \phi(v)\, i\, |1 - f\phi(v)|^{i-1}$$

As it has already been mentioned, $\phi(v)$ is an odd function, therefore $v\phi(v) > 0$, and c is the width of the hysteresis which is a positive scalar. Hence $\partial \xi_1(v, f)/\partial f < 0$.

If the DFO observer is designed based on reset-integrator model, then $\xi_1(v, f)$ is given by (6.5) and Condition 3 is always satisfied since

$$\frac{\partial \xi_1(v, f)}{\partial f} = -c \frac{\partial \phi^{-1}(f)}{\partial f} < 0$$

since $\phi^{-1}(f)$ is a monotonically increasing function.

6.5 Friction Estimation Without Velocity Measurements

The foregoing analysis was based on direct measurements of the velocity of the mass. However, if only the position of the mass can be observed, it is necessary to estimate the velocity as well. The resulting overall observer is configured as two coupled reduced-order observers as shown in Figure 3.1. The first uses the measured

position and the estimate of the friction to provide an estimate of the velocity, and the second uses the estimate of the velocity to estimate the friction.

The dynamics of the velocity observer are

$$\hat{v} = z_v + k_v x \tag{6.24}$$

$$\dot{z}_v = u - k_v \hat{v} \tag{6.25}$$

where $\hat{v}$ is the estimate of the velocity and k_v is the corresponding observer gain.

6.6 Combining Velocity and Friction Observers

When the velocity observer is used, the estimate $\hat{v}$ replaces the true velocity v in the friction observers.

The gains of the combined friction–velocity observers are established by placing the poles of the dynamic system defined by the estimation errors:

$$\dot{e}_v = \dot{v} - \dot{\hat{v}} = q_v(e_v, e_F) \tag{6.26}$$

$$\dot{e}_F = \dot{F} - \dot{\hat{F}} = q_F(e_v, e_F) \tag{6.27}$$

The error analysis will be studied below for each of the three friction observers.

6.6.1 Coulomb Friction Observer (CFO)

In the case of unmeasurable velocities the Coulomb friction observer is considered with $\mu = 1$. Then,

$$q_v(e_v, e_F) = -k_v e_v - e_F$$

$$q_F(e_v, e_F) = k_F\, k_v e_v + \dot{F}$$

and

$$\mathbf{\Psi} = \begin{bmatrix} -k_v & -1 \\ k_F k_v & 0 \end{bmatrix} \tag{6.28}$$

The error converges in a neighborhood of zero if $\dot{F}$ is bounded and the Jacobian matrix $\mathbf{\Psi}$ is negative definite, and bounded away from the origin. The conditions for the Jacobian matrix to be negative definite are the following:

1. $k_v > 0$

2. $k_F > 0$

6.6.2 Tracking Observer (TO)

For this observer

$$\begin{aligned} q_v(e_v, e_F) &= -k_v e_v - e_F \\ q_F(e_v, e_F) &= -(k_1 + k_2 k_v) e_v + \dot{F} \end{aligned}$$

and the Jacobian matrix is given by

$$\Psi = \begin{bmatrix} -k_v & -1 \\ -k_1 - k_2 k_v & 0 \end{bmatrix} \tag{6.29}$$

As in the case of the first observer, the error converges in a neighborhood of zero if $\dot{F}$ is bounded and the Jacobian matrix Ψ is negative definite, and bounded away from the origin. The conditions for the Jacobian matrix to be negative definite are the following:

1. $k_v > 0$

2. $k_1 + k_2 k_v < 0$

6.6.3 Dynamic Friction Observer (DFO)

The parameter–estimating observer has third–order dynamics; hence three differential equations are needed to characterize the error propagation:

$$\dot{e}_v = \dot{v} - \dot{\hat{v}} = q_v(e_v, e_a, e_f, v, F) \tag{6.30}$$

$$\dot{e}_a = \dot{a} - \dot{\hat{a}} = q_a(e_v, e_a, e_f, v, F) \tag{6.31}$$

$$\dot{e}_f = \dot{f} - \dot{\hat{f}} = q_f(e_v, e_a, e_f, v, F) \tag{6.32}$$

where

$$q_v(e_v, e_a, e_f, v, F) = -k_v e_v - e_F$$

$$q_a(e_v, e_a, e_f, v, F) = -k_a[(v - e_v)(k_{f1} + k_{f2}k_v) + k_v(f - e_f)]e_v$$

$$q_f(e_v, e_a, e_f, v, F) = -k_{f1}e_v - k_{f2}k_v e_v + \xi(v, f) - \xi_1(v - e_v, f - e_f)$$

The Jacobian matrix of the above equations, Ψ, where

$$\Psi = \begin{bmatrix} \frac{\partial q_v}{\partial e_v} & \frac{\partial q_v}{\partial e_a} & \frac{\partial q_v}{\partial e_f} \\ \frac{\partial q_a}{\partial e_v} & \frac{\partial q_a}{\partial e_a} & \frac{\partial q_a}{\partial e_f} \\ \frac{\partial q_f}{\partial e_v} & \frac{\partial q_f}{\partial e_a} & \frac{\partial q_f}{\partial e_f} \end{bmatrix}$$

$$= \begin{bmatrix} -k_v & -f & -a \\ -k_a(v(k_{f1} + k_{f2}k_v) + k_v f) & 0 & 0 \\ \frac{\partial \xi_1(v, f)}{\partial v} - k_{f1} - k_{f2}k_v & 0 & \frac{\partial \xi_1(v, f)}{\partial f} \end{bmatrix}$$

determines the local behavior of the estimation error. In order for the matrix Ψ to be negative definite, the following conditions are sufficent:

1. $k_v > a > 0$
2. $-k_a[vf(k_{f1} + k_{f2}k_v) + k_v f^2] > 0$
3. $\frac{\partial \xi_1(v, f)}{\partial f} < 0$

For the second condition, note that $vf > 0$. Thus, choosing $k_a < 0$ and $k_{f1} + k_{f2}k_v > 0$ ensures that Condition 2 is satisfied. The third condition is always valid for a Dahl or "reset integrator" model, as it has been shown in section 1.4.3. If these conditions are met $||\Psi||$ is bounded and $||\dot{\Psi}||$sufficiently small, the error differential equations are exponentially stable. Finally, since the error dynamic system is not homogeneous, another condition should be added ($|\xi(v, f) - \xi_1(v, f)| < \epsilon$), to ensure convergence of the error around zero.

6.7 Simulated Performance

The three observers are compared in a simulation study. For the simulations, we consider the ideal system (the system with no friction), with input u given by (6.8) where the gains g_1 and g_2 are chosen to be $g_1 = 200$ and $g_2 = 20$. The closed loop ideal system, with this input u, has a natural frequency of $10\sqrt{2}$ and a damping factor 0.707. In addition, the actual system, given by (6.1)–(6.2), is assumed to have the input w, given by (6.7), and u the same as the ideal. The reference position is a square wave with a frequency of 0.5 Hz. Moreover, white noise with an rms value of 0.1 is added to the measured position for verisimilitude.

As a dynamic friction model is assumed the reset integrator model. The function $\phi(\cdot)$, in the dynamic friction model, is approximated by

$$\phi^{-1}(f) = \begin{cases} D_1(f-1) + D_2, & f > 1 \\ D_2 f, & -1 < f < 1 \\ D_1(f+1) - D_2, & f < -1 \end{cases} \tag{6.33}$$

with $D_1 = 1000$ and $D_2 = 0.0001$. The friction coefficient a and the model gain c were set to 50 and 100, respectively. In addition, the third observer was designed based upon the reset integrator model.

As expected, the DFO observer, based upon the estimation of the parameters of an otherwise completely defined model, performs the best in estimating the friction level (Figure 6.1a). The tracking observer also performs remarkably well, even capturing the hysteresis effect (Figure 6.1b). The first observer, CFO, is most sensitive to observation noise. (The effect of noise is scarcely perceptible with the other observers.) But, although it does not capture the hysteresis effect, it estimates the friction level very well after a short transient period (Figure 6.1c).

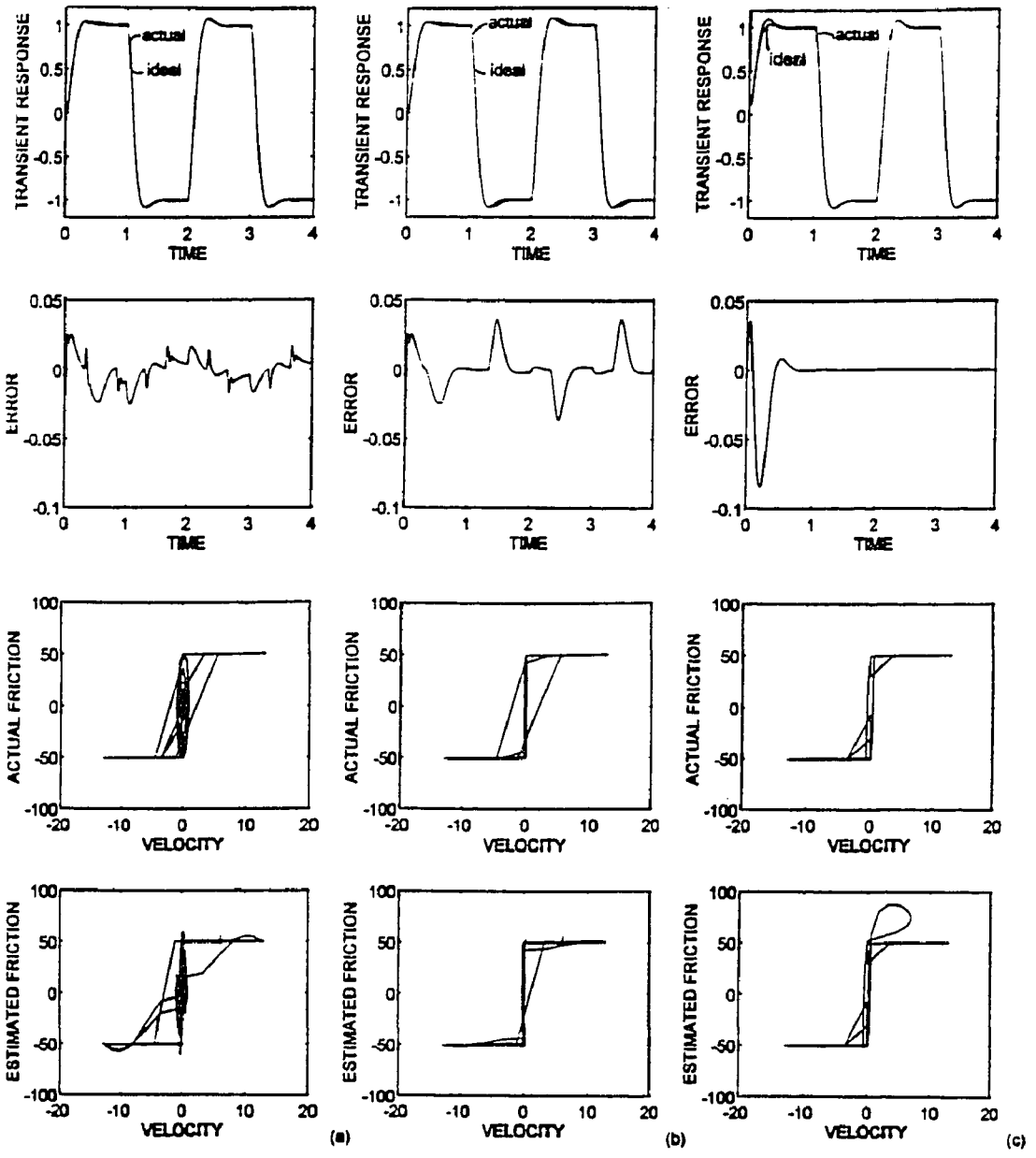

Figure 6.1 Actual and ideal transient response, error between the actual and ideal system response, actual friction, and estimated friction using (a) the CFO compensator, with $k_F = 100$, $\mu = 1$ and $k_v = 100$ (b) the TO compensator, with $k_1 = 0$, $k_2 = -100$ and $k_v = 100$ (c) the DFO compensator, with $k_{f1} = -0.01$, $k_{f2} = 0$, $k_a = -10$ and $k_v = 100$

CHAPTER 7

ADAPTIVE ESTIMATION OF DYNAMIC FRICTION IN A MULTIPLE DEGREE-OF-FREEDOM SYSTEM

7.1 Introduction

The problem considered in this chapter is the estimation of friction in a multiple degree-of-freedom system assuming that friction is described by a dynamic model. The results of this chapter are an extension to those presented in Chapter 6, for systems with multiple degrees-of-freedom and friction sources.

Two friction estimators, generalization of those presented before, are proposed and compared. The first is the generalized dynamic friction observer designed based on a dynamic friction model (GDFO); the second (GTO) is the generalized tracking observer presented in Chapter 4.

For the analysis both the cases of measurable and unmeasurable system "velocities" are considered.

Finally, favorable simulation results verify the theoretical analysis. The results indicate that the dynamic effects of friction in control systems can be dealt with effectively.

7.2 Statement of the Problem

A system with multiple degrees-of-freedom, as has already been mentioned, is consisted from one or more masses characterized by translational motion in one or more directions and/or rotational motion. In the following analysis the case of rotational motion perpendicular to planar translational will be considered as well as translational motion in three dimensions.

The dynamic model that describes such a system is the following

$$\dot{x} = v \tag{7.1}$$

$$M(x)\dot{v} = g(x,v,w) - F \tag{7.2}$$

where

$$x = [x_1\ x_2\ \cdots\ x_n]' \tag{7.3}$$

$$v = [v_1\ v_2\ \cdots\ v_n]' \tag{7.4}$$

and x_i and v_i are the ith "position" and "velocity". The mass matrix M is symmetric and positive definite. Vector $g(x,v,w)$ is a function of position and velocity, as well as of the external non-frictional input w to the system and represents the total system force vector; F is the friction vector.

Assuming that the friction between two surfaces is described by a "dynamic" model, then it can be shown (see Appendix A), that the friction force vector can be written in the following form

$$F = U\mathcal{A}\,f \tag{7.5}$$

where

$$\mathcal{A} = \mathrm{diag}\{a\} = \begin{bmatrix} a_1 & \cdots & 0 \\ \vdots & \ddots & \vdots \\ 0 & \cdots & a_\nu \end{bmatrix} \tag{7.6}$$

and

$$\dot{f} = \xi(U'v, f) \tag{7.7}$$

with

$$\xi(U'v,f) = [\xi_1(\bar{v}_1, f_1)\cdots\xi_\nu(\bar{v}_\nu, f_\nu)]' \tag{7.8}$$

and

$$f = [f_1 \cdots f_\nu]' \tag{7.9}$$

Vector a contains the unknown friction coefficients; U is a known $n \times \nu$ matrix; $\xi_i(\bar{v}_i, f_i)$ is a function that depends on the assuming dynamic model (Dahl, reset integrator, etc.) and for the analysis is assumed bounded if $\bar{v}_i$ and f_i are both bounded. Notice that $\xi_i(\cdot,\cdot)$ may not be the same as $\xi_j(\cdot,\cdot)$ for $i \neq j$.

The problem considered in this chapter is the estimation of the friction force vector F.

7.3 Observer Dynamics

Defining $\hat{a}$, $\hat{f}$ and $\hat{F}$ to represent the estimates of a, f and F respectively, the dynamics of the two friction observers studied in this chapter are:

7.3.1 Generalized Dynamic Friction Observer (GDFO)

This observer is based on the estimation of the friction coefficient a and the normalized friction f, using an assumed correct dynamic model for f. Specifically

$$\hat{a} = z_a + K_a \text{diag}\{\hat{f}\}U'v \tag{7.10}$$

$$\hat{f} = z_f + K_{f1}x + K_{f2}v \tag{7.11}$$

with

$$\dot{z}_a = -K_a \text{diag}\{U'v\}\xi(U'v, \hat{f}) - K_a \text{diag}\{\hat{f}\}U'M^{-1}(x)\,[g(x,v,w) - \hat{F}]$$

$$\dot{z}_f = -K_{f1}v - K_{f2}M^{-1}(x)\,[g(x,v,w) - \hat{F}] + \xi(U'v, \hat{f})$$

and

$$\hat{F} = U \text{diag}\{\hat{a}\}\hat{f} \tag{7.12}$$

where z_a, z_f are the observer states and K_a, K_{f1} and K_{f2} are the observer gains to be chosen by the designer to ensure convergence of the error to zero.

7.3.2 Generalized Tracking Observer (GTO)

Assuming that $\hat{F}$ is the estimate vector of F, the following alternate observer to estimate the dynamic friction vector F is proposed.

$$\hat{F} = z + K_1 x + K_2 v \tag{7.13}$$

with

$$\dot{z} = -K_1 v - K_2 M^{-1}(x)\,[g(x,v,w) - \hat{F}] \tag{7.14}$$

where K_1 and K_2 are matrices to be chosen by the designer to ensure convergence of the error to zero.

7.4 Selection of Gains and Error Analysis

To determine the gains K_1, K_2, K_a, K_{f1} and K_{f2} the error between the true and the estimated friction parameters is considered.

7.4.1 Generalized Dynamic Friction Observer (GDFO)

For this observer two sets of differential equations are needed to describe the propagation of the error. Define

$$e_a = a - \hat{a} \tag{7.15}$$

$$e_f = f - \hat{f} \tag{7.16}$$

Then, differentiating equations (7.15) and (7.16) and using (7.10) and (7.11), yields

$$\begin{aligned} \dot{e}_f &= \dot{f} - \dot{\hat{f}} \\ &= \xi(U'v, f) - \dot{z}_f - K_{f1}v - K_{f2}M^{-1}(x)\,[g(x,v,w) - U\mathrm{diag}\{a\}f] \\ &= K_{f2}M^{-1}(x)\,U[\mathrm{diag}\{\hat{f}\}e_a + \mathrm{diag}\{\hat{a}\}e_f - \mathrm{diag}\{\hat{e}_a\}e_f] + \xi(U'v, f) - \xi(U'v, \hat{f}) \end{aligned} \tag{7.17}$$

and

$$\begin{aligned} \dot{e}_a &= \dot{a} - \dot{\hat{a}} \\ &= -\dot{z}_a - K_a\mathrm{diag}\{U'v\}\dot{\hat{f}} - K_a\mathrm{diag}\{\hat{f}\}U'\dot{v} \\ &= K_a[\mathrm{diag}\{U'v\}K_{f2} + \mathrm{diag}\{\hat{f}\}U']M^{-1}(x)\,U[\mathrm{diag}\{\hat{f}\}e_a + \mathrm{diag}\{\hat{a}\}e_f \\ &\quad -\mathrm{diag}\{\hat{e}_a\}e_f] \end{aligned} \tag{7.18}$$

The equilibrium point for the above differential equations (7.17) and (7.18), is the origin, as it can easily be shown, i.e., $e_{f_0} = e_{a_0} = 0$. The local stability for the

above system is determined by the nature of the Jacobian matrix:

$$\Psi = \left[\begin{array}{cc} \frac{\partial \dot{e}_f}{\partial e_f} & \frac{\partial \dot{e}_f}{\partial e_a} \\ \\ \frac{\partial \dot{e}_a}{\partial e_f} & \frac{\partial \dot{e}_a}{\partial e_a} \end{array} \right]_{e=0} = \left[\begin{array}{cc} \Psi_{11} & \Psi_{12} \\ \Psi_{21} & \Psi_{22} \end{array} \right] \tag{7.19}$$

Analytically, we have

$$\begin{aligned} \Psi_{11} &= K_{f2} M^{-1}(x)\, U \mathrm{diag}\{a\} + \frac{\partial \xi(U'v, f)}{\partial f} \\ \Psi_{12} &= K_{f2} K^{-1} U \mathrm{diag}\{f\} \\ \Psi_{21} &= K_a [\mathrm{diag}\{U'v\} K_{f2} + \mathrm{diag}\{f\} U'] M^{-1}(x)\, U \mathrm{diag}\{a\} \\ \Psi_{22} &= K_a [\mathrm{diag}\{U'v\} K_{f2} + \mathrm{diag}\{f\} U'] M^{-1}(x)\, U \mathrm{diag}\{f\} \end{aligned}$$

To assure local exponential stability, the gains K_a and K_{f2}, should be picked such that the eigenvalues of Ψ lie in the open left half plane, $||\Psi||$ is bounded and $||\dot{\Psi}||$ is sufficient small. Notice that K_{f1} doesn't appear in matrix Ψ; therefore there is no restriction on how to choose it.

7.4.2 Generalized Tracking Observer (GTO)

Consider the error e_F between the friction force F and its estimate $\hat{F}$:

$$e_F = F - \hat{F} \tag{7.20}$$

Differentiating both sides of the above equation and using equations (7.7) through (7.12), the following analytic expression, that describes the rate of change of the error e_F, yields

$$\begin{aligned} \dot{e}_F &= \dot{F} - \dot{\hat{F}} \\ &= \dot{F} - \dot{z} - K_1 \dot{v} - K_2 \dot{v} \\ &= K_2 M^{-1}(x) e_F + \dot{F} \end{aligned} \tag{7.21}$$

The above differential equation is not homogeneous if vector F is not a constant. If the gain K_2 is picked to ensure exponential stability and $\dot{F}$ is bounded, the error will

be bounded in a neighborhood of the origin (Brockett, 1970). Notice that there is no any condition imposed on the gain K_1.

Next, it will be shown that the rate of change of the friction vector F is bounded when the normalized friction vector elements f_i are bounded.

The friction force vector is written in the form:

$$F = U\,\mathcal{A}\,f \tag{7.22}$$

Then, differentiating the above equation, yields

$$\dot{F} = \dot{U}\,\mathcal{A}\,f + U\dot{\mathcal{A}}\,f + U\mathcal{A}\dot{f} \tag{7.23}$$

Since the friction coefficients a_i are constants, matrix $\mathcal{A}$ is constant and $\dot{\mathcal{A}}$ is zero. Matrix U is in general a function of the positions x. It is reasonable to assume that the states x as well as the velocities are bounded and so matrices U and $\dot{U}$. It is reasonable also to assume the normalized friction vector f to be bounded when the system velocities and accelerations are bounded. In addition, vector $\dot{f}$ is bounded since, by assumption at the statement of the problem, $\xi_i(\bar{v}_i, f_i)$ are bounded when $\bar{v}_i$ and f_i are both bounded. Finally, since all the terms of equation (7.23) are bounded, $\dot{F}$ is bounded.

7.5 Friction Estimation Without Velocity Measurements

In the foregoing analysis, assuming that the entire state vector of the system is available for measurements, two nonlinear observers to estimate the friction force vector were proposed. In this section, however, only the position x is assumed to be measurable. Therefore, in order to estimate the unmeasurable velocities, an additional nonlinear reduced order state observer is used. This observer is combined in cascade with the observers of the previous sections to estimate the friction vector.

7.5.1 Velocity Observer "Architecture"

Assuming that $\hat{v}$ represents the estimate of the velocity v, the observer to estimate the velocity is:

$$\hat{v} = z_v + K_v x \tag{7.24}$$

with

$$\dot{z}_v = -K_v \hat{v} + M^{-1}(x)\,[g(x, \hat{v}, w) - \hat{F}] \tag{7.25}$$

where K_v is the designed parameter matrix.

The latter observer uses as inputs the measurements of the positions x as well as the estimates of the previously proposed observers (7.10)–(7.12) or (7.13)–(7.14), to estimate the velocities of the masses.

7.6 Combining Velocity and Friction Observers

When the velocity observer is used, the estimate $\hat{v}$ replaces in the friction observers the true velocity v.

7.6.1 Generalized Dynamic Friction Observer (GDFO)

For the parameter–estimating observer three sets of differential equations are needed to characterize the error propagation:

$$\dot{e}_v = \dot{v} - \dot{\hat{v}} = q_v(e_v, e_a, e_f, v, F) \tag{7.26}$$

$$\dot{e}_a = \dot{a} - \dot{\hat{a}} = q_a(e_v, e_a, e_f, v, F) \tag{7.27}$$

$$\dot{e}_f = \dot{f} - \dot{\hat{f}} = q_f(e_v, e_a, e_f, v, F) \tag{7.28}$$

where

$$\begin{aligned} q_v(e_v, e_a, e_f, v, F) &= -K_v e_v + M^{-1}(x)\,[g(x, v, w) - g(x, v - e_v, w)] \\ &\quad -M^{-1}(x)\,U[\mathrm{diag}\{f - e_f\}e_a + \mathrm{diag}\{a - e_a\}e_f - \mathrm{diag}\{e_a\}e_f] \\ q_a(e_v, e_a, e_f, v, F) &= -K_a \mathrm{diag}\{f - e_f\}U' K_v e_v - K_a \mathrm{diag}\{U'(v - e_v)\}(K_{f1} + K_{f2}K_v)e_v \\ q_f(e_v, e_a, e_f, v, F) &= -(K_{f1} + K_{f2}K_v)e_v + \xi(v, f) - \xi(v - e_v, f - e_f) \end{aligned}$$

The Jacobian matrix for the above system of differential equations is

$$\Psi = \left[\begin{array}{ccc} \frac{\partial q_v}{\partial e_v} & \frac{\partial q_v}{\partial e_a} & \frac{\partial q_v}{\partial e_f} \\ \frac{\partial q_a}{\partial e_v} & \frac{\partial q_a}{\partial e_a} & \frac{\partial q_a}{\partial e_f} \\ \frac{\partial q_f}{\partial e_v} & \frac{\partial q_f}{\partial e_a} & \frac{\partial q_f}{\partial e_f} \end{array} \right]_{e_v=e_f=e_a=0} = \left[\begin{array}{ccc} \Psi_{11} & \Psi_{12} & \Psi_{13} \\ \Psi_{21} & \Psi_{22} & \Psi_{23} \\ \Psi_{31} & \Psi_{32} & \Psi_{33} \end{array} \right]$$

where

$$\begin{aligned} \Psi_{11} &= -K_v + M^{-1}(x)\frac{\partial g(x,v,w)}{\partial v} \\ \Psi_{12} &= -M^{-1}(x)\, U\mathrm{diag}\{f\} \\ \Psi_{13} &= -M^{-1}(x)\, U\mathrm{diag}\{a\} \\ \Psi_{21} &= -K_a[\mathrm{diag}\{f\}U'K_v + \mathrm{diag}\{U'v\}(K_{f1} + K_{f2}K_v)] \\ \Psi_{22} &= 0 \\ \Psi_{23} &= 0 \\ \Psi_{31} &= \frac{\partial \xi(v,f)}{\partial v} - K_{f1}K_{f2}K_v \\ \Psi_{32} &= 0 \\ \Psi_{33} &= \frac{\partial \xi(v,f)}{\partial f} \end{aligned}$$

The error converges exponentially to zero if the gains K_v, K_a, K_{f1} and K_{f2} are picked such that the Jacobian matrix has eigenvalues in the left half plane, $||\Psi||$ is bounded and $||\dot{\Psi}||$ is sufficiently small.

7.6.2 Generalized Tracking Observer (GTO)

Let us define the errors e_v and e_F as follows

$$\dot{e}_v = \dot{v} - \dot{\hat{v}} = q_v(e_v, e_F, v, F) \tag{7.29}$$

$$\dot{e}_F = \dot{F} - \dot{\hat{F}} = q_F(e_v, e_F, v, F) \tag{7.30}$$

where,

$$q_v(e_v, e_F, v, F) = -K_v e_v - M^{-1}(x)\, e_F + M^{-1}(x)\,[g(x, v, w) - g(x, \hat{v}, w)]$$

$$q_F(e_v, e_F, v, F) = -(K_1 + K_2 K_v) e_v + \dot{F}$$

The above differential equations are not homogeneous. If the gains K_v, K_1 and K_2 are picked to ensure exponential stability and $\dot{F}$ is bounded, the error will be bounded near the origin (Brockett, 1970).

The Jacobian matrix of the error equations is

$$\Psi = \begin{bmatrix} M^{-1}(x)\dfrac{\partial g(x, v, w)}{\partial v} - K_v & -M^{-1}(x) \\ -(K_1 + K_2 K_v) & 0 \end{bmatrix} \tag{7.31}$$

If the gain matrices can be picked such that Ψ has eigenvalues in the left half plane, $||\Psi||$ is bounded and $||\dot{\Psi}||$ is sufficiently small, the estimation error is exponentially stable.

7.7 Example: Two–Mass System (Continued)

Let us consider again the two–mass system (Figure 4.2). The system differential equations are

$$\begin{aligned} m_1 \dot{v}_1 &= -(\eta_2 + \eta_3) x_1 + \eta_3 x_2 - F_1 \\ m_2 \dot{v}_2 &= \eta_3 x_1 - (\eta_1 + \eta_3) x_2 + w - F_2 \end{aligned} \tag{7.32}$$

where F_1 and F_2 are the total friction forces applied to the top and bottom mass respectively. Specifically

$$F_1 = a_1 f_1 \tag{7.33}$$

$$F_2 = -a_1 f_1 + a_2 f_2 \tag{7.34}$$

As a dynamic friction model is assumed the reset integrator model, which yields

$$\dot{f}_1 = c_1[v_1 - v_2 - \phi^{-1}(f_1)] \tag{7.35}$$

$$\dot{f}_2 = c_2[v_2 - \phi^{-1}(f_2)] \tag{7.36}$$

where c_1, c_2 are constants that determine the width of the hysteresis. The function $\phi(v)$ is an odd function of the velocity which varies between ± 1. The function $\phi^{-1}(f)$ is the inverse function of $\phi(v)$. For implementation purposes suitable analytical approximations for $\phi(\cdot)$ and its inverse will be used.

The problem considered in this example is the estimation of the friction forces.

7.7.1 Observer "Architectures"

Generalized Dynamic Friction Observer (GDFO)

The dynamics of this observer are

$$\begin{aligned}
\hat{a}_1 &= z_{a1} + K_{a1}\hat{f}_1(\hat{v}_1 - \hat{v}_2) \\
\hat{a}_2 &= z_{a2} + K_{a2}\hat{f}_2\hat{v}_2 \\
\hat{f}_1 &= z_{f1} + K_{f11}x_1 + K_{f21}\hat{v}_1 \\
\hat{f}_2 &= z_{f2} + K_{f12}x_2 + K_{f22}\hat{v}_2
\end{aligned}$$

where

$$\begin{aligned}
\dot{z}_{a1} &= -K_{a1}\xi_1(\hat{v}_1 - \hat{v}_2, \hat{f}_1)[\hat{v}_1 - \hat{v}_2] - K_{a1}\hat{f}_1\{(m_1)^{-1}[-(\eta_2 + \eta_3)x_1 + \eta_3 x_2 - \hat{F}_1] \\
&\quad -(m_2)^{-1}[\eta_3 x_1 - (\eta_1 + \eta_3)x_2 + w - \hat{F}_2]\} \\
\dot{z}_{a2} &= -K_{a2}\hat{v}_2\xi_2(v_2, \hat{f}_2) - K_{a2}\hat{f}_2(m_2)^{-1}[\eta_3 x_1 - (\eta_1 + \eta_3)x_2 + w - \hat{F}_2] \\
\dot{z}_{f1} &= \xi_1(\hat{v}_1 - \hat{v}_2, \hat{f}_1) - K_{f11}\hat{v}_1 - K_{f21}(m_1)^{-1}[-(\eta_2 + \eta_3)x_1 + \eta_3 x_2 - \hat{F}_1] \\
\dot{z}_{f1} &= \xi_2(\hat{v}_2, \hat{f}_2) - K_{f12}\hat{v}_2 - K_{f22}(m_2)^{-1}[\eta_3 x_1 - (\eta_1 + \eta_3)x_2 + w - \hat{F}_2]
\end{aligned}$$

and

$$\begin{aligned}
\hat{F}_1 &= \hat{a}_1\hat{f}_1 \\
\hat{F}_2 &= \hat{a}_2\hat{f}_2 - \hat{a}_1\hat{f}_1
\end{aligned}$$

In the above equations, the gains matrices are assumed to be diagonal

$$K_a = \text{diag}\{K_{a1}, K_{a2}\}$$

$$K_{f1} = \text{diag}\{K_{f11}, K_{f12}\}$$
$$K_{f2} = \text{diag}\{K_{f21}, K_{f22}\}$$

Generalized Tracking Observer (GTO)

The dynamics of this observer are:

$$\hat{F}_1 = z_1 - k_{11}x_1 + k_{21}\hat{v}_1 \tag{7.37}$$
$$\hat{F}_2 = z_2 - k_{12}x_2 + k_{22}\hat{v}_2 \tag{7.38}$$

and

$$\dot{z}_1 = -k_{11}\hat{v}_1 - k_{21}(m_1)^{-1}[-(\eta_2+\eta_3)x_1 + \eta_3 x_2 - \hat{F}_1]$$
$$\dot{z}_2 = -k_{12}\hat{v}_2 - k_{22}(m_2)^{-1}[\eta_3 x_1 - (\eta_1+\eta_3)x_2 + w - \hat{F}_2]$$

where

$$K_1 = \text{diag}\{k_{11}, k_{12}\}$$
$$K_2 = \text{diag}\{k_{21}, k_{22}\}$$

Velocity Observer "Architecture".

Assuming that only the position is available for measurements, the observer to estimate the velocity is the following:

$$\hat{v}_1 = z_{v_1} + k_{v_1}x_1 \tag{7.39}$$
$$\hat{v}_2 = z_{v_2} + k_{v_2}x_2 \tag{7.40}$$

and

$$\dot{z}_{v_1} = -k_{v_1}\hat{v}_1 + (m_1)^{-1}[-(\eta_2+\eta_3)x_1 + \eta_3 x_2 - \hat{F}_1]$$
$$\dot{z}_{v_2} = -k_{v_2}\hat{v}_2 + (m_2)^{-1}[\eta_3 x_1 - (\eta_1+\eta_3)x_2 + w - \hat{F}_2]$$

where, $K_v = \text{diag}\{k_{v_1}, k_{v_2}\}$.

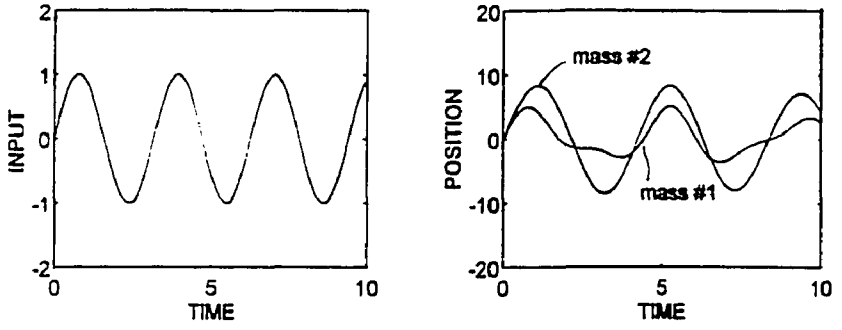

Figure 7.1 System input and transient response.

7.7.2 Simulation Results

For the simulations, the values of the system parameters are assumed to be $m_1 = 10$, $m_2 = 50$, $\eta_1 = 100$, $\eta_2 = 50$, $\eta_3 = 20$, $a_1 = 10$ and $a_2 = 20$. The measurements of the positions are considered to be contaminated with white noise with an rms value of 0.1. The input is sinusoidal with frequency π Hz. The system input and the transient response are shown in Figure 7.1.

As a dynamic friction model is assumed the reset integrator model. The function $\phi(\cdot)$, in the dynamic friction model, is approximated by

$$\phi^{-1}(f) = \begin{cases} D_1(f-1) + D_2, & f > 1 \\ D_2 f, & -1 < f < 1 \\ D_1(f+1) - D_2, & f < -1 \end{cases} \tag{7.41}$$

with $D_1 = 1000$ and $D_2 = 0.0001$. The friction coefficients a_1 and a_2 are picked 10 and 20, respectively. The friction model gains c_1 and c_2 are set to 100.

The results for the GDFO are shown in Figure 7.2a. The observer gain matrices used in the simulations are

$$\begin{aligned} K_a &= \text{diag}\{-30, -100\} \\ K_{f1} &= \text{diag}\{0.01, 0.01\} \\ K_{f2} &= \text{diag}\{0, 0\} \\ K_v &= \text{diag}\{10, 10\} \end{aligned}$$

Figure 7.2b shows the results for the GTO observer. The observers gain matrices, used at the simulations, are

$$\begin{aligned} K_1 &= \text{diag}\{0, 0\} \\ K_2 &= \text{diag}\{-1000, -5000\} \\ K_v &= \text{diag}\{10, 10\} \end{aligned}$$

As it can be seen from the simulations, the GDFO observer that is designed based on the actual friction model performs the best. The GTO observer is not able to track the hysteresis without a high gain, which results in a high transient response overshoot. Although it doesn't capture the hysteresis effect accurately, it estimates the friction level very well after a short transient period.

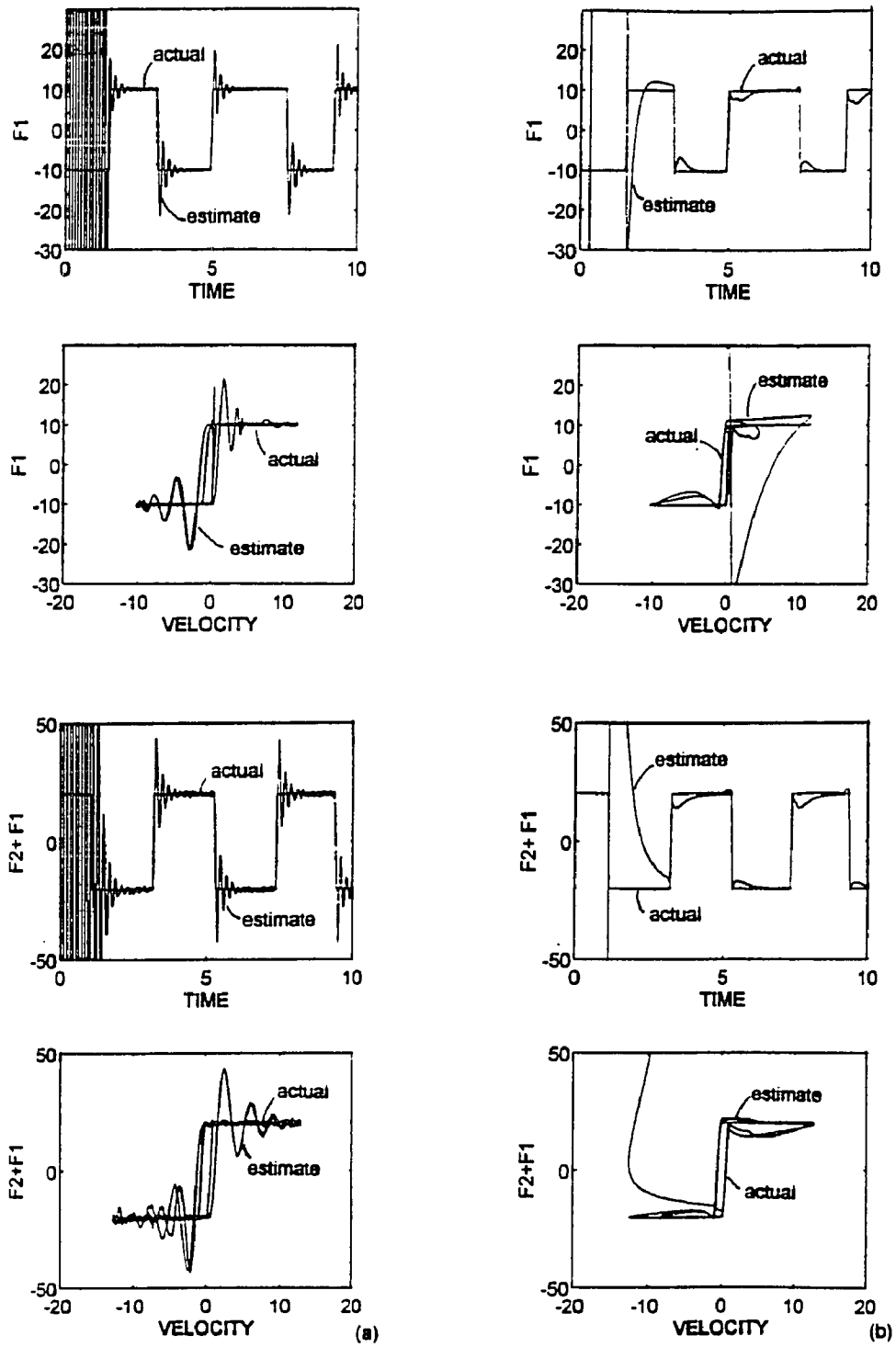

Figure 7.2 (a) Performance of the GDFO observer in estimating dynamic friction F_1 between the two masses and $(F_1 + F_2)$ between the second mass and the ground (b) Performance of the GTO observer in estimating the system friction forces.

CHAPTER 8

EXPERIMENTAL EVALUATION OF FRICTION ESTIMATION AND COMPENSATION TECHNIQUES

8.1 Introduction

In this chapter experimental results are reported on friction estimation and compensation. The goal of this experimental study is to help understand the nature of friction as well as to demonstrate the effectiveness of the algorithms proposed in the previous chapters.

The results reported in this chapter are a comparative study of four methods for estimating and cancelling the friction between two parallel rubbing surfaces. Four different observers are investigated for estimating the friction force. The first observer (CFO) is designed based on the classic Coulomb friction model; the second (TO) tracks the friction force as if it were an unknown bias; the third (DFOa) is based on the reset integrator dynamic model; and the fourth (DFOb) is based on Dahl's model of friction. The above observers were presented in Chapters 2, 3 and 6.

The results demonstrate not only the friction cancellation but also show the advantages and disadvantages of a dynamic friction description versus the classical "zero memory" friction representation.

8.2 Experimental Apparatus

The experimental apparatus used is shown in Figure 8.1. It consists of a motor driving one of two parallel metal circular plates. The position of the fixed plate can be adjusted with a micrometer screw thereby adjusting the normal force and hence the level of friction. Attached to the fixed surface is a disk of material to be used in the experiment.

The movable plate is driven by a d–c motor, the angular position of which is measured by an incremental encoder with an effective resolution of 2000 pulses

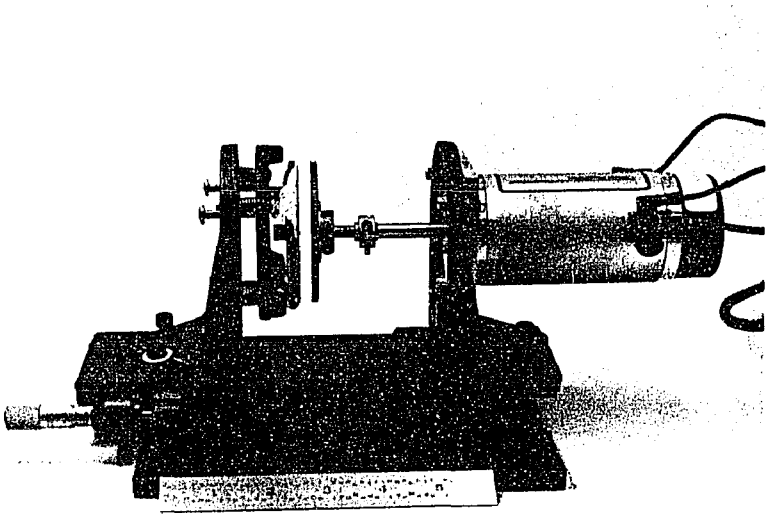

Figure 8.1 Experimental apparatus.

per revolution. Through an interfacing circuit consisting of a Hewlett–Packard HCTL2016 counter and some other interfacing logic, the output of the encoder is transmitted to an IBM Data Acquisition and Control Adapter (DACA) board residing in an MS–DOS (386–20) personal computer where the position count is converted to a 16 bit word. The algorithm to be evaluated is coded in C and implemented on the 386–20. The resulting control signal command, generated by the DACA board, is externally amplified in a power amplifier to provide the input to the brushes of the motor (Figure 8.2) .

The experiments, whose results are reported here, were conducted with a sampling frequency of 100 Hz; the integrals in the algorithms described below were computed numerically using a first-order Euler scheme.

The algorithms were tested by applying an internally–generated square wave reference input of ± 50 degrees amplitude. Without compensation, there is a steady

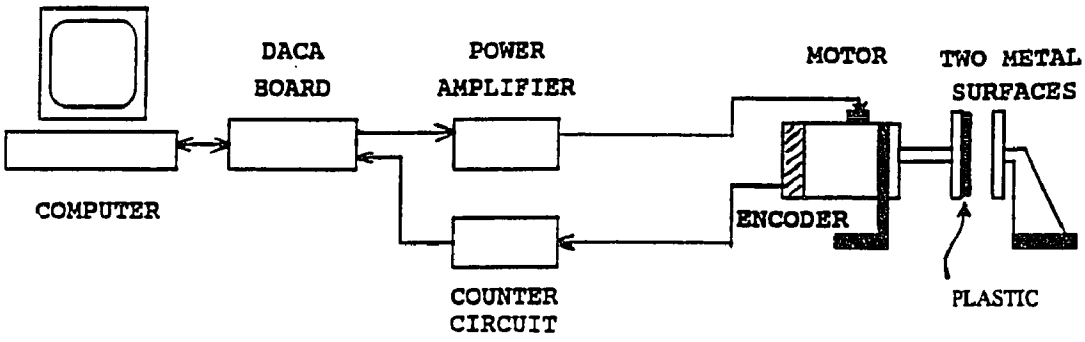

Figure 8.2 Experiment configuration.

state position error ("hang-off") proportional to the magnitude of the friction force which increases as the fixed plate is pressed harder against the movable plate.

8.3 Algorithms

The goal of this experiment is to evaluate the estimation and cancellation of friction. To this end, four different friction observers were studied and compared. Each observer comprises a velocity observer (which furnishes an estimate of the relative angular velocity of the surfaces) driving the friction observer under investigation.

Angular velocity estimation

The dynamics of the velocity observer are defined by

$$\hat{\omega} = z_\omega + k_\omega \theta \tag{8.1}$$

$$\dot{z}_\omega = -\hat{F} + \mathtt{w} - k_\omega \hat{\omega} \tag{8.2}$$

where $\hat{\omega}$ is the estimate of the angular velocity ω and k_ω is the scalar designed observer parameter.

The latter observer uses as inputs the measurements of the position θ, the estimate $\hat{F}$ of the friction force F, the external input $\mathtt{w}$ and estimates the shaft angular velocity

Friction estimation

For the analysis, the friction force F is assumed of the form

$$F = a\, f \tag{8.3}$$

where the parameter a is the coefficient of friction that multiplies the normalized friction f.

Defining $\hat{a}$, $\hat{f}$ and $\hat{F}$ to represent the estimates of a, f and F, respectively, the dynamics of the four friction observers are as follows:

Coulomb Friction Observer (CFO)

This observer is estimating the friction coefficient a under the assumption that $f = \mathrm{sgn}(\omega)$, and is given by

$$\hat{F} = (z_F + k_F \mid \hat{\omega} \mid)\mathrm{sgn}(\hat{\omega}) \tag{8.4}$$

$$\dot{z}_F = -k_F(\mathtt{w} - \hat{F})\mathrm{sgn}(\hat{\omega}) \tag{8.5}$$

where z_F is the observer state, and k_F is the observer gain to be chosen by the designer to ensure convergence of the error to zero, while θ and ω are the relative position and velocity of the surfaces, respectively.

Tracking Observer (TO)

This observer is based on the tracking of the total friction force F. Its dynamics are given by:

$$\hat{F} = z + k_1\theta + k_2\hat{\omega} \tag{8.6}$$

$$\dot{z} = -k_1\hat{\omega} - k_2(\mathtt{w} - \hat{F}) \tag{8.7}$$

where z is the observer state and k_1, k_2 are the observer gains to be chosen by the designer to ensure convergence of the error to zero.

"Reset Integrator Model" Based Observer (DFOa)

This observer is based on estimating the friction coefficient a and the normalized friction force f, using an assumed dynamic model for f. In accordance with the theory developed in Chapter 4, the observer dynamics are defined by

$$\hat{a} = z_a + k_a \hat{f}\hat{\omega} \tag{8.8}$$

$$\hat{f} = z_f + k_{f1}\theta + k_{f2}\hat{\omega} \tag{8.9}$$

with

$$\dot{z}_a = -k_a c\hat{\omega}^2 + k_a c\hat{\omega}\phi^{s1}(\hat{f}) + k_a \hat{a}\hat{f}^2 - k_a \hat{f}u$$

$$\dot{z}_f = -k_{f1}\hat{\omega} - k_{f2}(\mathtt{w} - \hat{a}\hat{f}) + c(\hat{\omega} - \phi^{-1}(\hat{f}))$$

and

$$\hat{F} = \hat{a}\hat{f} \tag{8.10}$$

where z_a, z_f are the observer states and k_a, k_{f1} and k_{f2} are the observer gains to be chosen by the designer to ensure convergence of the error to zero. The constant c determines the width of the hysteresis of the friction at low velocities and $\phi^{-1}(f)$ is the inverse function of $\phi(\cdot)$, an odd function that varies between ± 1. For implementation purposes suitable analytical approximations for $\phi(\cdot)$ and its inverse would be used.

"Dahl Model" Based Observer (DFOb)

This observer has similar structure to the DFOa observer. It is designed, however, based on the Dahl friction model. In accordance with the theory developed in Chapter 6, the observer dynamics are defined by

$$\hat{a} = z_a + k_d \hat{f}\hat{\omega} \tag{8.11}$$

$$\hat{f} = z_f + k_{d1}\theta + k_{d2}\hat{\omega} \tag{8.12}$$

with

$$\begin{aligned} \dot{z}_a &= -k_d c\hat{\omega}^2|1-\hat{f}\mathrm{sgn}(\hat{\omega})|^i\mathrm{sgn}(1-\mathrm{sgn}(\hat{\omega})) - k_d\hat{f}(\mathtt{w}-\hat{f}\hat{a}) \\ \dot{z}_f &= -k_{d1}\hat{\omega} - k_{d2}(\mathtt{w}-\hat{a}\hat{f}) + c\hat{\omega}|1-\hat{f}\mathrm{sgn}(\hat{\omega})|^i\mathrm{sgn}(1-\mathrm{sgn}(\hat{\omega})) \end{aligned}$$

and

$$\hat{F} = \hat{a}\hat{f} \tag{8.13}$$

where z_a, z_f are the observer states and k_d, k_{d1} and k_{d2} are the observer gains to be chosen by the designer to ensure convergence of the error to zero.

8.3.1 Friction Cancellation

The estimate of the friction force was also used to cancel the actual friction developed between the rubbing surfaces. This was achieved by making the input voltage to the motor w to be

$$\mathtt{w} = u + \hat{F} \tag{8.14}$$

where $\hat{F}$ is the estimated value of the friction force and u is given by

$$u = -g_1(\theta - \theta_r(t)) - g_2\hat{\omega} \tag{8.15}$$

where $\theta_r(t)$ is a reference angular position. The coefficients g_1 and g_2 were selected to satisfy desired performance specifications (Friedland, 1986).

All the above observers use as inputs the angular position θ as well as the estimated angular velocity $\hat{\omega}$.

8.4 Experimental Results

A series of eight experiments were performed, each in two stages. During the first stage the parallel plates were separated; during the second stage they were brought into contact by adjusting the micrometer screw (Figure 8.1). During the first phase, when the plates are not in contact, the observer estimates the friction present in

the motor alone. In the second phase, when the plates are in contact, the observer estimates the sum of the friction in the motor and the friction developed between the contacting surfaces.

The control law without compensation of friction is

$$\mathtt{w} = -g_1[\theta - \theta_r(t)] - g_2\hat{\omega}$$

where $\theta_r(t)$ is the reference square wave with amplitude 50 degrees and $\hat{\omega}$ is the estimated angular velocity produced by the observer. The feedback gains of the input u were chosen as $g_1 = 200$ and $g_2 = 50$.

To assess the capabilities of the friction estimation algorithms and the effectiveness of friction compensation, two experiments were performed for each friction observer. In the first experiment the friction was estimated but the estimate was not used to compensate for friction; in the second, the friction was compensated by generating a component of control torque equal and opposite to the estimated friction torque.

Figures 8.3a, 8.4a, 8.5a and 8.6a show the reference and actual angular positions versus time, the error between the actual and the reference angular positions versus time, the frictional acceleration versus time and the frictional acceleration versus velocity in the case where only friction estimation was performed; Figures 8.3b, 8.4b, 8.5b and 8.6b show these quantities with friction compensation.

In the first phase of the experiments, where the surfaces are not in contact, the magnitude of friction is small. When the surfaces are brought in contact, the friction increases substantially. The increase in friction shows up clearly in the experimental results.

As expected, the presence of friction affects the angular hang–off of the motor: without compensation, the steady state hang–off error increases with increased friction (Figures 8.3a, 8.4a, 8.5a and 8.6a). Friction compensation, however, all but eliminates the hang–off and excellent performance is exhibited. The performance

improvement is seen by comparing Figures 8.3a, 8.4a, 8.5a and 8.6a with 8.3b, 8.4b, 8.5b and 8.6b, respectively.

Implementation of the DFO observers, based on dynamic friction models, requires substantial experimental tuning because of the number of parameters in each model. Nevertheless, the results of these observers are quite similar.

The tracking observer (TO) gives results between those of the DFO's and the CFO. Figures 8.3b and 8.4b are very similar as well as figures 8.4a, 8.5a and 8.6a.

The plots of estimated friction versus velocity shown for each experiment emphasize the effect of adding the external friction. The lower level is due to the friction in the motor alone; the upper level is the sum of the friction in the motor and the external friction. It is interesting to note that the friction in the motor exhibits the hysteresis phenomenon observed by a number of investigators. When the external friction load is applied the friction level increases but the hysteresis loop does not change very much. This suggests that the external load (dry friction) does not produce much hysteresis.

Upon comparing the performance of the four observers, it can be inferred that the CFO observer (Figure 8.3) seems to give the best results both for estimation of friction and for compensation.

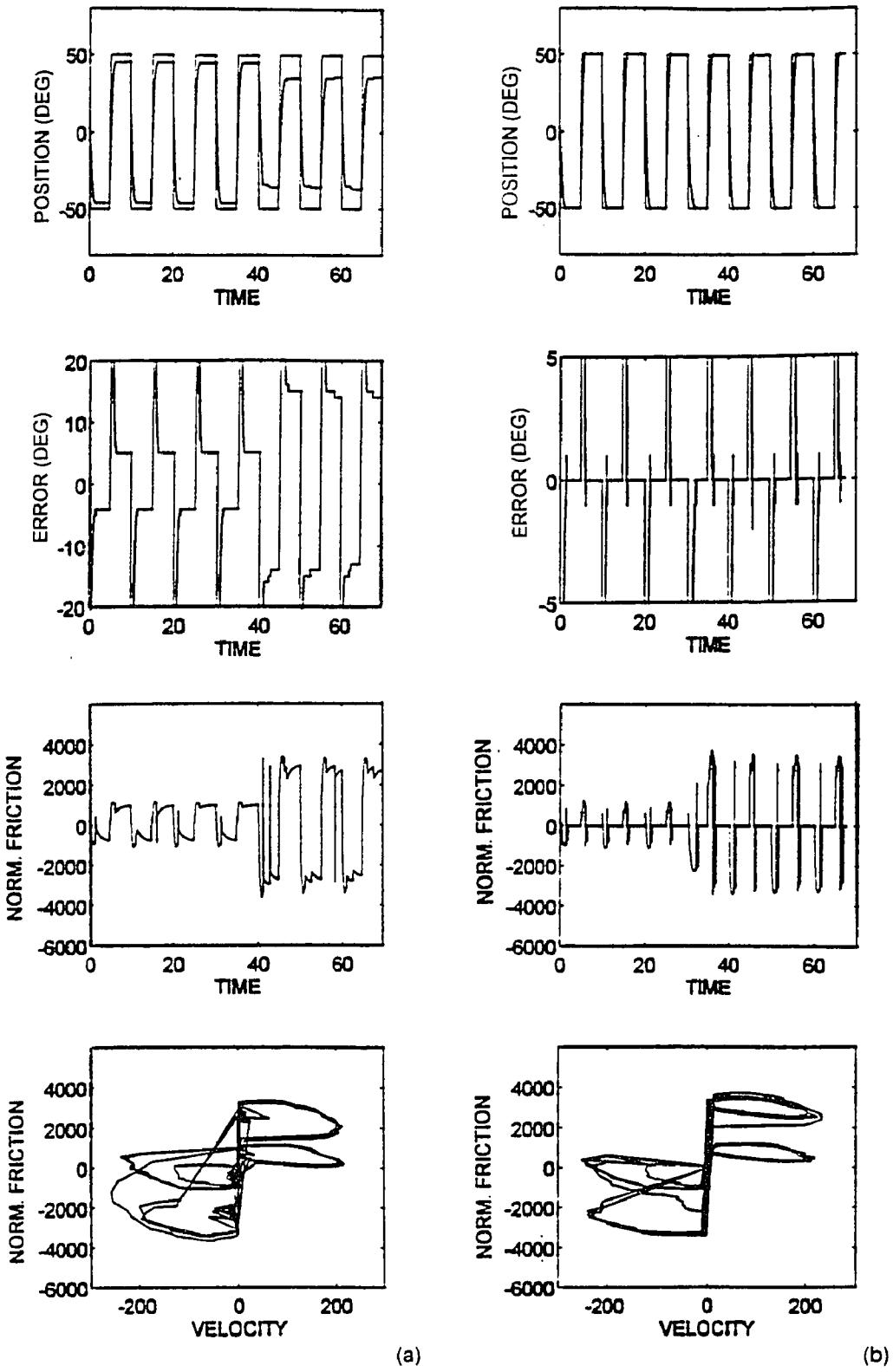

Figure 8.3 System transient response and friction estimate using the CFO observer (a) without friction cancellation (b) with friction cancellation.

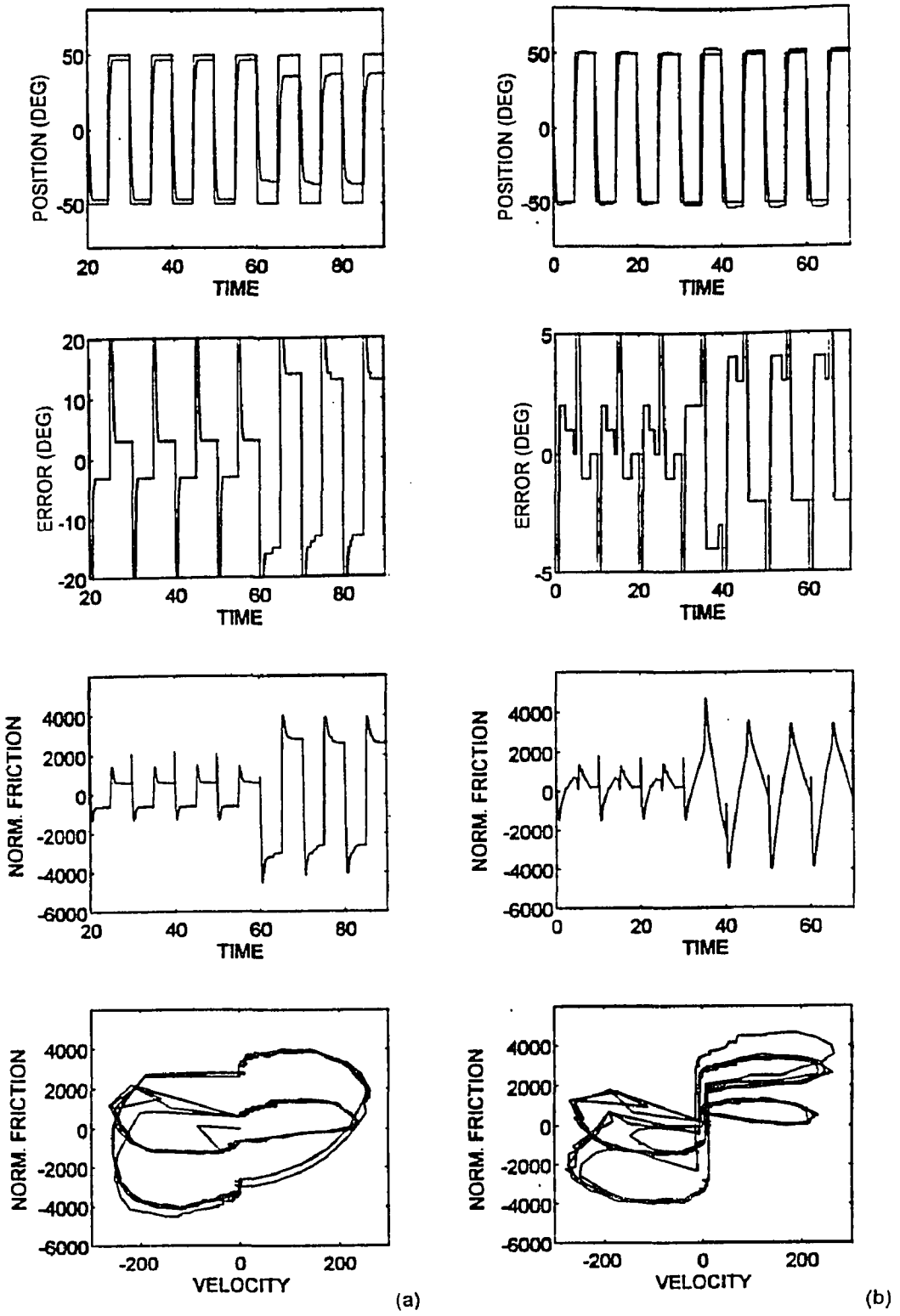

Figure 8.4 System transient response and friction estimate using the TO observer (a) without friction cancellation (b) with friction cancellation.

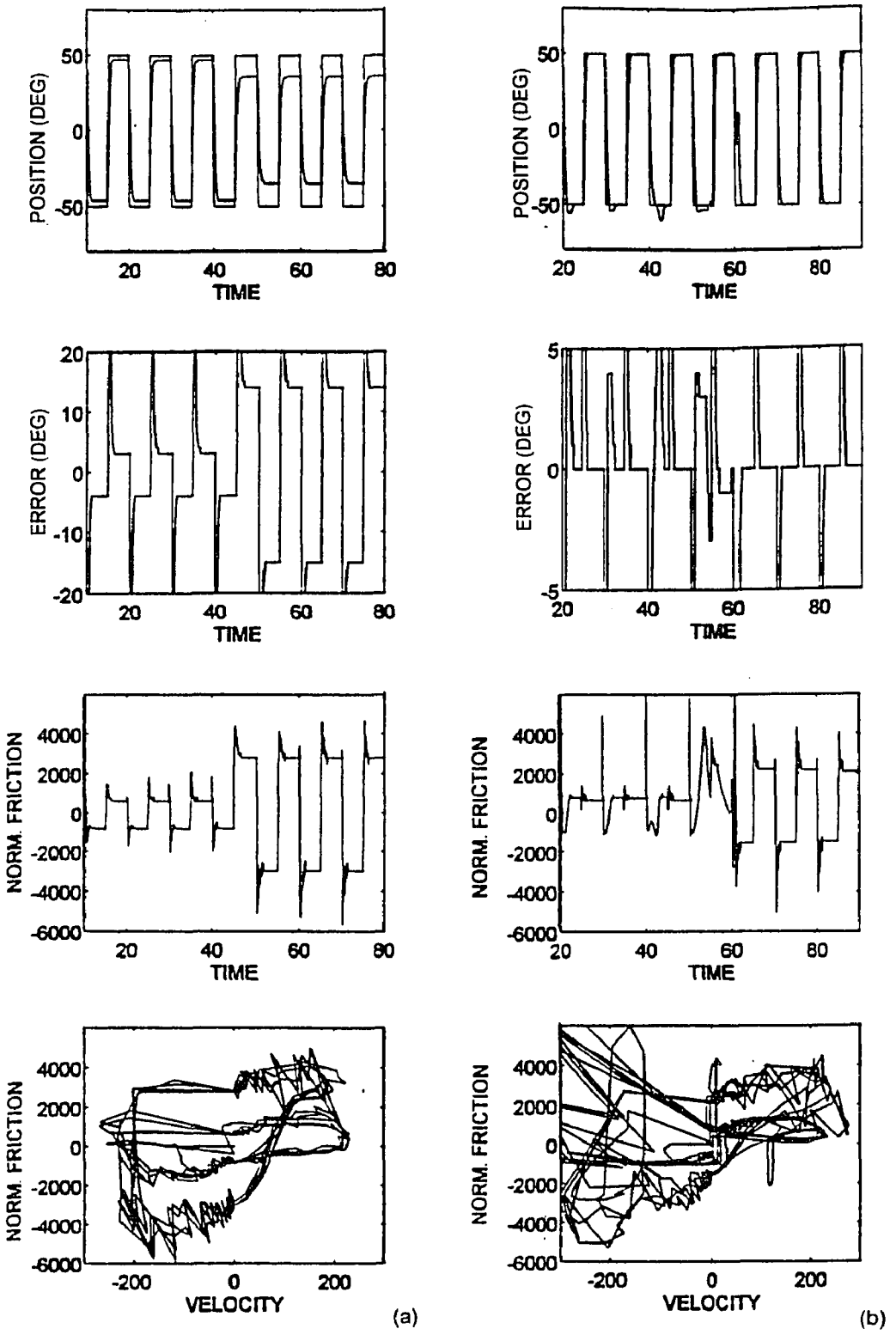

Figure 8.5 System transient response and friction estimate using the DFOa observer (a) without friction cancellation (b) with friction cancellation.

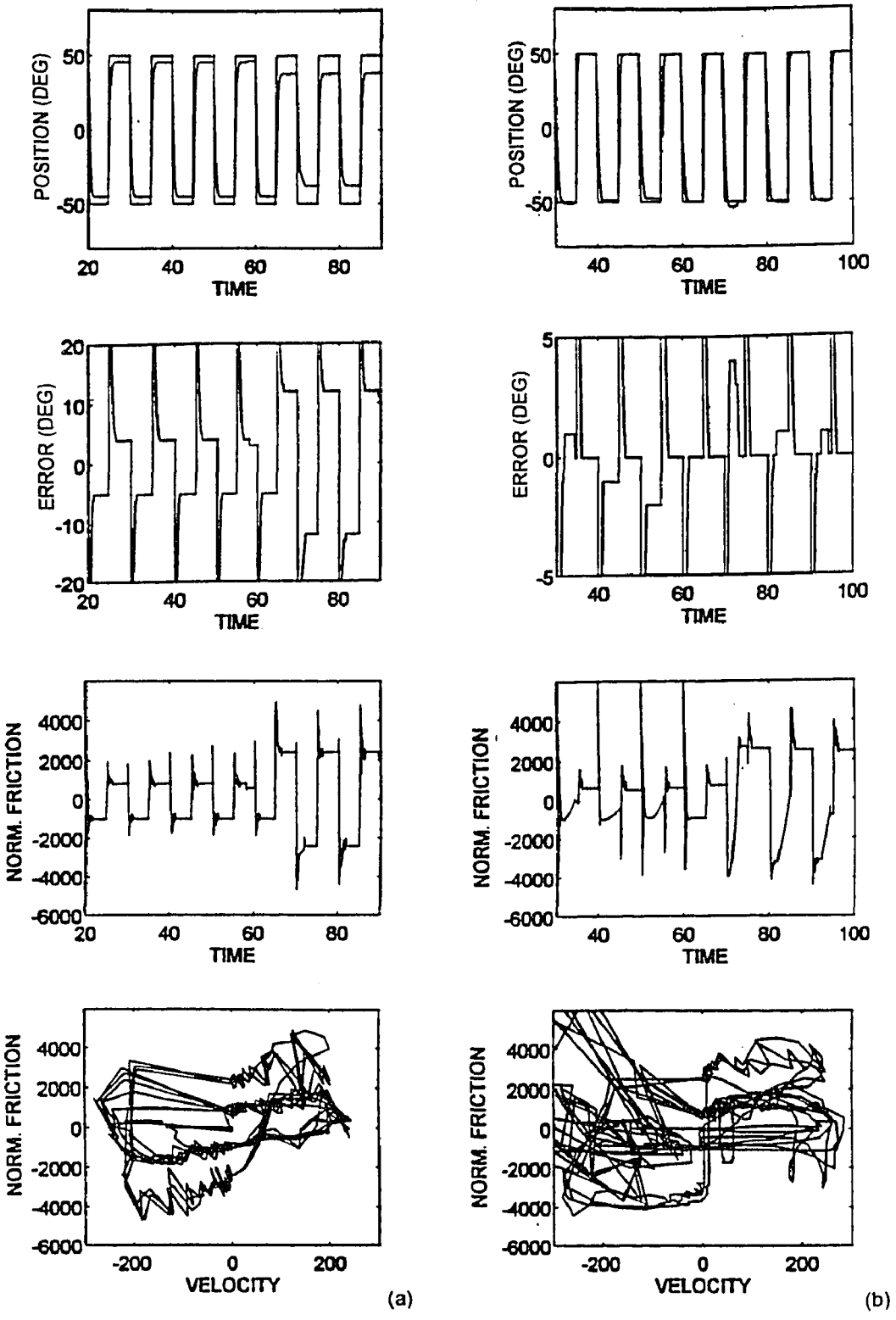

Figure 8.6 System transient response and friction estimate using the DFOb observer (a) without friction cancellation (b) with friction cancellation.

CHAPTER 9

CONCLUSIONS AND RECOMMENDATIONS

9.1 Conclusions

Friction in a control system can be successfully estimated using one of the three observers presented in this thesis:

1. The "Generalized Coulomb Friction Observer," (GCFO), which is designed based on a Coulomb friction model, performs well in estimating not only Coulomb friction but also "extended" Coulomb and dynamic friction. In the case of dynamic friction, however, it doesn't capture the hysteresis effect very well. Despite this fact, the GCFO observer demonstrated excellent experimental performance.

2. The "Generalized Dynamic Friction Observer," (GDFO), which is designed based on a general first order dynamic friction model, gives good results in tracking a friction model that contains hysteresis effects at low velocities. The GDFO observer performs well not only in simulations but also, in the experiments despite the fact of the high complexity of the dynamic friction models.

3. The "Generalized Tracking Observer," which considers friction as an unknown system parameter, is the simplest in structure It gives reasonable performance but not as good as the more complex observers. Moreover, in order for the GTO to estimate detailed friction characteristics, such as hysteresis, a high gain is required. This results in a large transient overshoot.

All the observers presented use as inputs the measured "positions" and "velocities" of the system.

When the velocity cannot be measured, it can be estimated using an additional observer in cascade with the friction observers. Use of this velocity observer introduces no significant degradation of performance in estimation of friction.

Friction cancellation has also been studied in this thesis. Perfect friction cancellation depends on the system topology and is not always possible. When the topology is suitable, the friction estimates can be used to cancel the friction (almost) perfectly. When the topology is not suitable, partial friction cancellation may be considered. A procedure for accomplishing this was presented.

To verify the validity and effectiveness of the theory presented in this thesis, several experiments were conducted where all of the observers were tested for friction estimation and cancellation. With a simple apparatus to produce varying levels of friction, four friction estimation and compensation algorithms were investigated. Experimental data were collected for each. The experimental results verified the capability of the observer–based friction compensators to cancel the effects of friction in control systems. The friction estimates that the observers give are reasonable in that they produce estimates that increase as the load is increased and that they display the hysteresis phenomenon reported by other investigators. The experimental results revealed that all the algorithms tested are effective for compensation of friction but behave differently in estimation of friction. Particularly, the CFO seems to give the most satisfactory results. The TO overcompensate friction. The DFOa and DFOb exhibit good performance but they are very complicated to tune.

The results indicate that the performance of a friction observer does not necessarily improve as its complexity is increased. The first observer based on the Coulomb friction model seems to perform the best, although it is quite simple. The tracking observer is slightly simpler, but its performance does not seem to be as good. The additional complexity of observers that are based on dynamic models does not seem justified in view of the performance they yield in cancelling friction. Their use,

however, may be justified when the goal is not only cancelling friction, but also gaining a better understanding of the underlying physics.

9.2 Recommendations

A comparative experimental study of the various friction estimation and compensation techniques presented in the literature should be undertaken.

A theoretical analysis of the global convergence of the estimation error to zero is needed.

More also research is needed in the case of minimizing the ill–effects of friction when the topology does not allow for perfect cancellation. When friction cannot be cancelled, its effects can be regarded as a bias system input. This merits further investigation.

Finally, the general problem of friction modeling still remains. The algorithms proposed by this dissertation could be helpful in this application.

APPENDIX A

MATRIX FORM OF FRICTION FORCES

Consider a system containing n masses subjected simultaneously to several forces including Coulomb friction forces, with the following dynamic description

$$M\ddot{x} = g(x, v, w) - F \tag{A.1}$$

where the vectors x and v belong to $\mathcal{R}^k$ $(k \geq n)$ represent "positions" and "velocities", respectively. Here, $g(x, v, w)$ is the total non–frictional force applied to the system, F is the friction force, and M is the "mass" matrix.

Next the general expressions of the friction vector F will be derived explicitly for the following cases:

1. Coulomb friction
2. "Extended" Coulomb friction
3. Dynamic friction
4. "Extended" dynamic friction

A.1 Vector Coulomb Friction Force

It will be shown that for a system with Coulomb friction, the friction force F can be written:

$$F = F(a, v) = U\mathcal{A}\,\mathrm{sgn}(U'v) \tag{A.2}$$

with

$$a = [a_1 \cdots a_\nu]$$

$$\mathcal{A} = \mathrm{diag}\{a\}$$

where U is a known matrix, U' is the transpose matrix of U, a is a vector containing the friction coefficients (which we assume constants), $\mathcal{A}$ is a diagonal matrix containing all the different friction coefficients and ν is the number of the different friction forces applied to the system.

The following cases will be considered for the motion of the system:

1. Motion with no constraints
   (a) Translational motion in one direction
   (b) Translational motion in more than one direction.
   (c) Rotational motion.
   (d) Translational motion on a plane with rotation perpendicular to that plane.
2. Motion with holonomic constraints.

For each of the above cases, the form of the dynamic equations and the friction vector characterizing the system will be investigated.

A.1.1 Translational Motion in One Direction with no Constraints

By applying Newton's second Law of motion to a multiple mass system with transitional motion in one direction, the resulting dynamic description of the system is the following

$$\dot{\bar{x}} = \bar{v} \tag{A.3}$$

$$\bar{M}\dot{\bar{v}} = \bar{g}(\bar{x}, \bar{v}, w) - \bar{F}(a, \bar{v}) \tag{A.4}$$

where

$$\bar{M} = diag\{m_1, \cdots, m_n\}' \text{ and } m_i > 0 \tag{A.5}$$

$$\bar{F}(a, \bar{v}) = [\bar{F}_1(a, \bar{v}), \cdots, \bar{F}_n(a, \bar{v})]' \tag{A.6}$$

and the vectors $\bar{x}$ and $\bar{v}$ represent positions and velocities, respectively. Furthermore, $\bar{g}(\bar{x}, \bar{v}, w)$ is the total non–frictional force applied to the system and $\bar{F}_i(a, \bar{v})$ is the friction force applied to the ith degree–of–freedom.

Analytically, from the definition of Coulomb friction, $\bar{F}_i(a, \bar{v})$ can be written as the sum of the relative friction forces which are proportional to the sgn of the relative velocities of the particular mass with the other masses, i.e.

$$\bar{F}_i(a, \bar{v}) = a_{i0}\ \mathrm{sgn}(\bar{v}_i) + \sum_{j=1,\, i \neq j}^{n} a_{ij}\ \mathrm{sgn}(\bar{v}_i - \bar{v}_j) \tag{A.7}$$

or equivalently

$$\bar{F}(a, \bar{v}) = \begin{bmatrix} a_{10}\mathrm{sgn}(\bar{v}_1) + a_{12}\mathrm{sgn}(\bar{v}_1 - \bar{v}_2) + \cdots + a_{1n}\mathrm{sgn}(\bar{v}_1 - \bar{v}_n) \\ a_{20}\mathrm{sgn}(\bar{v}_2) + a_{21}\mathrm{sgn}(\bar{v}_2 - \bar{v}_1) + \cdots + a_{2n}\mathrm{sgn}(\bar{v}_2 - \bar{v}_n) \\ \vdots \\ a_{n0}\mathrm{sgn}(\bar{v}_n) + a_{n1}\mathrm{sgn}(\bar{v}_n - \bar{v}_1) + \cdots + a_{n,n-1}\mathrm{sgn}(\bar{v}_n - \bar{v}_{n-1}) \end{bmatrix} \tag{A.8}$$

where a_{ij} is the friction coefficient corresponding to the friction developed between the ith and the jth mass and a_{i0} is the friction coefficient corresponding to the friction relative to a fixed base ("ground").

Next, considering the fact that the friction developed between two masses is unique (action = reaction), i.e $a_{ij} = a_{ji}$, it is shown that the following lemma holds:

Lemma A.1 *Assuming that $a_{ij} = a_{ji}$, matrices $\bar{U}_o$ and $\mathcal{A}_o$ can always be found such that*

$$\bar{F}(a, \bar{v}) = \bar{U}_o \mathcal{A}_o\ \mathrm{sgn}(\bar{U}_o' \bar{v}) \tag{A.9}$$

where $\bar{U}_o$ is a matrix containing zeroes and ones and has dimension $n \times n(n+1)/2$, while $\mathcal{A}_o$ is a diagonal matrix containing all the different friction coefficients.

Proof:

Due to the symmetry property, i.e $a_{ij} = a_{ji}$, and

$$a_{ij}\text{sgn}(\bar{v}_i - \bar{v}_j) = -a_{ji}\text{sgn}(\bar{v}_j - \bar{v}_i) \tag{A.10}$$

Next, let us define the vector d_o to be

$$d_o = \begin{bmatrix} d_1 \\ d_2 \\ d_3 \\ \vdots \\ d_n \end{bmatrix} \tag{A.11}$$

where

$$d_1 = \begin{bmatrix} a_{10}\text{sgn}(\bar{v}_1) \\ a_{12}\text{sgn}(\bar{v}_1 - \bar{v}_2) \\ a_{13}\text{sgn}(\bar{v}_1 - \bar{v}_3) \\ a_{14}\text{sgn}(\bar{v}_1 - \bar{v}_4) \\ a_{15}\text{sgn}(\bar{v}_1 - \bar{v}_5) \\ \vdots \\ a_{1n}\text{sgn}(\bar{v}_1 - \bar{v}_n) \end{bmatrix}, \quad d_2 = \begin{bmatrix} a_{20}\text{sgn}(\bar{v}_2) \\ a_{23}\text{sgn}(\bar{v}_2 - \bar{v}_3) \\ a_{24}\text{sgn}(\bar{v}_2 - \bar{v}_4) \\ a_{25}\text{sgn}(\bar{v}_2 - \bar{v}_5) \\ \vdots \\ a_{2n}\text{sgn}(\bar{v}_2 - \bar{v}_n) \end{bmatrix}, \tag{A.12}$$

$$d_3 = \begin{bmatrix} a_{30}\text{sgn}(\bar{v}_3) \\ a_{34}\text{sgn}(\bar{v}_3 - \bar{v}_4) \\ a_{35}\text{sgn}(\bar{v}_3 - \bar{v}_5) \\ \vdots \\ a_{3n}\text{sgn}(\bar{v}_3 - \bar{v}_n) \end{bmatrix}, \cdots, d_n = \begin{bmatrix} a_{n0}\text{sgn}(\bar{v}_n) \end{bmatrix} \tag{A.13}$$

As it can be seen, d_o does not contain the elements $a_{ij}\text{sgn}(\bar{v}_i - \bar{v}_j)$ if $i > j$.

Furthermore, let us rewrite equation (A.7), describing the ith friction force $\bar{F}_i(a, \bar{v})$ as follows

$$\begin{aligned} \bar{F}_i(a, \bar{v}) &= a_{i0}\ \text{sgn}(\bar{v}_i) + \sum_{j=1,\ i\neq j}^{n} a_{ij}\ \text{sgn}(\bar{v}_i - \bar{v}_j) \\ &= a_{i0}\ \text{sgn}(\bar{v}_i) + \sum_{j=1}^{i-1} a_{ij}\ \text{sgn}(\bar{v}_i - \bar{v}_j) + \sum_{j=i+1}^{n} a_{ij}\ \text{sgn}(\bar{v}_i - \bar{v}_j) \end{aligned} \tag{A.14}$$

Using property (A.10), equation (A.14) can be written as:

$$\bar{F}_i(a, \bar{v}) = a_{i0}\ \text{sgn}(\bar{v}_i) - \sum_{j=1}^{i-1} a_{ji}\ \text{sgn}(\bar{v}_j - \bar{v}_i) + \sum_{j=i+1}^{n} a_{ij}\ \text{sgn}(\bar{v}_i - \bar{v}_j) \tag{A.15}$$

Analytically, writing equation (A.15) for every i and using the vector d_o, yields

$$\begin{aligned}\bar{F}_1(a,\bar{v}) &= a_{10}\,\mathrm{sgn}(\bar{v}_1) + a_{12}\,\mathrm{sgn}(\bar{v}_1-\bar{v}_2) + \cdots + a_{1n}\,\mathrm{sgn}(\bar{v}_1-\bar{v}_n) \\ &= w_{11}d_1 + w_{12}d_2 + \cdots + w_{1n}d_n \end{aligned} \tag{A.16}$$

where

$$w_{11} = [\,1\ \ 1\ \ 1\ \ \cdots\ \ 1]$$

The successive row vectors w_{1j}, for every $j > 1$ contain only zero elements.

Furthermore,

$$\begin{aligned}\bar{F}_2(a,\bar{v}) &= a_{20}\,\mathrm{sgn}(\bar{v}_1) - a_{12}\,\mathrm{sgn}(\bar{v}_1-\bar{v}_2) + a_{23}\,\mathrm{sgn}(\bar{v}_2-\bar{v}_3) + \cdots \\ &\quad + a_{2n}\,\mathrm{sgn}(\bar{v}_2-\bar{v}_n) \\ &= w_{21}d_1 + w_{22}d_2 + \cdots + w_{2n}d_n \end{aligned} \tag{A.17}$$

where

$$\begin{aligned} w_{21} &= [\,0\ \ -1\ \ 0\ \ \cdots\ \ 0] \\ w_{22} &= [\,1\ \ 1\ \ 1\ \ \cdots\ \ 1] \end{aligned}$$

The row vectors w_{2j}, for every $j > 2$ contain only zero elements.

Moreover,

$$\begin{aligned}\bar{F}_3(a,\bar{v}) &= a_{30}\,\mathrm{sgn}(\bar{v}_1) - a_{13}\,\mathrm{sgn}(\bar{v}_1-\bar{v}_3) - a_{23}\,\mathrm{sgn}(\bar{v}_2-\bar{v}_3) \\ &\quad + a_{34}\,\mathrm{sgn}(\bar{v}_3-\bar{v}_4) + \cdots + a_{3n}\,\mathrm{sgn}(\bar{v}_3-\bar{v}_n) \\ &= w_{31}d_1 + w_{32}d_2 + w_{33}d_3 + \cdots + w_{3n}d_n \end{aligned} \tag{A.18}$$

where

$$\begin{aligned} w_{31} &= [\,0\ \ 0\ \ -1\ \ 0\ \ \cdots\ \ 0] \\ w_{32} &= [\,0\ \ -1\ \ 0\cdots\ \ 0] \\ w_{33} &= [\,1\ \ 1\ \ 1\cdots\ \ 1] \end{aligned}$$

The row vectors w_{3j}, for every $j > 3$ contain only zero elements.

Finally,

$$\begin{aligned} \bar{F}_n(a, \bar{v}) &= a_{n0}\,\mathrm{sgn}(\bar{v}_1) - a_{1n}\,\mathrm{sgn}(\bar{v}_1 - \bar{v}_n) - \cdots - a_{n-1,n}\,\mathrm{sgn}(\bar{v}_{n-1} - \bar{v}_n) \\ &= w_{n1}d_1 + w_{n2}d_2 + w_{n3}d_3 + \cdots + w_{nn}d_n \end{aligned} \tag{A.19}$$

where

$$\begin{aligned} w_{n1} &= [\,0\ 0\ 0\ \cdots\ 0\ -1\,] \\ w_{n2} &= [\,0\ 0\ 0\ \cdots\ -1\,] \\ &\vdots \\ w_{nn} &= [1] \end{aligned} \tag{A.20}$$

Next we define matrices W_i such

$$W_1 = \begin{bmatrix} w_{11} \\ w_{21} \\ w_{31} \\ \vdots \\ w_{n1} \end{bmatrix} = \begin{bmatrix} 1 & 1 & 1 & \cdots & \cdots & 1 \\ 0 & -1 & 0 & \cdots & \cdots & 0 \\ 0 & 0 & -1 & \ddots & \cdots & 0 \\ \vdots & \vdots & \ddots & \ddots & \ddots & \vdots \\ \vdots & \vdots & & \ddots & \ddots & 0 \\ 0 & 0 & \cdots & \cdots & 0 & -1 \end{bmatrix} \tag{A.21}$$

$$W_2 = \begin{bmatrix} w_{12} \\ w_{22} \\ w_{32} \\ \vdots \\ w_{n2} \end{bmatrix} = \begin{bmatrix} 0 & 0 & 0 & \cdots & 0 \\ 1 & 1 & 1 & \cdots & 1 \\ 0 & -1 & 0 & \cdots & 0 \\ 0 & 0 & -1 & \ddots & \vdots \\ \vdots & \vdots & \ddots & \ddots & 0 \\ 0 & 0 & \cdots & 0 & -1 \end{bmatrix} \tag{A.22}$$

$$W_3 = \begin{bmatrix} w_{13} \\ w_{23} \\ w_{33} \\ \vdots \\ w_{n3} \end{bmatrix} = \begin{bmatrix} 0 & 0 & \cdots & 0 \\ 0 & 0 & \cdots & 0 \\ 1 & 1 & \cdots & 1 \\ 0 & -1 & \cdots & 0 \\ \vdots & \vdots & \ddots & \vdots \\ 0 & 0 & \cdots & -1 \end{bmatrix} \tag{A.23}$$

Finally,

$$W_n = \begin{bmatrix} w_{1n} \\ w_{2n} \\ w_{3n} \\ \vdots \\ w_{nn} \end{bmatrix} = \begin{bmatrix} 0 \\ 0 \\ 0 \\ \vdots \\ 0 \\ 1 \end{bmatrix} \tag{A.24}$$

The matrices W_i have dimensions $n \times (n - i + 1)$.

Substituting equations (A.21)-(A.24) into (A.16)-(A.19) and then using (A.6), yields

$$\bar{F}(a, \bar{v}) = \bar{U}_o d_o \tag{A.25}$$

where

$$\bar{U}_o = [W_1 \;\; W_2 \;\; \cdots \;\; W_n] \tag{A.26}$$

Next, let us define the matrix $\mathcal{A}_o$ to be

$$\mathcal{A}_o = diag\{a_{10},\ a_{12},\ a_{13},\ \cdots,\ a_{1n},\ a_{20},\ a_{23},\ \cdots,\ a_{2n},\ \cdots,\ a_{n-1,n},\ a_{n0}\} \tag{A.27}$$

Using equation (A.27), the vector d_o given by (A.11) can be written as

$$d_o = \mathcal{A}_o \;\; \text{sgn}\left(\begin{bmatrix} \mathbf{v}_{o1} \\ \mathbf{v}_{o2} \\ \vdots \\ \mathbf{v}_{on} \end{bmatrix} \right) \tag{A.28}$$

where

$$\mathbf{v}_{o1} = \begin{bmatrix} \bar{v}_1 \\ \bar{v}_1 - \bar{v}_2 \\ \bar{v}_1 - \bar{v}_3 \\ \bar{v}_1 - \bar{v}_4 \\ \vdots \\ \bar{v}_1 - \bar{v}_n \end{bmatrix}, \quad \mathbf{v}_{o2} = \begin{bmatrix} \bar{v}_2 \\ \bar{v}_2 - \bar{v}_3 \\ \bar{v}_2 - \bar{v}_4 \\ \vdots \\ \bar{v}_2 - \bar{v}_n \end{bmatrix}, \cdots, \mathbf{v}_{on} = \begin{bmatrix} \bar{v}_n \end{bmatrix} \tag{A.29}$$

In addition, it can be easily proven that

$$\underbrace{\begin{bmatrix} \bar{v}_1 \\ \bar{v}_1 - \bar{v}_2 \\ \bar{v}_1 - \bar{v}_3 \\ \bar{v}_1 - \bar{v}_4 \\ \vdots \\ \bar{v}_1 - \bar{v}_n \end{bmatrix}}_{\mathbf{v}_{o1}} = \underbrace{\begin{bmatrix} 1 & 0 & 0 & 0 & \cdots & 0 \\ 1 & -1 & 0 & 0 & \cdots & 0 \\ 1 & 0 & -1 & 0 & \cdots & 0 \\ 1 & 0 & 0 & -1 & \cdots & 0 \\ \vdots & \vdots & \vdots & & \ddots & \vdots \\ 1 & 0 & 0 & 0 & \cdots & -1 \end{bmatrix}}_{W_1'} \begin{bmatrix} \bar{v}_1 \\ \bar{v}_2 \\ \bar{v}_3 \\ \bar{v}_4 \\ \vdots \\ \bar{v}_n \end{bmatrix} \tag{A.30}$$

$$\underbrace{\begin{bmatrix} \bar{v}_2 \\ \bar{v}_2 - \bar{v}_3 \\ \bar{v}_2 - \bar{v}_4 \\ \vdots \\ \bar{v}_2 - \bar{v}_n \end{bmatrix}}_{\mathbf{v}_{o2}} = \underbrace{\begin{bmatrix} 0 & 1 & 0 & 0 & \cdots & 0 \\ 0 & 1 & -1 & 0 & \cdots & 0 \\ 0 & 1 & 0 & -1 & \cdots & 0 \\ \vdots & \vdots & \vdots & & \ddots & \vdots \\ 0 & 1 & 0 & 0 & \cdots & -1 \end{bmatrix}}_{W_2'} \begin{bmatrix} \bar{v}_1 \\ \bar{v}_2 \\ \bar{v}_3 \\ \bar{v}_4 \\ \vdots \\ \bar{v}_n \end{bmatrix} \tag{A.31}$$

$$\underbrace{\begin{bmatrix} \bar{v}_3 \\ \bar{v}_3 - \bar{v}_4 \\ \vdots \\ \bar{v}_3 - \bar{v}_n \end{bmatrix}}_{\mathbf{v}_{o3}} = \underbrace{\begin{bmatrix} 0 & 0 & 1 & 0 & \cdots & 0 \\ 0 & 0 & 1 & -1 & \cdots & 0 \\ \vdots & \vdots & \vdots & & \ddots & \vdots \\ 0 & 0 & 1 & 0 & \cdots & -1 \end{bmatrix}}_{W_3'} \begin{bmatrix} \bar{v}_1 \\ \bar{v}_2 \\ \bar{v}_3 \\ \bar{v}_4 \\ \vdots \\ \bar{v}_n \end{bmatrix} \tag{A.32}$$

$$\vdots$$

$$\underbrace{\begin{bmatrix} \bar{v}_n \end{bmatrix}}_{\mathbf{v}_{on}} = \underbrace{\begin{bmatrix} 0 & 0 & 0 & 0 & \cdots & 0 \end{bmatrix}}_{W_n'} \begin{bmatrix} \bar{v}_1 \\ \bar{v}_2 \\ \bar{v}_3 \\ \bar{v}_4 \\ \vdots \\ \bar{v}_n \end{bmatrix} \tag{A.33}$$

Hence, substituting equations (A.30)–(A.33) into (A.28), yields

$$d_o = \mathcal{A}_o \text{sgn}(\bar{U}_o' \bar{v}) \tag{A.34}$$

Finally, substituting (A.34) into (A.25), yields

$$\bar{F}(a,\bar{v}) = \bar{U}_o \mathcal{A}_o \text{sgn}(\bar{U}_o'\bar{v}) \tag{A.35}$$

where, the matrices $\bar{U}_o$ and $\mathcal{A}_o$ are given by equations (A.26) and (A.27) respectively.

Obviously, $\bar{U}_o$ is unique for a particular $\mathcal{A}_o$. However, by changing the order of the diagonal elements of $\mathcal{A}_o$, matrix $\bar{U}_o$ changes. Specifically, an interchange between the ith and the jth diagonal elements of $\mathcal{A}_o$ results in an interchange between the ith and the jth columns of $\bar{U}_o$. Hence, many different sets of matrices $\bar{U}_o$ and $\mathcal{A}_o$ can be found such that equation (A.35) is valid.

The proof is complete. △

The representation of the friction vector $\bar{F}(a,\bar{v})$ by (A.9) however, is too general to represent a typical mechanical system. The latter has a considerably simpler topology for which

$$\bar{F}(a,\bar{v}) = \bar{U}\mathcal{A}\ \text{sgn}(\bar{U}'\bar{v}) \tag{A.36}$$

Matrix $\mathcal{A}$ is diagonal and is obtained from $\mathcal{A}_o$ after eliminating the known zero friction coefficients a_{ij}. Moreover, $\bar{U}$ is a submatrix of $\bar{U}_o$ where the columns corresponding to the zero rows of $\mathcal{A}_o$, have been eliminated. The matrices $\mathcal{A}$ and $\bar{U}$ obviously have smaller dimensions than $\mathcal{A}_o$ and $\bar{U}_o$ respectively.

Finally, representations (A.3), (A.4) and (A.36) can be generalized through a unitary matrix transformation T as follows

$$\begin{aligned} x &= T\bar{x} \\ v &= T\bar{v} \\ M &= T\bar{M}T' \\ \bar{g}(\bar{x},\bar{v},w) &= T'g(x,v,w) \end{aligned} \tag{A.37}$$

$$\begin{aligned} \bar{F}(a,\bar{v}) &= T'F(a,v) \\ U &= T\bar{U} \end{aligned}$$

since M is a symmetric positive definite matrix.

A.1.2 Translational Motion in More than One Direction with no Constraints

Without loss of generality 3–dimensional motion is considered.

According to the results of the previous section, the dynamic equations describing a system of n masses in Cartesian coordinates are

$$\begin{aligned} \dot{\bar{x}} &= \bar{v}_x \\ \dot{\bar{y}} &= \bar{v}_y \\ \dot{\bar{z}} &= \bar{v}_z \\ \bar{M}\dot{\bar{v}}_x &= \bar{g}_x(\bar{x},\bar{v}_x,w) - \bar{F}_x(a_x,\bar{v}_x) \\ \bar{M}\dot{\bar{v}}_y &= \bar{g}_y(\bar{x},\bar{v}_y,w) - \bar{F}_y(a_y,\bar{v}_y) \\ \bar{M}\dot{\bar{v}}_z &= \bar{g}_z(\bar{x},\bar{v}_z,w) - \bar{F}_z(a_z,\bar{v}_z) \end{aligned} \tag{A.38}$$

where the mass matrix M is given by (A.5), $\bar{g}_x(\bar{x},\bar{v}_x,w)$, $\bar{g}_y(\bar{y},\bar{v}_y,w)$, $\bar{g}_z(\bar{z},\bar{v}_z,w)$ represent the total forces in the x,y,z directions, respectively, excluding friction, while $\bar{F}_x(a_x,\bar{v}_x)$, $\bar{F}_y(a_y,\bar{v}_y)$, $\bar{F}_z(a_z,\bar{v}_z)$ are the friction forces in the three dimensions. Furthermore, according to (A.36),

$$\begin{aligned} \bar{F}_x(a_x,\bar{v}_x) &= \bar{U}_x\mathcal{A}_x\ \mathrm{sgn}(\bar{U}_x'\bar{v}_x) \\ \bar{F}_y(a_y,\bar{v}_y) &= \bar{U}_y\mathcal{A}_y\ \mathrm{sgn}(\bar{U}_y'\bar{v}_y) \\ \bar{F}_z(a_z,\bar{v}_z) &= \bar{U}_z\mathcal{A}_z\ \mathrm{sgn}(\bar{U}_z'\bar{v}_z) \end{aligned} \tag{A.39}$$

Equations (A.38) and (A.39) can be written in matrix form as follows:

$$\begin{aligned} \dot{\bar{\mathbf{x}}} &= \bar{\mathbf{v}} \\ \bar{\mathbf{M}}\dot{\bar{\mathbf{v}}} &= \bar{\mathbf{g}}(\bar{\mathbf{x}},\bar{\mathbf{v}},\mathbf{w}) - \bar{\mathbf{F}}(\mathbf{a},\bar{\mathbf{v}}) \end{aligned} \tag{A.40}$$

where

$$\bar{\mathbf{x}} = \begin{bmatrix} \bar{x} & \bar{y} & \bar{z} \end{bmatrix}' \tag{A.41}$$

$$\bar{\mathbf{v}} = \begin{bmatrix} \bar{v}_x & \bar{v}_y & \bar{v}_z \end{bmatrix}' \tag{A.42}$$

$$\bar{\mathbf{M}} = diag\{\bar{M},\ \bar{M},\ \bar{M}\} \tag{A.43}$$

$$\bar{\mathbf{g}}(\bar{\mathbf{x}}, \bar{\mathbf{v}}, \mathbf{w}) = diag\{\bar{g}_x(\bar{x}, \bar{v}_x, w),\ \bar{g}_y(\bar{y}, \bar{v}_y, w),\ \bar{g}_z(\bar{z}, \bar{v}_z, w)\} \tag{A.44}$$

and

$$\bar{\mathbf{F}}(\mathbf{a}, \bar{\mathbf{v}}) = diag\{\bar{F}_x(a_x, \bar{v}_x),\ \bar{F}_y(a_y, \bar{v}_y),\ \bar{F}_z(a_z, \bar{v}_z)\}$$

$$= \begin{bmatrix} \bar{U}_x & 0 & 0 \\ 0 & \bar{U}_y & 0 \\ 0 & 0 & \bar{U}_z \end{bmatrix} \begin{bmatrix} \mathcal{A}_x & 0 & 0 \\ 0 & \mathcal{A}_y & 0 \\ 0 & 0 & \mathcal{A}_z \end{bmatrix} \text{sgn}\left(\begin{bmatrix} \bar{U}'_x & 0 & 0 \\ 0 & \bar{U}'_y & 0 \\ 0 & 0 & \bar{U}'_z \end{bmatrix} \mathbf{v} \right)$$

A.1.3 Rotational Motion with no Constraints

This case is similar to the one presented above. Therefore it will not be investigated separately.

A.1.4 Translational Motion on a Plane and Rotation Perpendicular to that Plane with no Constraints

It can be easily seen that this case is analogous to pure rotational motion or purely translational motion with no constraints.

A.1.5 Motion with Holonomic Constraints

Let us rewrite the dynamic equations describing an n–mass system as follows

$$M_x \ddot{x} = g_x(x, \dot{x}, w) - F_x(a, \dot{x}) \tag{A.45}$$

where the vectors $x \in \mathcal{R}^k$ and $\dot{x} \in \mathcal{R}^k$ represent "positions" and "velocities", respectively. Here $g_x(x, \dot{x}, w)$ is the total force applied to the system, excluding friction, $F_x(a, \dot{x})$ is the friction force, M_x is the "mass" matrix and a is a vector containing the friction coefficients.

It has been shown in the previous sections that the friction for a system with unconstrained motion can be written as follows

$$F_x(a, \dot{x}) = U_x \mathcal{A} \operatorname{sgn}(U_x' \dot{x}) \tag{A.46}$$

where U_x is a known constant matrix, while $\mathcal{A}$ is a diagonal matrix containing all the different friction coefficients in a proper order.

Now assume that the motion of the masses is subject to λ holonomic constraints,

$$\begin{aligned} \psi_1(x,t) &= 0 \\ \psi_2(x,t) &= 0 \\ &\vdots \\ \psi_\lambda(x,t) &= 0 \end{aligned} \tag{A.47}$$

The coordinates of the vector x of the differential equations (A.45), under the constraints (A.47), become dependent on each other. Now, since the constraints (A.47) are holonomic, the coordinates of x can be transformed to a new set of coordinates $q \in \mathcal{R}^m$, which are called *generalized.* In these new coordinates the system (A.45)–(A.47) takes the form:

$$M_q \ddot{q} = g_q(q, \dot{q}, w) - F_q(a, \dot{q}) \tag{A.48}$$

where M_q is the new mass matrix, $g_q(q, \dot{q}, w)$ the new non–frictional force vector, and $F_q(a, \dot{q})$ the friction force. For the system (A.48) the following lemma holds:

Lemma A.2 *The friction force vector in the generalized coordinates q can be written in the standard form*

$$F_q(a, \dot{q}) = U_q \mathcal{A} \operatorname{sgn}(U_q' \dot{q}) \tag{A.49}$$

where U_q the new distribution matrix of the system friction forces.

Proof

To show that the friction force vector remains in the standard form in the new coordinates q, equation (A.48) will be derived explicitly from (A.45). To derive equation (A.48), the Lagrangian equations will be used (Synge, 1942)

$$\frac{d}{dt}(\frac{\partial E}{\partial \dot{q}})' - (\frac{\partial E}{\partial q})' = \Phi_q \tag{A.50}$$

where

$$\frac{\partial E}{\partial q} = \left[\begin{array}{ccc} \frac{\partial E}{\partial q_1} & \cdots & \frac{\partial E}{\partial q_m} \end{array} \right] \tag{A.51}$$

$$\frac{\partial E}{\partial \dot{q}} = \left[\begin{array}{ccc} \frac{\partial E}{\partial \dot{q}_1} & \cdots & \frac{\partial E}{\partial \dot{q}_m} \end{array} \right] \tag{A.52}$$

and

$$\Phi_q = T_q' \Phi_x \tag{A.53}$$

$$\Phi_x = g_x(x, \dot{x}, w) - F_x(a, \dot{x}) \tag{A.54}$$

In the above equations, E is the kinetic energy of the system, Φ_q is the generalized total force vector in q coordinates and Φ_x is the total force vector in x coordinates as can be seen from (A.54). Notice that the vector $g_x(x, \dot{x}, w)$ may include conservative forces, which would have the form $-\frac{\partial V}{\partial x}$ where V is the potential energy (Timoshenko, 1948).

The kinetic energy of system (A.45) is

$$E = \frac{1}{2} \dot{x}' M_x \dot{x} \tag{A.55}$$

and has a unique value independently of the coordinates used to describe the system dynamics.

Consider x as a function of q. Then the following relations can be easily derived

$$\dot{x} = T_q \dot{q} \tag{A.56}$$

and

$$\ddot{x} = \dot{T}_q \dot{q} + T_q \ddot{q} \tag{A.57}$$

where

$$\begin{aligned} T_q &= \frac{\partial x}{\partial q} \\ &= \begin{bmatrix} \frac{\partial x_1}{\partial q_1} & \cdots & \frac{\partial x_1}{\partial q_m} \\ \vdots & \ddots & \vdots \\ \frac{\partial x_k}{\partial q_1} & \cdots & \frac{\partial x_k}{\partial q_m} \end{bmatrix} \end{aligned} \tag{A.58}$$

while

$$m = k - \lambda$$

$$\dot{T}_q = \frac{d}{\mathrm{d}t} T_q = \frac{\partial \dot{x}}{\partial q} \tag{A.59}$$

Furthermore, using equations (A.59) and (A.55) yields

$$\begin{aligned} \frac{\partial E}{\partial q} &= \frac{\partial E}{\partial \dot{x}} \frac{\partial \dot{x}}{\partial q} \\ &= \dot{q}' T_q' M \dot{T}_q \end{aligned} \tag{A.60}$$

Similarly, using (A.55) and (A.56)

$$\begin{aligned} \frac{\partial E}{\partial \dot{q}} &= \frac{\partial E}{\partial \dot{x}} \frac{\partial \dot{x}}{\partial \dot{q}} \\ &= \dot{q}' T_q' M T_q \end{aligned} \tag{A.61}$$

Differentiating (A.61) yields

$$\frac{d}{dt}\left(\frac{\partial E}{\partial \dot{q}}\right)' = T_q' M \dot{T}_q \dot{q} + T_q' M T_q \ddot{q} + (\dot{T}_q)' M T_q \dot{q} \tag{A.62}$$

Substituting (A.62), (A.60), (A.53), (A.54), (A.46) and (A.56) into (A.50) yields

$$T_q' M T_q \ddot{q} = -T_q' M \dot{T}_q \dot{q} + T_q' g_x(x, \dot{x}, w) - T_q' U_x \mathcal{A} \mathrm{sgn}(U_x' T_q \dot{q}) \tag{A.63}$$

Defining

$$M_q = T_q' M T_q \tag{A.64}$$

$$U_q = T_q' U_x \tag{A.65}$$

$$g_q(q, \dot{q}, w) = T_q' g_x(x, T\dot{q}, w) - T_q' M \dot{T}_q \dot{q} \tag{A.66}$$

$$\tag{A.67}$$

equation (A.63) takes the form (A.48) and the friction force vector is described by the standard form (A.49).

The proof is complete. △

A.2 Vector "Extended" Coulomb Friction Force

In this case the friction coefficients a_i are written as

$$a_i = a_{i1} + a_{i2} e^{-a_{i3}|\bar{v}_i|} + a_{i4}|\bar{v}_i| \tag{A.68}$$

where a_{i1}, a_{i2}, a_{i3} and a_{i4} are constant coefficients and $\bar{v}_i$ is the ith element of the vector $U'v$.

Using equation (A.68), the vector friction coefficient a takes the form

$$a = \begin{bmatrix} a_1 \\ \vdots \\ a_\nu \end{bmatrix} = \begin{bmatrix} a_{11} + a_{12} e^{-a_{13}|\bar{v}_1|} + a_{14}|\bar{v}_1| \\ \vdots \\ a_{\nu 1} + a_{\nu 2} e^{-a_{\nu 3}|\bar{v}_\nu|} + a_{\nu 4}|\bar{v}_\nu| \end{bmatrix} \tag{A.69}$$

or equivalently,

$$\underbrace{\begin{bmatrix} a_1 & \cdots & 0 \\ \vdots & \ddots & \vdots \\ 0 & \cdots & a_\nu \end{bmatrix}}_{\mathcal{A}} = \underbrace{\begin{bmatrix} a_{11} & \cdots & 0 \\ \vdots & \ddots & \vdots \\ 0 & \cdots & a_{\nu 1} \end{bmatrix}}_{\mathcal{A}_1} + \underbrace{\begin{bmatrix} a_{14}|\bar{v}|_1 & \cdots & 0 \\ \vdots & \ddots & \vdots \\ 0 & \cdots & a_{\nu 4}|\bar{v}_\nu| \end{bmatrix}}_{\mathcal{A}_4}$$

$$+ \underbrace{\begin{bmatrix} a_{12} & \cdots & 0 \\ \vdots & \ddots & \vdots \\ 0 & \cdots & a_{\nu 2} \end{bmatrix}}_{\mathcal{A}_2} e \underbrace{\begin{bmatrix} a_{13}|\bar{v}_1| & \cdots & 0 \\ \vdots & \ddots & \vdots \\ 0 & \cdots & a_{\nu 3}|\bar{v}_\nu| \end{bmatrix}}_{\mathcal{A}_3}$$

Finally, the total friction force vector is written as

$$F(a,v) = U\mathcal{A}_v \operatorname{sgn}(U'v) \tag{A.70}$$

where

$$\mathcal{A}_v = \mathcal{A}_1 + \mathcal{A}_2 e^{-\mathcal{A}_3 \operatorname{diag}\{|U'v|\}} + \mathcal{A}_4 \operatorname{diag}\{|U'v|\} \tag{A.71}$$

A.3 Vector Dynamic Friction Force

In the case of dynamic friction, each particular friction force is described as follows

$$F_i = a_i\, f_i \tag{A.72}$$

and

$$\dot{f}_i = \xi_i(\bar{v}_i, f_i) \tag{A.73}$$

where $\xi_i(\bar{v}_i, f_i)$ is a function that depends on the assumed dynamic model (Dahl, "reset integrator", etc.)

In vector form the total friction can be written as follows:

$$F(a,v) = U\mathcal{A}\, f \tag{A.74}$$

and

$$\dot{f} = \xi(U'v, f) \tag{A.75}$$

Notice that $\xi_i(.,.)$ may not be the same as $\xi_j(.,.)$ for $i \neq j$.

A.4 Vector "Extended" Dynamic Friction Force

This case is a combination of the "extended" Coulomb friction with the dynamic effects and is described as follows

$$F(a,v) = U\mathcal{A}_v\, f \tag{A.76}$$

where $\mathcal{A}_v$ and f are given by (A.71) and (A.75), respectively.

APPENDIX B

A SPECIAL CASE SOLUTION OF EQUATION $AX = B$

Let us consider the following equation:

$$AX = B \tag{B.1}$$

with A and B known real matrices with dimensions $m \times n$ and $m \times l$, respectively. Moreover, it is assumed that $n > m$ and $\text{rank}(A) = m$.

Equation (B.1) has an infinite number of solutions. To find one of them, the following procedure may be used.

Step 1: Find a cofactor D of the matrix A such that D is a square matrix with dimension $m \times m$ and $\text{rank}(D) = m$.

Step 2: Assume that matrix D consists of the $i_{1th}, \cdots i_{mth}$ columns of the matrix A. Then, define a matrix $\hat{X}$ containing the $i_{1th}, \cdots i_{mth}$ rows of the matrix X.

Step 3: Solve the following equation:

$$D\hat{X} = B \rightarrow \hat{X} = D^{-1}B$$

Step 4: The solution of the equation $AX = B$ is

$$[X_{ij}] = \begin{cases} [\hat{X}_{kj}] & \text{if } i = i_k \quad \forall k = 1, \cdots, m \\ 0 & \text{otherwise} \end{cases}$$

where $[X_{ij}]$ and $[\hat{X}_{ij}]$, are the ijth element of the matrices X and $\hat{X}$, respectively.

REFERENCES

Armstrong–Hélouvry, B. 1991. Control of Machines with Friction. Boston, Kluwer Academic Press.

—- 1988. "Friction: Experimental Determination, Modeling and Compensation." *Proceedings of the 1988 International Conference on Robotics and Automation,* Philadelphia, U.S.A, 3: 1422-1427.

—- 1989. "Control of Machines with Non-Linear Low-Velocity Friction: A Dimensional Analysis." *Proceedings of the 1st International Symposium on Experimental Robotics,* Montreal, Quebec, 180-195.

—- 1990. "Stick-Slip Arising from Stribeck Friction." *Proceedings of the International Conference on Robotics and Automation,* Cincinnati, U.S.A, 1377-1382.

—- 1993. "Stick-slip and Control in Low-Speed Motion." *IEEE Transactions on Automatic Control,* 38(10): 1483-1496.

Baril, C. 1993. "Control of Mechanical Systems Affected by Friction and Other Nondifferentiable Nonlinearities." *Ph.D. Dissertation*, Technion, Israel Institute of Technology.

Bell, R., and M. Burdekin. 1966. "Dynamic Behavior of Plain Sideways." *Proceedings of the Institute of Mechanical Engineers,* 181: 1(8): 169-183.

—- 1969. "A Study of the Stick-Slip Motion of Machine Tool Feed Drives." *Proceedings of the Institute of Mechanical Engineers,* 184: 1(29): 543-560.

Bo, L., and D. Pavelescu. 1982. "The Friction–Speed Relation and Its Influence on the Critical Velocity of Slip–Stick Motion." *Wear,* 82: 277-289.

Brandenburg, G., and U. Schäfer. 1988. "Stability Analysis and Optimization of a Position–Controlled Elastic Two Mass System With Backlash and Coulomb Friction." *Proceedings of the 12th IMACS World Congress,* Paris, France, 220-223.

—- 1991. "Influence and Compensation of Coulomb Friction in Industrial Pointing and Tracking Systems." *Proceedings of the 1991 IEEE IAS Annual Meeting,* Detroit-Dearborn, 2: 1407-1413.

Brockett, R.W. 1970. Finite Dimensional Linear Systems. John Wiley and Sons, Inc.

Canudas de Wit, C., K.J. Åström, and K. Braun. 1987. "Adaptive Friction Compensation in DC–Motor Drives." *IEEE Transactions on Robotics and Automation,* RA-3(6): 681-685.

Canudas de Wit, C. 1988. Adaptive Control for Partially Known Systems: Theory and Applications. Elsevier Science Publishers, Studies in automation and Control, Vol. 7.

Canudas de Wit, C., and V. Seront. 1990. "Robust Adaptive Friction Compensation." *IEEE- RD Congress,* Cincinnati.

Canudas de Wit, C., P. Noel, A. Aubin, and B. Brogliato. 1991. "Adaptive Friction Compensation in Robot Manipulators: Low Velocities." *The International Journal of Robotic Research,* 10(3): 189-199.

Canudas de Wit, C., H. Olsson, K.J. Åström, and P. Lischinsky. 1993. "Dynamic Friction Models and Control Design." *Proceedings of the American Control Conference,* San Francisco, CA, 2: 1920-1926.

Cetinkunt, S., W. Yu, J. Filliben, and A. Donmez. 1992. "Friction Characterization Experiments for Precision Machine Tool Control at Very Low Speed." *Proceedings of the 1992 American Control Conference,* Chicago, Illinois, 1: 404-408.

Craig, J.J. 1987. Adaptive Control of Mechanical Manipulators. Addison-Wesley Publishing Company.

Dahl, P.R. 1976. "Solid Friction Damping of Mechanical Vibrations." *AIAA Journal,* 14(12): 1675-1682.

Dupont, P. 1993. "The Effect of Friction on the Forward Dynamics Problem." *International Journal of Robotics Research,* 12(2): 164-179.

Dupont, P., and E. Dunlap. 1993a. "Friction Modeling and Control in Boundary Lubrication." *Proceedings of the 1993 American Control Conference,* San Francisco, CA, 2: 1910-1914.

Dupont, P. 1994. "Avoiding Stick-Slip Through PD Control." To appear in *IEEE Transactions on Automatic Control.*

Ehrich, N.E., and P.S. Krishnaprasad. 1992. "Adaptive Friction Compensation for Bi-Directional Low Velocity Position Tracking." *Proceedings of the 31st IEEE Conference on Decision and Control,* 267-273.

Friedland, B., F.M. Hutton, C. Williams, and B. Ljung. 1976. "Design of Servo for Gyro Test Table Using Linear Optimum Control Theory." *IEEE Transactions on Automatic Control,* 4: 293-296.

Friedland, B. 1986. Control System Design-An Introduction to State Space Methods. MacGraw Hill Publ. Co .

Friedland, B., and Y.J. Park. 1991. "On Adaptive Friction Compensation." *Proceedings of the 30th IEEE Conference on Decision and Control,* Brighton, England, 2899-2903.

Friedland, B., and S.E. Mentzelopoulou. 1992. "On Adaptive Friction Compensation Without Velocity Measurements." *Proceedings of the IEEE International Conference on Control Applications,* Dayton, OH, 2: 1076-1081.

—- 1993. "On Estimation of Dynamic Friction." *Proceedings of the 32nd IEEE Conference on Decision and Control,* San Antonio, TX, 2: 1919-1924.

Friedland, B., S.E. Mentzelopoulou, and Y.J. Park. 1993a. "Friction Estimation in Multimass Systems." *Proceedings of the 1993 American Control Conference,* San Francisco, CA, 2: 1927-1931.

Fuller, D.D. 1984. Theory and Practice of Lubrication for Engineers. New York: John Wiley and Sons.

Gantmacher, F.R. 1959. The Theory of Matrices. Vol.1, Chelsea Publishing Company, New York, N.Y .

Gilbart, J.W., and G.C. Winston. 1974. "Adaptive Compensation of an Optical Tracking Telescope." *Automatica,* 10: 125-131.

Gogoussis, A., and M. Donath. 1987. "Coulomb Friction and Drive Effects in Robot Mechanisms." *Proceedings of the IEEE International Conference on Robotics and Automation,* Raleigh, NC, 2: 828-836.

—- 1990. "A Method for the Real Time Solution of the Forward Dynamics Problem for Robots Incorporating Friction." *Transactions of the ASME,* 112: 630-639.

—- 1993. "Determining the Effects of Coulomb Friction on the Dynamics of Bearings and Transmissions in Robot Mechanisms." *ASME Journal of Mechanical Design.*

Grossman, W. 1991. "An Observer Based Design for Control of Nonlinear Systems and Applications to Robot Manipulators." *Degree of Engineer Thesis,* Electrical Engineering Department, Polytechnic University.

Haessig, Jr. D.A., and B. Friedland. 1991. "On the Modeling and Simulation of Friction." *ASME Journal of Dynamic Systems, Measurement and Control,* 113: 354-362.

Handlykken, M., and T. Turner. 1980. "Control System Analysis and Synthesis for a Six Degree of Freedom Universal Force–Reflecting Hand Controller." *Proceedings of the 19th IEEE Conference on Decision and Control,* 2: 1197-1205.

Harnoy, A., and B. Friedland. 1993. "Dynamic Friction Model of Lubricated Surfaces for Precise Motion Control." *Proceedings of the STLE/ASME Tribology Conference,* New Orleans, Louisiana.

Harnoy, A., B. Friedland, and H. Rachoor. 1994. "Modeling and Simulation of Elastic and Friction Forces in Lubricated bearings for Precise Motion Control." To appear in *Wear.*

Hess, D.P., and A. Soom. 1990. "Friction at a Lubricated Line Contact Operating at Oscillating Sliding Velocities." *Journal of Tribology,* 112: 1: 147-152.

Hsu, J.C., and A.U. Meyer. 1968. Modern Control Principles and Applications. New York, N.Y.: MacGraw Hill Publ. Co.

Johnson, C.T., and R.D. Lorenz. 1991. "Experimental Identification of Friction and Its Compensation in Precise Position Controlled Mechanisms." *Proceedings of the Industrial Applications Social Annual Meeting,* Dearborn, Michigan: IEEE, 1400-1406.

Karnopp, D. 1985. "Computer Simulation of Slip-Stick Friction in Mechanical Dynamic Systems." *ASME Journal of Dynamic Systems, Measurement and Control,* 107: 100-103.

Klamechi, B.E. 1985. "A Catastrophe Theory Description of Slip-Stick Motion in Sliding." *Wear.* 101: 325-332.

Kolston, P.J. 1988. "Modeling Mechanical Stick-Slip Friction Using Electric Circuit Analysis." *Trans. ASME,* 110: 440-443.

Kubo, T., G. Anwar, and M. Tomizuka. 1986. "Application of Nonlinear Friction Compensation to Robot Arm Control." *Proceedings of the IEEE Conference of Robotics and Automation,* San Francisco, CA, 722-727.

Linker, M.F., and J.H. Dieterich. 1992. "Effects of Variable Normal Stress on Rock Friction: Observations and Constitutive Equations." *Journal of Geophysical Research,* 97(B4): 4923-40.

Luh, J.Y.S., W.D. Fisher, and R.P.C. Paul. 1983. "Joint Torque Control by a Direct Feedback for Industrial Robots." *IEEE Transactions on Automatic Control.* 28: 2: 153-161.

Maqueira, B., and K.K. Masten. 1993. "Adaptive Friction Compensation for Line–of–Sight Pointing and Stabilization." *Proceedings of the 1993 American Control Conference.* 2: 1942-1946.

Marui, E., and S. Kato. 1984. "Forced Vibrations of a Base Exited Single Degree of Freedom System with Coulomb Friction. *Transaction of the ASME,* 106: 280-285.

Mentzelopoulou, S. 1993. "Friction Estimation in Two Robot Arm Manipulator." *Proceeding of the 2nd IEEE Regional Conference on Control Systems,* Newark, NJ, 54-57.

Mentzelopoulou, S., B. Friedland, D. Hur, and O. Manzhura. 1993a. "Experimental Measurements and Compensation of Friction." *Proceeding of the 2nd IEEE Regional Conference on Control Systems*, Newark, NJ, 162-165.

Mentzelopoulou, S., and B. Friedland. 1994. "Experimental Evaluation of Friction Estimation and Compensation Techniques." to be presented at the *1994 American Control Conference.*

—- 1994a. "On Adaptive Estimation of Dynamic Friction on a Nth Degree of Freedom System." submitted to the *33rd IEEE Conference on Decision and Control.*

Mukerjee, A., and D.H. Ballard. 1985. "Self–Calibration in Robot Manipulators." *Proceedings of the IEEE International Conference on Robotics and Automation.* St. Louis, 1050-1057.

Pfeffer, L., J. Khatib, and J. Hake. 1989. "Joint Torque Control Sensory Feedback in the Control of a PUMA Manipulator." *IEEE Transactions on Robotics and Automation*, 5(4): 418-425.

Polycarpou, A., and A. Soom. 1992. "Transitions Between Sticking and Slipping." *Friction Induced Vibration, Chatter, Squeal, and Chaos, Proc. ASME Winter Annual Meeting*, Anaheim, New York: ASME 49: 139-148.

Rabinowicz, E. 1951. "The Nature of the Static and Kinetic Coefficients of Friction." *Journal of Applied Physics,* 22(11): 1373-1379

Rabinowicz, E. 1958. "The Intrinsic Variables Affecting the Stick–Slip Process." *Proceedings of Physical Society of London,* 71(4): 668-675.

Rabinowicz, E. 1965. Friction and Wear of Materials. New York, John Wiley and Sons.

Rice, J.R., and A.L. Ruina. 1983. "Stability of Steady Frictional Slipping." *Journal of Applied Mechanics.* 50(2): 343-349.

Salisbury, J.K. 1980. "Active Stiffness Control of a Manipulator in Cartesian Coordinates." *Proceedings of the 19th IEEE Conference on Decision and Control*, 1: 95-100.

Sampson, J.B., F. Morgan, D.W. Reed, and M. Muskat. 1943. "Friction Behavior During the Slip Portion of the Stick-Slip Process." *Journal of Applied Physics,* 14(12): 689-700.

Satyendra, K.N. 1956. "Describing Functions Representing the Effect of Inertia, Backlash and Coulomb Friction on the Stability of an Automatic Control System." *AIEE Transactions,* 75: 2: 243-249.

Schäfer, U., and G. Brandenburg. 1991. "State Position Control of Elastic Pointing and Tracking Systems with Gear Play and Coulomb Friction." *4th EPE Congress,* Florence, Italy, 596-602.

—- 1993. "Model Reference Position Control of an Elastic Two-Mass System with Compensation of Coulomb Friction." *Proceedings of the 1993 American Control Conference,* San Francisco, CA. 2: 1937-1941.

Shen, C.N. 1962. "Synthesis of High Order Nonlinear Control Systems with Ramp Input." *IRE Transactions on Automatic Control,* 7(2): 22-37.

Shen, C.N., and H. Wang. 1964. "Nonlinear Compensation of a Second- and Third Order System with Dry Friction." *IEEE Transactions on Applications in Industry,* 83(71): 128-136.

Southward, S.C., C.J. Radcliffe, and C.R. MacCluer. 1991. "Robust Nonlinear Stick-Slip Friction Compensation." *Journal of Dynamic Systems, Measurement, and Control,* 113: 639-645.

Timoshenko, S., and D.H. Young. 1948. Advanced Dynamics. McGraw-Hill Book Company, Inc.

Tou, J., and P.M. Schultheiss. 1953. "Static and Sliding Friction in Feedback Systems." *Journal of Applied Physics,* 24: 9: 1210-1217.

Tomlinson, G.R., and J.H. Hibbert. 1979. "Identification of the Dynamic Characteristics of a Structure with Coulomb Friction." *Journal of Sound and Vibration,* 64: 2: 233-242.

Townsend, W.T. and J.K. Salisbury. 1987. "The Effect of Coulomb Friction and Stiction on Force–Control." *Proceedings of the IEEE International Conference on Robotics and Automation,* 883-889.

Tung, E.D., G. Anwar, and M. Tomizuka. 1991. "Low Velocity Friction Compensation and Feedforward Solution Based on Repetitive Control." *Proceedings of the 1991 American Control Conference,* 3: 2615-2620.

Tung, E.D., Y. Urishisaki, and M. Tomizuka. 1993. "Low Velocity Friction Compensation for Machine Tool Feed Drives." *Proceedings of the 1993 American Control Conference,* San Francisco, CA, 2: 1932-1936.

Tustin, A. 1947. "The Effects of Backlash and of Speed- Dependent Friction on the Stability of Closed–Cycle Control Systems." *Journal of the Institution of Electrical Engineers,* 94(2A): 143-151.

Walrath, C.D. 1984. "Adaptive Bearing Friction Compensation Based on Recent Knowledge of Dynamic Friction." *Automatica,* 20: 717-727.

Wu, C.H., and R.P. Paul. 1980. "Manipulator Compliance based on Joint Torque Control." *Proceedings of the 19th IEEE Conference on Decision and Control,* 1: 88-94.

Yang, S., and M. Tomizuka. 1988. "Adaptive Pulse Width Control For Precise Positioning Under Influence of Stiction and Coulomb friction." *ASME Journal of Dynamic Systems, Measurement and Control,* 110(3): 221-227.